Development and Evaluation of a Thermal Model for Haptic Interfaces

by

Hsin-Ni Ho

B.S. Mechanical Engineering, 2000
National Taiwan University

M.S. Mechanical Engineering, 2002
National Taiwan University

Submitted to the Department of Mechanical Engineering
in Partial Fulfillment of the Requirements for the Degree of
Doctor of Philosophy in Mechanical Engineering

at the

Massachusetts Institute of Technology

February 2007

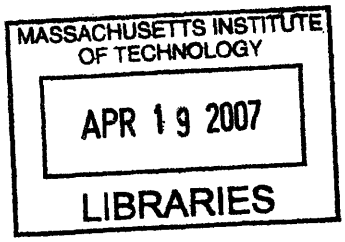

Signature of Author.....
Department of Mechanical Engineering
September 20, 2006

Certified by.....
Lynette A. Jones
Principal Research Scientist in Mechanical Engineering
Thesis Supervisor

Accepted by.....
Lallit Anand
Chairman, Department Committee on Graduate Students

Development and Evaluation of a Thermal Model for Haptic Interfaces

by

Hsin-Ni Ho

Submitted to the Department of Mechanical Engineering
on September 22, 2006 in partial fulfillment of the
requirements for the degree of Doctor of Philosophy in
Mechanical Engineering

ABSTRACT

The thermal interaction between the skin and an object is influenced by the thermal properties and initial temperatures of the skin and object, and by the contact force and surface roughness of the contact surfaces. This thermal interaction is modeled in this research which characterizes the transient thermal responses during contact. The thermal model was evaluated in psychophysical and physiological experiments by determining whether simulated thermal feedback generated based on the model was capable of conveying information to users that was similar to that provided by real materials, and by comparing the temperature responses of the skin predicted by the model and elicited by real materials. In order to obtain precise skin temperature measurements, an infrared thermal measurement system was designed to overcome the limitations imposed by thermal sensors and to determine the influence of contact pressure on the skin temperature responses during contact. The results from the psychophysical and physiological experiments validated the thermal model proposed in this research within the typical contact force range of manual exploration. A thermal display based on this model is able to convey thermal cues that can be used to perceive and identify objects as effectively as those provided by real materials.

Thesis Supervisor: Lynette A. Jones
Title: Principal Research Scientist in Mechanical Engineering

ACKNOWLEDGMENTS

I would like to express my sincere gratitude to my advisor, Dr. Lynette A. Jones for her guidance throughout my PhD years. Her wisdom and kindness helped me adapt to the foreign environment and shaped me into a researcher. This thesis would not be possible without her expertise and advice, and the countless hours that she spent on reviewing and editing the manuscript.

I also would like to thank my committee members, Prof. John H. Lienhard and Prof. Ioannis Yannas, for their valuable suggestions and support for this work. Prof. Lienhard's teaching stimulated my great interest in heat transfer, and the suggestions from Prof. Yannas always showed me the importance of considering the problems in other perspectives. Their expertise enabled me to build the foundation of this work.

My special thanks also go to Prof. Ian Hunter for providing the wonderful research environment and resources. I am also grateful to Prof. Bora Mikic for his enthusiasm when discussing the thermal modeling with me.

I want to thank all the members in Bio-instrumentation lab for their help and support. My MIT experience would not be so joyful without having Erin Piateski as an officemate and a best friend. Her company and encouragement made our office feel like home. Robert David is always very kind and helpful to me. His insights in heat transfer are inspiring and his attitude of conducting research sets a good example to me. Andrew Taberner and James Tangora have always been the great sources of expertise when I faced the challenges of my research. Not to mention Dawn Wendell, Brian Hemond, Craig Forest, Mike Garcia-Webb, Angela Chen, and Kate Melvin for making the lab a friendly place.

For all my friends, without you standing by my side, the summer in Boston would not be so joyous and the winter would be longer and darker. The laughs that we shared are the most precious memory of my life in USA.

Lastly and most importantly, I would like to thank my parents, Ting-Keng Ho and Ho-Tze Lin, for their bottomless support and always having faith in me. This thesis is dedicated to them.

This research was supported in part through the Advanced Decision Architectures Collaborative Technology Alliance sponsored by the U.S. Army Research Laboratory under Cooperative Agreement DAAD 19-01-2-0009.

Dedicated to my parents, Ting-Keng Ho and Ho-Tze Lin

獻給我的父母，何鋌鏗與林鶴子。

TABLE OF CONTENTS

CHAPTER 1

INTRODUCTION

1.1 HAPTIC INTERFACES

The haptic sensory system involves the tactile and proprioceptive senses and is the only sensory system that can both sense and act on stimuli. The tactile sense refers to the 'sense of touch' which is involved in perceiving the surface features, mechanical properties and thermal characteristics of objects in contact with the skin. The proprioceptive sense encodes the position and movement of our limbs. In our daily lives, we rely on both senses to observe and explore the environment. Tactile and proprioceptive inputs therefore play an important role in assessing the properties of objects that we used to interact with the environment. Without the haptic sense, this interaction would be extremely limited and most manual activities would be performed very inefficiently.

In order to assist in the physical interaction with a virtual environment or teleoperated robotic system, it is important to provide haptic feedback to the human operator. A haptic interface is defined as a device which is able to communicate with the user's sensory system through tactile and force feedback. Depending on the application, the haptic interface can either be a display which provides tactile or force feedback or it can use the operator's response as an input and display the appropriate feedback based on the user's response.

Current tactile displays are able to convey the shape, texture or contour of an object by deforming the skin or changing the distribution of contact forces (for a review see Burdea & Coiffet, 2003). Tactile displays are able to convey detailed localized contact information, whereas force displays provide feedback of the forces produced during interaction. Force displays are usually configured as hand controllers or exoskeletal devices that are mounted on the back of the hand and arm. The grounding of force displays is necessary to prevent slippage and potential accidents during force transmission. With the integration of sensors and actuators, these force displays are capable of sensing force and measuring limb position and therefore form a closed loop for force feedback control (for a review see Burdea & Coiffet, 2003).

With the objective of providing a complete image of a virtual environment, multimodal haptic displays have been developed to generate tactile, kinesthetic and thermal feedback simultaneously to convey the characteristics of an object during hand-object interactions (Benali-Khoudja & Hafez, 2004; Caldwell & Gosney, 1993; Citerin et al., 2006; Kron & Schmidt, 2003; Yang et al., 2006a). These multimodal displays are configured in various forms ranging from a haptic glove to a computer mouse. The tactile feedback is typically generated with a miniature motor, pin array, micro coils or piezoelectric bimorphs, whereas the thermal feedback is provided by a Peltier device with temperature control. With such an interface, the degree of immersion in a virtual environment can be enhanced.

1.2 Utility and Development of Thermal Displays

For applications involving virtual environments and teleoperated robotic systems, the object that interacts with the hand is either a virtual object or an object that is actually at a remote site. Users can therefore only interact physically with the object through a haptic interface. In order to provide a holistic image of a virtual object, the integration of thermal feedback into haptic interfaces has received increasing attention. With such a

display, the thermal characteristics of an object and thermal sensations associated with contact can be reproduced to assist users in identifying the object.

Typical thermal displays consist of thermal stimulators, thermal sensors, and a temperature control system that is used to monitor and control the surface temperature of the displays (Benali-Khoudja & Hafez, 2004; Caldwell & Gosney, 1993; Citerin et al., 2006; Deml et al., 2006; Ho & Jones, 2004; Ino et al., 1993; Kron & Schmidt, 2003; MacLean & Roderick, 1999; Ottensmeyer & Salisbury, 1997; Yamamoto et al., 2004; Yang et al., 2006a). In some studies, infrared lamps or fans have also used to provide thermal information about the environment through thermal convection or radiation (Dionisio et al., 1997; Lecuyer et al., 2003).

The Data Glove Input System designed by Caldwell and Gosney (1993) is a haptic interface that provides force, tactile, and thermal feedback. The thermal feedback unit is a Peltier device which makes contact with the dorsal surface of the index finger. Using this device, Caldwell and Gosney (1993) recorded the thermal changes on a teleoperated robotic hand as it made contact with a variety of objects (a cube of ice, a soldering iron, insulating foam, and a block of aluminum), and then presented these thermal transients to subjects who were required to identify the virtual material based on the simulated thermal cues. Subjects achieved an 80% success rate in identifying the various materials based only on these thermal cues.

Ino et al. (1993) also developed a thermal display which provided thermal cues associated with contact. They measured the decreases in finger temperature upon contact as subjects tried to identify various materials (aluminum, glass, rubber, polyacrylate, and wood), and the measured decreases in finger temperature were then used to simulate the thermal transients associated with contact. Subjects were required to identify the materials using only the simulated thermal cues. Ino et al. (1993) found that the recognition rates for the various materials presented with the thermal display were equivalent to those measured using real materials (61% correct with the real materials and 56% correct with the display), and that there was no significant difference in the

information transmission rates associated with the real object and the Peltier-based thermal display.

Besides empirically measuring temperature changes and re-creating them in a display, model-based thermal displays have also been developed to simulate different materials. Using an electrical analogy (Benali-Khoudja et al., 2003) as the basis of their thermal model, Benali-Khoudja and Hafez (2004) built a vibrotactile and thermal interface, VITAL. The simulation of the virtual material was achieved by integrating four Peltier devices with the vibrotactile interface so that the interface could generate thermal and tactile stimulation simultaneously. They demonstrated that the model predictions of the skin temperature responses when making contact with glass, copper and aluminum were similar to those measured when making contact with the corresponding real materials.

Another thermal display that was built to assist in material identification was designed and fabricated by Yamamoto et al. (2004) who used a thermal model to predict changes in skin temperature. The display was based on a Peltier device with thermal sensors, and a PID (proportional-integral-derivative) controller. The performance of the display was evaluated with four simulated materials (EPS, wood, ceramic, and brass) that subjects were required to identify. Subjects achieved an 80% success rate in identifying EPS and brass with the thermal cues generated by the thermal display, but were less accurate with the other two materials.

In order to enhance the ability of subjects to identify materials, multi-finger thermal displays have also been developed to present thermal information about an object to all of the fingers in one hand (Deml et al., 2006; Kron & Schmidt, 2003; Yang et al., 2006a, 2006b). These thermal displays are all model-based and utilize Peltier devices as the thermal stimulator. Deml et al. (2006) found that the simulated skin temperature responses during contact based on their thermal model were only slightly different from those recorded with real materials. In addition, subjects achieved similar performance in material identification tasks with real materials and those simulated with the thermal display. Kron and Schmidt (2003) evaluated their display using a pairwise material

discrimination task with four real (aluminum, ceramic, PVC, and wood) and simulated materials. Subjects' performance in material discrimination was comparable when the materials were presented physically or with the thermal display. Yang et al. (2006a, 2006b) further suggested that subjects' performance in material identification improves as the number of the fingers simulated increases, but that most of the improvement occurs when three rather than a single finger is used.

Other displays have been fabricated using Peltier devices to simulate changes in temperature in virtual environments. A thermal display, the Thermostylus, has also been built that can be incorporated into the PHANTOM interface (SensAble Technologies), a commercially available force reflecting device (Ottensmeyer & Salisbury, 1997). It utilizes a Peltier device to provide thermal feedback together with the force feedback of PHAMTON interface. The heating and cooling rates of this unit are 11 ^{o}C/s and 4.5 ^{o}C/s, respectively.

As a new medium of communication, a haptic doorknob was designed by MacLean and Roderick (1999) to convey information about the space beyond the door using thermal, tactile, and auditory feedback. The thermal feedback unit in this haptic display consisted of a Peltier device controlled by a PID temperature controller. This unit was able to output approximately 10 ^{o}C above and below the ambient temperature within 30 s.

Thermal feedback can also be presented without physical contact between the device and the user. In 1997, Dionisio et al. introduced the Thermopad which consists of a Peltier device, a fan and an IR lamp. The purpose of the Peltier device is to induce changes in skin temperature based on the virtual scenario. The IR lamp serves to warm the environment, and the fan is used to cool it. With this configuration, the Thermopad is able to generate thermal feedback in the form of conduction, convection and radiation, and is able to simulate different thermal scenarios in virtual reality environments, such as the perception of a fire blazing in a fire place.

Another type of non-contact thermal display called the HOMERE system was designed to assist visually-impaired people in virtual reality environments. (Lecuyer et al., 2003). The thermal feedback in this system is generated by twelve IR lamps located around a circular structure. They provide the warm feeling of the 'virtual sun' with 30 degree resolution for the direction of sunlight.

1.3 THERMAL MODELS FOR HAND-OBJECT INTERACTIONS

One of the most crucial processes in developing a thermal display is the characterization of the thermal responses that occur on the hand as it makes contact with a material. In the early stages of thermal display development, the simulation of a virtual material in contact with the fingertip was based on empirical data of the changes in skin temperature when the hand made contact with the corresponding real material (Caldwell & Gosney, 1993; Ino et al., 1993). In other words, numerous measurements needed to be completed in order to simulate every material and condition that could appear in the virtual scenario. The time and labor needed for these measurements was considerable and there was not a consistent measurement protocol which introduced variability in the results obtained.

These limitations were overcome as thermal modeling has become the major methodology used for predicting the thermal interaction between the skin and an object (Bergamasco et al., 1997; Citerin et al., 2006; Deml et al., 2006; Ho & Jones, 2004, 2006b; Kron & Schmidt, 2003; Shitzer et al., 1996; Yamamoto et al., 2004; Yang et al., 2006a). A thermal model is able to incorporate various material properties and contact conditions for different hand-object interaction scenarios. It can predict the thermal responses of the skin and an object during contact and the algorithms used for the thermal display should elicit the correct skin temperature response that simulates the intended thermal sensation. By working with a thermal model, a thermal display is able to simulate any object and environmental condition.

Most of the existing analytical thermal models are developed based on the bio-heat equation (Pennes, 1948), which is able to account for the effects of metabolic heat generation and blood perfusion with thermal diffusion to describe the energy balance within the tissue:

$$\rho c \frac{dT}{dt} = \nabla(k \nabla T) + (\rho c)_b \omega_b (T_a - T) + q_m \qquad (1\text{-}1)$$

where ρc is the heat capacity of the tissue, T is the tissue temperature, t is time, k is the conductivity of the tissue, $(\rho c)_b$ is the heat capacity of the blood, ω_b is the perfusion rate of blood, T_a is the temperature of arterial blood before entering the capillaries, and q_m is the metabolic heat generation.

This bio-heat equation describes a transient, conduction-dominated heat transfer process within tissue with the assumptions that metabolic heat generation, q_m, is homogeneously distributed throughout the tissue of interest, that the blood perfusion effect $(\rho c)_b \omega_b (T_a - T)$ is homogeneous and isotropic, and that thermal equilibration occurs in the microcirculatory capillary bed. An important advantage of Pennes' bio-heat equation is that the blood perfusion term is linear with temperature, which means that the equation can be solved by methods commonly used to solve the heat-conduction equation. Numerous alternative models have been proposed for bio-heat transfer over the past 50 years (for a review see Charny, 1992), but the simplicity of Pennes' bio-heat equation and its agreement with experimental data have made it the quantitative foundation for the field of bio-heat transfer (Charny, 1992).

Using the bio-heat equation, existing thermal models predict the skin temperature responses during hand-object interactions with different assumptions and boundary conditions. In these thermal models, the initial temperatures and thermal properties of the skin and materials, and the effects of blood perfusion have generally been considered.

Shitzer et al. (1996) proposed a lumped heat transfer model for bio-heat transfer of a gloved semi-spherical fingertip with the cold environment based on the assumptions that the fingertip is supplied and drained by a single artery and a single vein, that the thermal properties of the tissue are homogeneous, and that the conduction of heat along the finger is neglected. The heat balance at the fingertip is given by:

$$\rho cV\frac{dT}{dt} = hA(T_o - T) + (\rho c)_b \omega_b (T_b - T) \tag{1-2}$$

where ρc is the heat capacity of the fingertip, V is fingertip volume, T is fingertip temperature, t is time, h is the heat transfer coefficient between the fingertip and the environment, A is fingertip surface area, and ω is blood perfusion rate. Subscripts o and b are for the properties of the environment and blood, respectively. In this model, the effects of heat storage and blood perfusion within the tissue are described by $\rho cV\frac{dT}{dt}$ and $(\rho c)_b \omega_b (T_b - T)$ respectively. In spite of the assumptions made to simplify the complicated heat transfer process, Shitzer et al. (1996) found a good conformity between the analytic and measured results.

The thermal model proposed by Yamamoto et al. (2004) attempted to simulate the early time sensation (ETS) when the hand is brought into contact with an object. The skin and object were therefore regarded as two homogenous materials with uniform initial temperatures and the effect of thermal contact resistance was neglected. According to the model, the contact temperature within the ETS is constant with time and can be calculated based on the material properties and initial temperatures of the skin and object. In order to reproduce the thermal sensations with a thermal display, Yamamoto et al. (2004) determined a static temperature based on the contact temperature and the thermal properties of the display. This temperature was presented with the display before contact was made. After the finger made contact with the display, the surface temperature of the display changed to the contact temperature. The contact temperature was then maintained for the rest of the contact period. Based on the same assumptions and governing

equations as Yamamoto et al. (2004), Yang et al. (2006a) calculated the time dependent temperature profile during contact at 1.24 mm from the skin surface. This technique attempted to provide the same thermal stimuli to the thermoreceptors with the thermal display as if the hand was making contact with a real object.

In 1997, Bergamasco et al. proposed two thermal models, a partial differential equation (PDE) and an ordinary differential equation (ODE) thermal model of the finger, to describe thermal contact phenomena for virtual reality applications. The goal of these models was to calculate the transient skin temperature gradient in the direction perpendicular to finger pad surface when the finger rested in air and when it made contact with an object. The PDE model for the finger in air was based on the one-dimensional bio-heat equation with the assumption that the thermal properties of the tissue are spatially uniform. For modeling contact with an object, the PDE model treated it as a one-dimensional conduction problem with the assumptions that the object is a semi-infinite body and no heat exchange occurs at the tissue boundary which is some distance from the interface. Instead of regarding skin as a tissue with uniform thermal properties, the ODE model divided the skin into 10 layers with different material properties. In this model, the heat storage within each layer, the continuum of the one-dimensional heat conduction at the interfaces, blood perfusion, and metabolic heat generation were all considered for both non-contact and contact situations.

The ODE model proposed by Bergamasco et al. has been adapted by others to include the three layers of skin based on its anatomical structure, namely epidermis, dermis and endodermis (Deml et al., 2006; Kron & Schmidt, 2003). The model proposed by Kron and Schmidt (2003) is able to determine the temperature distribution inside the fingertip when the fingertip moves in air or makes contact with an object. The effects of metabolic heat generation and blood perfusion are considered within the dermal and hypodermal layers. However, these effects were only taken into account for the hypodermal layer in a similar model developed by Deml et al. (2006).

In order to capture the temperature response within the fingertip more precisely, Citerin et al. (2006) utilized the superposition property of the thermal system and solved the skin temperature responses during the different stages of contact using an analytical and finite element method. At the early stage of contact, the temperature distribution was solved analytically by assuming that both the skin and object were semi-infinite materials. For the remainder of the contact period, the effects of metabolic heat generation and blood perfusion were considered and the temperature distribution was solved using finite-element methods.

1.4 PROPOSAL AND OVERVIEW

The objectives of the research conducted for this thesis were to understand what happens thermally during hand-object interactions and to develop a thermal model that was able to describe this contact process. Based on the thermal model, a thermal display was constructed to generate realistic thermal feedback when interacting with a virtual object. With this thermal feedback, the essential thermal information about an object could be conveyed and a complete image of the virtual object could be created.

The thesis is organized in the following manner. In Chapter 2, the characteristics of human thermal perception are described; the role of thermal cues in material discrimination is further examined in Chapter 3. In this chapter a thermal model is presented and two psychophysical experiments are described which were designed to evaluate how people perceive thermal sensations during hand-object interactions.

In Chapter 4, a thermal display was constructed based on the proposed thermal model and was evaluated with both psychophysical and physiological experimentation. The results indicated that there was an inconsistency between the model predictions and the measured skin temperature responses during contact. This discrepancy may have resulted from inaccuracies in skin temperature measurement and/or from inadequacies in the proposed thermal model. An infrared thermal measurement system was therefore

designed to improve the accuracy of temperature measurement. A detailed description of the system is provided in Chapter 5.

Chapter 6 describes the revision and validation of the thermal model. The thermal model now takes into account the influence of thermal contact resistance on the skin temperature response during contact. This model was evaluated using the physiological measurements recorded with the infrared thermal measurement system. The results indicated that the revised thermal model is accurate within the typical contact force range used for manual exploration.

Finally, Chapter 7 provides a summary of the conclusions of the research, and possible future research.

CHAPTER 2

THERMAL SENSATION

2.1 Skin Anatomy and Properties

2.2 Thermoreceptors

2.3 Thresholds

2.4 Spatial Summation and Localization

When making contact with an object, the skin is the surface that interacts with the object and receives thermal information during the interaction. Knowledge of the anatomy and properties of the skin is an important starting point in understanding what happens thermally in the skin during contact. The thermal stimuli generated during contact are sensed by thermoreceptors located in the skin, of which there are two sub-modalities that respond to different ranges of thermal stimuli. Humans can only perceive a thermal stimulus when it exceeds some specific threshold and this threshold depends on the stimulated site and if the stimulus is warm or cold. Human thermal perception has been shown to have good spatial summation and poor localization for thermal stimuli at low intensities. These characteristics influence how people perceive temperature.

2.1 SKIN ANATOMY AND PROPERTIES

Skin, the largest organ of the human body, defines the boundary between the body and the outer world. For an average adult human, the skin has a surface area of approximately 1.8 m^2 with a thickness typically between 2-3 mm and a mass of about 4.5 to 5 kg (Tortora & Grabowski, 1993). With both low thermal conductivity (0.37 W/mK) and thermal diffusivity (10^{-7} m^2/s), skin is a good thermal insulator that helps maintain core body temperature and minimize environmentally-induced surface temperature

fluctuations. The skin contains sweat glands, blood vessels, and numerous nerve endings. With these characteristics, it is able to guard against bacterial invasion, protect underlying muscles and organs, regulate temperature (Moore & Agur, 1995), and is also the sensing surface that permits us to explore our environment tactually.

Skin is composed of two principal layers: the epidermis and dermis. The epidermis is the outermost layer and its thickness ranges between 65-115 μm. It provides a barrier to the outside world and houses free nerve endings. With no blood vessels in the epidermis, its cells are nourished by the capillaries extending from the upper layers of the dermis. The second major layer of the skin is the dermis. The thickness of the dermis ranges between 0.3 – 3 mm. Within the dermis, there are sensory nerve endings which respond to touch and pressure, temperature changes and painful stimuli. The papillary folds that interconnect the epidermis and dermis form the fingerprints and footprints that are the basis of unique identify. Lying below the dermis is the hypodermis which is the subcutaneous tissue that attaches the skin to underlying bone and muscle and supplies it with blood vessels and nerves. The subcutaneous fat within the hypodermis serves as a protective padding and insulation for the body.

2.2 THERMORECEPTORS

Changes in skin temperature are encoded by two classes of thermoreceptors located in the dermis of the skin, cold and warm receptors. Warm receptors are located 0.3-0.6 mm below the skin surface, whereas cold receptors are 0.15-0.17 mm in depth, which is immediately beneath the epidermis. The receptive field of thermoreceptors is typically less than 1 mm in diameter (Hensel, 1981). The density of thermoreceptors varies from one body region to another, but cold receptors are always more numerous than warm receptors (Darian-Smith, 1984).

Although there is little morphological evidence regarding the structure of thermoreceptors, it appears that areas sensitive to cold or warmth in humans are not

associated with any encapsulated or corpuscular nerve endings (Hensel, 1981). Nerve conduction studies on afferent fibers excited by cutaneous thermal stimulation indicate that the afferent fibers from cold and warm receptors are small myelinated Aδ and unmyelinated C fibers, respectively. Because myelinated axons have larger diameters than unmyelinated axons, the conduction velocity of cold receptors is much faster (5-30 m/s) than that of warm receptors (0.5-2 m/s) (Brown, 1989).

In the neutral thermal zone between 30 and 36 °C, both thermoreceptors discharge spontaneously at low rates and no thermal sensation is noted. When the skin temperature drifts away from this neutral thermal zone, the relative discharge rate of the warm and cold receptors changes. In general, increases in skin temperature induce warm receptors to fire, and decreases in temperature result in cold receptors discharging. The warm receptors respond to a temperature range between 30-50 °C with peak intensities between 38-43 °C. Cold receptors fire in bursts at temperatures below 30°C with peak intensities between 23-28 °C. They are silent between 37-44°C and then fire paradoxically at 45° C (Darian-Smith, 1984; Spray, 1986). When the skin temperature rise above 45 °C or falls below 13°C, nocioceptors respond to the extreme thermal stimuli which results in the perception of pain.

2.3 THRESHOLDS

The ability to perceive thermal changes depends on many factors including the site stimulated, the amplitude and rate of temperature change, and the baseline temperature of the skin (for reviews see Darian-Smith, 1984; Stevens, 1991). Thermal sensitivity varies by approximately 100-fold at different body sites. The face, especially the mouth, is the most sensitive region and the extremities are the least sensitive. All body regions are more sensitive to cold than to warmth which might result from the fact that cold receptors are more numerous than warm receptors (Stevens & Choo, 1998).

The threshold for discriminating the difference in the amplitudes of two temperature pulses delivered to the thenar eminence of the hand is 0.02-0.07 °C for cooling pulses, and 0.03-0.09 °C for warming pulses (Johnson et al., 1973; Johnson et al., 1979). This is considerably lower than the threshold for discriminating a change in skin temperature. When the skin temperature of the thenar eminence is maintained at 33 °C, the differential threshold for warming is 0.11 °C and for cooling, 0.07 °C (Stevens & Choo, 1998). If skin temperature changes very slowly, for example at a rate of less than 0.5 °C/minute, then an observer can be unaware of a change of up to 4-5 °C, provided that the temperature remains within the neutral thermal zone of 30-36 °C (Kenshalo, 1976).

2.4 Spatial Summation and Localization

Human thermal sensibility has been shown to have good spatial summation for thermal stimuli at low intensities (Hardy & Oppel, 1937; Marks et al., 1976; Taus et al., 1975). Spatial summation refers to the effect of the size of the simulated area on the perceived amplitude of the stimulus. The intensity and areal extent of a thermal stimulus can be traded to preserve the same thermal sensation. The rules governing spatial summation for warmth and cold differ in that the degree of spatial summation for warmth declines with increasing stimulus intensity, whereas the summation for cold tends to remain about the same with decreases in temperature ranging from 1.5 to 12 °C (Stevens & Marks, 1979). For both warm and cold sensation, spatial summation decreases as the thermal stimulus approaches the thermal pain threshold. (Stevens, 1991).

The localization of thermal stimuli has been shown to be extremely poor compared to that of tactile stimuli (Taus et al., 1975). With a pure thermal stimulus, such as a radiation source, it is possible for a subject to misjudge whether the stimulus is on the front or back of the torso (Cain, 1973). The localization of a thermal stimulus can be facilitated by the tactile input associated with contact. However, the interaction of thermal and tactile inputs can also lead to mislocalization of thermal sensations when adjacent parts of the skin are differentially stimulated. Green (1977) described a thermal

illusion involving the hand in which the thermal sensation experienced by the middle finger changed as a function of the sensations experienced at the two adjacent fingers. When the index and ring fingers were placed on cold (or warm) thermal stimulators and the middle finger was placed on a thermally neutral stimulator, cold (or warmth) was felt on all three fingers. The perceived magnitude of these thermal sensations was the same as that experienced in the control condition in which the temperature of the thermal stimulator under the middle finger was varied and the outer two stimulators remained thermally neutral. This referral of thermal sensations required equivalent tactile experiences on the three fingers, in that it did not occur when the middle finger was held above the stimulator (Green, 1977).

With poor spatial localization but good spatial summation for both warm (Hardy & Oppel, 1937; Marks & Stevens, 1973; Marks et al., 1976) and cold (Hardy & Oppel, 1938; Stevens & Marks, 1979) stimuli, it is difficult for the thermal perceptual system to identify precisely where a specific thermal change occurs. As a result, thermal illusion can occur under some conditions as described by Green (1977) and this will affect the ability to identify the nature of the thermal stimulus.

CHAPTER 3

CONTRIBUTION OF THERMAL CUES TO MATERIAL DISCRIMINATION AND LOCALIZATION

The ability to discriminate between objects by touch is based on the perception of a number of properties including shape, surface texture, compliance, and thermal characteristics. These cues become particularly important when objects must be identified in the absence of vision. The human hand is capable of resolving remarkably fine variations in texture, as shown by its capacity to detect periodically ordered elements that are only 0.06 μm high when there is a relative motion between the texture and the finger pad (LaMotte & Srinivasan, 1991). The ability to discriminate between the compliance of objects depends on whether the objects have deformable or rigid surfaces. With deformable surfaces, cutaneous cues from skin deformation are sufficient to discriminate compliance, whereas for rigid objects both cutaneous and proprioceptive cues are necessary for discrimination (Srinivasan & LaMotte, 1995). The thermal cues that are used to assist in identifying an object arise from changes in skin temperature that occur when the object is held in the hand. Warm and cold thermoreceptors in the skin discharge in response to these local thermal transients. The resting temperature of the skin is generally higher than the temperature of objects in contact with the skin, and so it is the cold thermoreceptors that signal the decrease in skin temperature upon contact.

Several studies have suggested that subjects can identify objects varying in thermal properties using only thermal cues. Jones and Berris (2003) evaluated the performance of subjects in a material discrimination task in which thermal cues were the main source of information about the materials. Of the materials presented to the hands (copper, brass, nickel, stainless steel and nylon), nylon was the only material that could be reliably discriminated from the other materials. Caldwell and Gosney (1993) presented the simulated thermal transients associated with various materials (ice cube, a heated soldering iron, an aluminum block, and a piece of insulation foam) to the hands of subjects with their thermal display and found that subjects achieved an 80% success rate in identifying the various materials based only on these thermal cues. In a further study of thermal cues and object identification, Ino et al. (1993) found that of the five materials presented to the fingertip, subjects could reliably identify aluminum and wood with success rates higher than 80%, but confused glass, rubber and polyacrylate. In these studies (Caldwell & Gosney, 1993; Ino et al., 1993; Jones & Berris, 2003), subjects were required to identify the material based on the pattern of thermal cues presented to the hand, and subjects knew in advance the types of material being presented. These results suggest that subjects can use thermal cues effectively to identify objects when the thermal transients associated with contact are perceptually distinct.

A thermal model was developed and the two psychophysical experiments were conducted to determine what thermal cues are used to discriminate between objects. The thermal model can predict the changes in temperature during contact and from these predictions and psychophysical results, it is possible to determine the magnitude of the thermal changes required for subjects to discriminate between materials. In the material discrimination experiment, subjects were required to discriminate between two materials presented to the left and right index fingers by selecting the material that felt colder. The second experiment focused on identifying which of three fingers was in contact with a material that differed from the other two. In this study, the ability to localize thermal changes was evaluated.

3.1 MODELING THE THERMAL PROCESS

The resting temperature of the skin on the hand ranges from 25 to 36 °C (Verrillo et al., 1998), and is typically higher than the ambient temperature of materials encountered in the environment. The thermal cues used to identify a material by touch are influenced by the interface temperature and the heat flux conducted out of the skin upon contact. These are in turn a function of thermal properties such as conductivity and heat capacity, and the initial temperatures of the skin and material.

The thermal interaction between the skin and a material in contact with the skin is a transient process that is dominated by heat conduction. The interface temperature during contact is the only temperature load imposed on the skin, and the heat transfer within the skin depends mainly on this temperature. To model this process, a simple but representative model was sought that was able to characterize the interface temperature. The 'two semi-infinite bodies in contact' model was a reasonable initial choice to model the contact between the finger and an object (Ho & Jones, 2004; 2006a). The assumptions of this model were that the contact time was short enough for the fingerpad and material to behave as semi-infinite bodies (Lienhard & Lienhard, 2003), that the heat flux due to blood perfusion and metabolic heat generation was insignificant, that the thermal contact resistance was negligible, and that the temperature variation was only significant in the direction perpendicular to the contact interface. The validity of the last assumption was confirmed by a two-dimensional finite element simulation of the temperature responses of the finger and object during contact conducted by Sarda et al. (2004). Their results indicated that the isotherms within the temperature gradient are almost parallel to the contact surface and this suggested that thermal interaction between the skin and object is essentially one-dimensional in the direction perpendicular to the contact surface (Sarda et al., 2004).

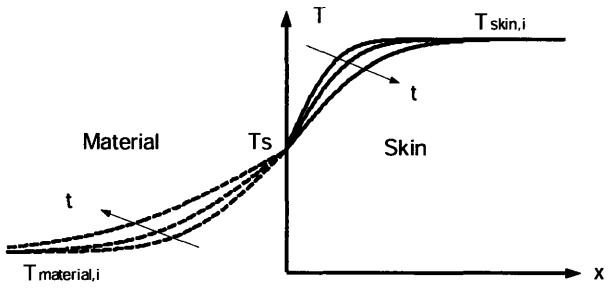

Figure 3-1. Heat transfer process between the fingerpad skin and a material during contact based on the semi-infinite body model

With the 'two semi-infinite bodies in contact' model, the temperature profiles of the skin and a material during contact can be described as shown in Figure 3-1. At the moment of contact (t = 0), the surface temperatures of the skin and material change instantaneously to the interface temperature, T_s, and remain constant throughout the whole contact process. The interface temperature, T_s, is determined by the thermal properties and initial temperatures of the skin and object. Based on this model, the interface temperature, T_s, can be calculated as:

$$T_s = \frac{T_{material,i}(k\rho c)^{1/2}_{material} + T_{skin,i}(k\rho c)^{1/2}_{skin}}{(k\rho c)^{1/2}_{material} + (k\rho c)^{1/2}_{skin}} \tag{3-1}$$

where T_s is the interface temperature, k is the thermal conductivity, ρ is density, c is specific heat, $T_{material,i}$ is the initial temperature of the material, $T_{skin,i}$ is the initial temperature of the skin, and $(k\rho c)^{1/2}$ is the contact coefficient. The thermal property that influences this process is the contact coefficient $(k\rho c)^{1/2}$ which acts as a weighting factor that determines whether T_s will more closely approach $T_{skin,i}$ or $T_{material,i}$ (Incropera & DeWitt, 1996). In this thermal model, the contact coefficient is used to characterize the thermal properties of objects during hand-object interactions. Although the interface temperature remains constant during contact, the temperature profiles within the skin (for x > 0) change with time and can be calculated based on the following equation:

$$\frac{T_{skin}(x,t)-T_s}{T_{skin,i}-T_s}=erf\left(\frac{x}{2\sqrt{\alpha_{skin}t}}\right) \tag{3-2}$$

where α_{skin} is the thermal diffusivity of the skin. The heat fluxes, which are created by the difference between the interface temperature and the initial temperatures of the skin and material, penetrate into the skin and material and change the temperatures of both the skin and material with time. The heat flux conducted out of the skin during contact is time dependent in this process and can be calculated from Equation (3-3):

$$q''_{skin}=\frac{k_{skin}(T_s-T_{skin,i})}{(\pi\alpha_{skin}t)^{1/2}} \tag{3-3}$$

where q''_{skin} is the heat flux conducted out of the skin during contact, k_{skin} is the thermal conductivity of the skin, and t is time. Because the heat flux conducted out of the skin depends on the interface temperature, T_s, the decrease in skin temperature during contact, ΔT ($T_{skin,i} - T_s$), can be used as an index of how cold subjects would feel a material is when making contact. When a person makes contact with an object, the contact coefficients of the skin and material determine the interface temperature and the heat flux conducted out of the skin. The change in temperature within the skin is encoded by thermoreceptors in the dermis (x ~ 0.16 mm for cold receptors, Hensel, 1981) and is transmitted to the central nervous system to assist in object identification.

The Fourier number of the material can be used to determine whether the time is short enough for the semi-infinite body model to be valid. The definition of the Fourier number, Fo, is:

$$Fo=\frac{\alpha t}{L_c^2} \tag{3-4}$$

where α is the thermal diffusivity of the material, L_c is the characteristic length, which is defined as the material volume divided by the contact area, and t is time. Generally speaking, the semi-infinite body model is valid under the condition that the Fourier number of the material in the process is less than 0.05 (Mills, 1999). For materials whose Fourier numbers are larger than 0.05, the semi-infinite body model can still serve as a reasonable description of the transient thermal process.

3.2 MATERIAL DISCRIMINATION

Jones and Berris (2003) found that subjects were able to discriminate between materials presented to the right and left index fingers using only thermal cues when the thermal properties of the materials were considerably different. The goal of this experiment was to further quantify the difference in thermal properties that is required for subjects to discriminate reliably between materials.

3.2.1 Method

Subjects. Ten normal healthy adults (five women and five men) aged between 20 and 35 years, participated in this experiment. They included undergraduate and graduate students and research staff in the Department of Mechanical Engineering at MIT. They had no known abnormalities of the tactile or thermal sensory systems and no history of peripheral vascular disease. They all reported that they were right-handed. This research was approved by the local ethics committee.

Apparatus. Six materials that covered a broad range of thermal properties were selected. They were: copper, bronze, stainless steel, glass reinforced epoxy (G10), plastic (ABS), and foam. Their thermal properties are listed in Table 3-1. Based on the semi-infinite body model, the corresponding skin temperature upon contact with the materials is shown in Table 3-1 and Figure 3-2 (A), and the corresponding heat flux conducted out of the skin with contact is shown in Figure 3-2 (B)

Table 3-1. Thermal properties of the materials.

Material	Copper	Bronze	Stainless Steel	G10	ABS	Foam
Conductivity k (W/mK)	398	54	13.5	0.29	0.18	0.029
Density ρ (kg/m^3)	8954	8780	8000	1800	1010	24
Specific heat c (J/kgK)	384	355	460	1600	1386	1210
Contact coefficient $(k\rho c)^{1/2}$ ($J/m^2s^{1/2}K$)	36992	12973	7048	910	501	29
Skin temperature upon contact T_s (°C)[1]	24.3	24.7	25.3	29.0	30.3	32.8
Fourier number Fo[2]	3.58	0.54	0.11	0.003	0.004	0.03

[1.] Based on semi-infinite body model with initial skin temperature at 33 °C and initial material temperature at 24 °C
[2.] Based on 5 s contact time and sample dimensions

The materials were stored at room temperature which was maintained at 24 °C. Each sample was 12.4 mm in diameter and 100 mm long, and had a flat upper surface which was 12 mm by 60 mm. They were turned from 12.7 mm (½ inch) rod stock, milled and then sanded to provide a flat, smooth contact surface. Their surface roughness was measured with a Mitutoyo Surface Roughness Tester (Model SV-3000S4). The surface roughness was measured to ensure that textural differences among the material samples were minimized. These values and the Young's modulus (the tensile elastic modulus) of the materials are listed in Table 3-2.

Two pieces of delrin were used to make a material presentation fixture as shown in Figure 3-3. The combined size of these pieces when screwed together was 103 x 63 x 46 mm^3. Two 22 x 20 mm^2 rectangular holes were machined into the upper piece to allow insertion of the fingers. In the lower piece of delrin, two 12.5 mm diameter compartments were machined 43 mm apart directly under the holes. The material samples slid into these slots and were flush with the surrounding surface. An extended roof was added on top of the fixture to prevent subjects from seeing the material samples.

(A)

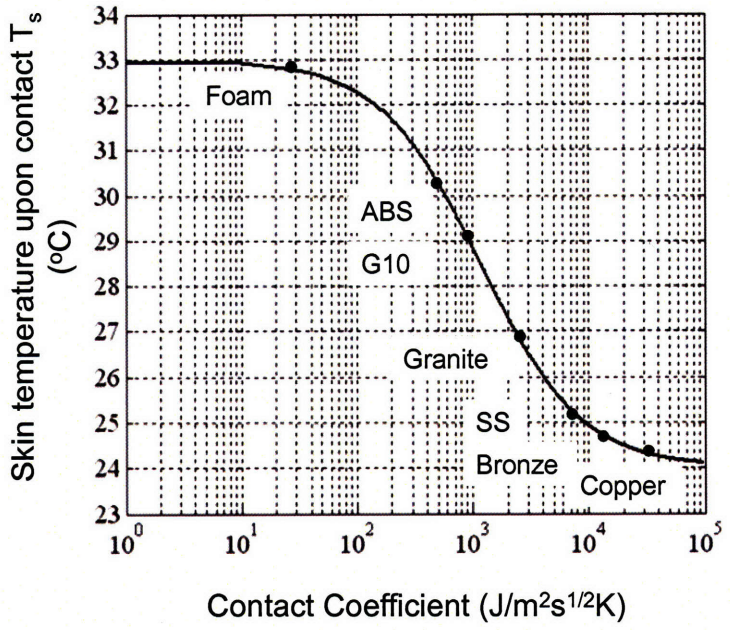

(B)

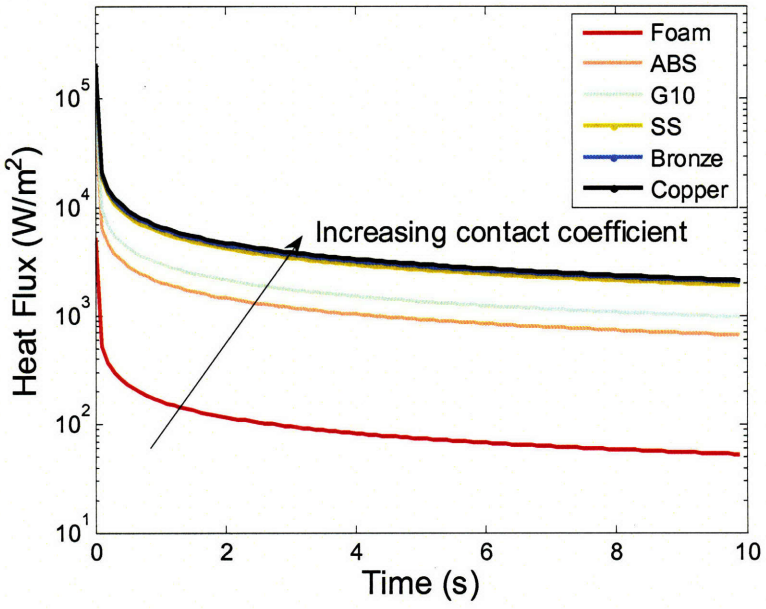

Figure 3-2. Skin thermal responses based on model predictions. (A) Skin temperatures and (B) corresponding heat fluxes conducted out of the skin during contact with the identified materials. Granite was used in the material localization experiment.

Table 3-2. Surface roughness and Young's modulus of the material samples

Material[1]	Mean Rq[2] (μm)	Young's Modulus (GPa)
Copper	0.40	110.0
Bronze	0.32	93.0
SS	0.43	193.0
ABS	0.20	2.3
G10	1.50	17.0
Granite	1.47	53
Foam	15.22	1.50E-03

[1] Copper, bronze, stainless steel (SS), G10, ABS, and foam were used in the first experiment. Copper, stainless steel, ABS, granite, and foam were used in the second experiment.
[2] Rq: Root-mean-square surface roughness.

A thermistor (457 μm in diameter and 3.18 mm in length; Model 56A1002-C8, Alpha Technics) measured the skin temperature of the index finger. The thermistors were connected to a Data Acquisition Unit (Model 34970A, Agilent Technologies) which was controlled using a Visual Basic program. Temperature data were sampled at 20 Hz. To ensure that the skin temperature of the hand was maintained constant, a fixture was made using a recirculating chiller (Model 1167P, VWR International). The chiller was connected to a spiral folded tube (ID 4.8mm, OD 7.9 mm) that was placed in a delrin fixture. A 2 mm thick copper plate was placed on the tube to improve the temperature uniformity of the surface. A 3.2 mm thick rubber pad was then added on top of the copper plate to increase comfort for subjects when they placed their hands on the fixture to maintain skin temperature.

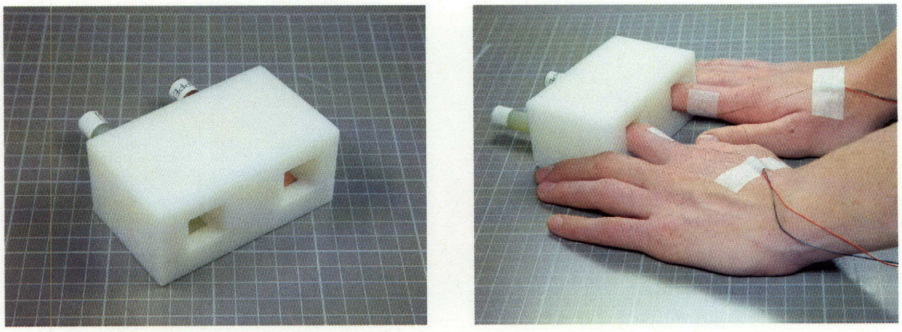

Figure 3-3. Material discrimination fixture. The thermistors are glued to the index fingers.

Procedure. Subjects washed their hands with soap prior to participating in the experiment. A thermistor was glued to the fingerpads of each index finger using biocompatible cyanoacrylate (Liquid Bandage™, Johnson & Johnson). The thermistor was 457 μm in diameter and 3.18 mm in length, and was chosen on the basis of its small dimensions and thermal mass. To ensure that skin temperature measurements were not influenced by contact force directly, baking soda was used to mark the contact area of the skin with the material and the thermistor was glued on the edge of the contact area as shown in Figure 3-4. Subjects' initial skin temperatures ranged from 30 to 35.5 °C and the average value was 33 °C. The ambient temperature in the room was maintained at 24°C, as measured with a k-type thermocouple (Omega) in free air.

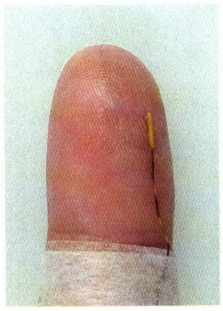

Figure 3-4. Thermistor position on the fingerpad.

Each of the six materials was paired with all other materials including itself, which gave a total of 21 different combinations. These 21 combinations were repeated four times for a total of 84 trials. Within each block of 21 trials the order of presentation of the materials was randomized. There was at least a 1-minute break between each block of trials, during which the subjects placed their hands on the recirculating chiller.

Prior to each trial, subjects were instructed to place both of their hands on the recirculating chiller to maintain their skin temperature at 33 °C. For the first part of the experiment, two material samples were inserted into the two separate compartments as shown in Figure 3-3. Subjects inserted their left and right index fingers into the compartments after hearing a sound cue. The data acquisition system recorded temperature from the thermistors attached to the subjects' fingerpads after the sound cue.

At the end of each trial, subjects withdrew their hands from the fixture and placed them on the recirculating chiller pad. A maximum of 10 s was allowed for each trial.

A two-alternative forced choice (2AFC) method was used in which subjects were instructed to choose the colder of the two materials presented by reporting which hand made contact with the colder material. Subjects were not told which materials were used and no feedback was given regarding the correctness of their judgments. They were encouraged to lift and replace their fingers on the material samples during each trial, but were discouraged from lateral scanning of the sample surface.

Subjects lifted and replaced their fingers on the material repeatedly during each trial, which meant that the temperature responses fluctuated and so it was difficult to record meaningful temperature data. The measurement of the decrease in skin temperature on contact was therefore undertaken separately. The procedure in this second part of the experiment was similar to that in the first, except that subjects were instructed to leave their index fingers on the sample surface for 5 seconds after inserting their left and right index fingers into the compartments. The goal of this part of the experiment was to measure the change in skin temperature upon contact.

3.2.2 Results

In this experiment, the responses for the trials involving different materials were analyzed in terms of the number of correct responses, that is, correctly identifying the "colder" of the two materials as defined in terms of the predicted thermal responses at the skin surface-material interface. The chance level in this experiment was 50%, and a threshold level of 72% correct was chosen as indicating that subjects could reliably discriminate between a pair of materials. An initial analysis of the results from trials in which the same material was presented to both hands indicated that there was a bias towards reporting that the material on the right index finger was colder ($t=2.08$, $p=0.04$). This did not reflect any temperature difference between the hands as they were both maintained at 33 °C.

Table 3-3. Percentages of correct discriminations for different pairs of materials. SS is stainless steel, G10 is glass-reinforced epoxy and ABS is a plastic.

	Copper	Bronze	SS	G10	ABS	Foam
Copper		70	75	95	98	100
Bronze			68	98	98	100
SS				98	100	95
G10					78	90
ABS						85
Foam						

The percentage of correct discriminations for the various combinations of materials is shown in Table 3-3. For all combinations except copper-bronze and bronze-stainless steel the percentages were above 72%. This means that subjects were able to discriminate reliably between two materials when the ratio of the contact coefficients of the materials exceeded three. For combinations involving foam, the percentage of correct discriminations ranged from 85-100%. This high performance presumably reflects the distinct thermal and textural properties of foam, in particular its much greater surface roughness when compared to the other materials, as shown in Table 3-2. Analyses of covariance (ANCOVA) were conducted to determine whether the surface roughness and elasticity of the materials (the latter defined in terms of Young's modulus which is the ratio of the stress to strain) influenced subjects' performance. The covariates were the ratio of the surface roughness of the two materials being compared or the ratio of their Young's moduli. The analyses indicated that there was no significant effect of the ratio of the materials' surface roughness ($p=0.53$) or Young's modulus ($p=0.20$) on the percentage of correct responses.

In the second part of the experiment, the change in temperature upon contact was recorded for each of the materials presented. These data are shown in Figure 3-5 where it can be seen that the decrease in skin temperature was small, ranging from a mean of 0.25 for foam to 1.44 °C for bronze. A one-way ANOVA indicated that there was no significant difference in the decrease in skin temperature across the six materials

presented (F(5, 48)=1.927; p=0.11). With the exception of foam, the decreases in skin temperature as the finger made contact with the six materials were considerably smaller than the theoretical values listed in Table 3-1, which were calculated using an initial skin temperature of 33 °C and an initial material temperature of 24 °C.

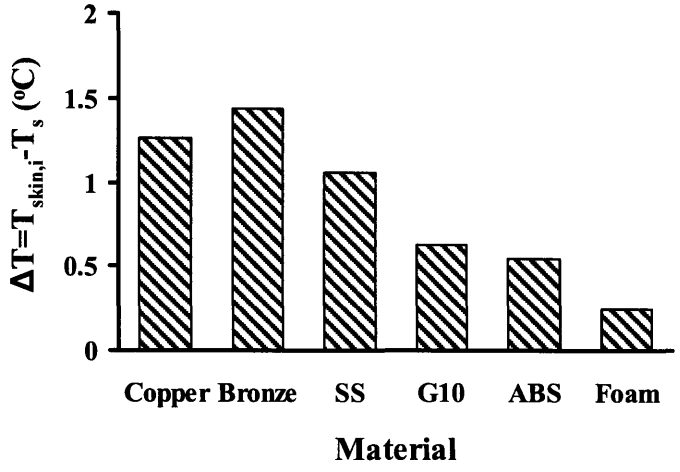

Figure 3-5. Group mean decrease in skin temperature after 5 s of contact with the six materials. SS, stainless steel; G10, glass reinforced epoxy; ABS, a plastic.

3.2.3 Discussion

In this material discrimination task, subjects perceived thermal cues by lifting and replacing their fingers on the surfaces, and the local thermal transients associated with contact were presumably used to discriminate between the materials. The results from this experiment indicate that when textural cues are minimized, thermal cues can be used to discriminate between materials when the differences in the contact coefficients are relatively large. The only two combinations that could not be reliably discriminated were copper and bronze, and bronze and stainless steel. The thermal cues used to discriminate between these materials, such as the heat fluxes conducted out of skin, were so similar that they did not facilitate discrimination. These results are consistent with the semi-infinite body model illustrated in Figures 3-2 (A) and 2 (B), which show the similarity in the predicted heat fluxes for copper and bronze, and bronze and stainless steel.

Although the thermal cues associated with contact were presumably used to discriminate between the materials, differences in surface texture and elasticity could have influenced subjects' performance. However, the analyses indicated that the percentage of correct responses was not significantly affected by the ratio of the surface roughness or the Young's moduli of the materials being compared. The ease with which foam was discriminated when presented with any of the other materials is probably due to its distinctive thermal characteristics, surface roughness and elasticity. Of all the materials presented, foam changed the skin temperature the least. The average decrease in skin temperature when making contact with foam was 0.25 °C, which is above the threshold of 0.14 °C for discriminating decreases in skin temperature on the fingertip (Stevens & Choo, 1998). Although the surface roughness and compliance of foam may have provided additional cues to assist in material discrimination, the percentages of correct discriminations for the combinations including foam decreased progressively from copper to ABS. This suggests that even with the extra tactile cues, the ability to discriminate foam from the other materials was influenced by their thermal properties.

The elastic moduli (i.e., Young's modulus) of the materials varied considerably, with foam being the most elastic. The typical contact force during this type of thermal discrimination experiment would have been between 1.5-2 N (Jones & Berris, 2003) and the average contact area was 135 mm^2. Based on these force and contact area estimates and the Young's modulus for each material, the strain of the materials (i.e., the change in length of the material normalized by the initial length) was calculated. The estimated strain for foam is 0.01 and for the other materials it ranged between 10^{-6}-10^{-7}. From these values, it would seem reasonable to assume that, with the exception of foam, no deformation occurred during contact with these materials.

The present findings are consistent with those of Dyck et al. (1974) who designed a set of thermal stimulators known as the "Minnesota Thermal Disks." These disks are made from copper, stainless steel, glass and polyvinyl chloride (PVC), and were developed as a clinical tool to measure thermal sensation. Dyck et al. (1974) found that the pairs of disks that normal healthy subjects reliably distinguished on the palm of the

hand as "cold" and "warm" were copper and PVC, and copper and glass. The contact coefficients of copper, PVC, and glass are 36992, 406, and 1510 $J/m^2s^{1/2}K$ respectively. The contact coefficient ratios of the pairs that Dyck et al. (1974) reported were distinguished are both greater than three, consistent with the present findings.

The decreases in skin temperature upon contact with the materials (shown in Figure 3-5) were considerably smaller than the theoretical values predicted from the semi-infinite body model (Table 3-1). The difference between these two sets of values results from the fact that skin is not a 'semi-infinite' inanimate object as assumed in the semi-infinite body model, but has an internal source of heat generation. Moreover, the thermal properties of skin make it a good thermal insulator ($\alpha=10^{-7}$ m^2/s), which means that changes in temperature can be localized to a small region of skin (Eberhart, 1985). Because of the localized nature of the change in skin temperature, the thermistor attached to the edge of the contact area may not have detected the full extent of the temperature change. The absence of any significant difference in the decrease in skin temperature after contact with the various materials also reflects the variability between subjects in the measured thermal changes. Factors such as the volume and width of the finger pad, the contact area and contact force can all affect the thermal response of the finger (Jones & Berris, 2003).

The semi-infinite body model was used to predict the interaction between the skin and the materials, and the Fourier numbers of the materials in contact with the skin for 5 seconds were calculated (see Table 3-1). The Fourier numbers for G10, ABS, and foam confirmed that the semi-infinite body model was valid for them, but copper, bronze, and stainless steel all had Fourier numbers well above 0.05. Thus the semi-infinite body model can only give an approximate description of the skin-material interaction for these materials.

Although the measured decreases in temperature upon contact with the materials in this experiment were small, ranging from 0.25 to 1.44 °C, they were presumably perceived by subjects. Psychophysical studies of thermal thresholds indicate that at a skin

temperature of 33 °C, the threshold for detecting a decrease in temperature is 0.14 °C on the tip of the index finger and 0.07 °C on the thenar eminence (Stevens & Choo, 1998). These threshold values are smaller than the thermal changes measured as the index finger made contact with the materials. The time course and amplitude of the thermal responses are, however, markedly different from those reported by Ino et al. (1993) who, for a single subject, showed an immediate decline in skin temperature upon contact with all materials. The decreases in skin temperature that they reported ranged from 0.1 °C for wood to 7 °C for aluminum, and occurred within 1 s and then stabilized within 500 ms, which is an extremely rapid and dramatic response for the peripheral thermal system. Caldwell and Gosney (1993) reported that it took 3-5 s to obtain a successful thermal reading from the hand as it made contact with a range of materials, and in the present study the change in skin temperature did not stabilize for 5 s. These latter data are consistent with the long reaction and decision times reported for thermal stimuli (Lederman & Klatzky, 1997; Stevens, 1991).

3.3 MATERIAL LOCALIZATION

This experiment was conducted to examine how accurately subjects can localize a thermal stimulus in the presence of other thermal stimuli on the same hand, and to determine if this changes as a function of the location of the target stimulus and the thermal properties of the stimuli. The thermal perceptual system has been shown to have poor spatial localization but good spatial summation for both warm (Hardy & Oppel, 1937; Marks & Stevens, 1973; Marks et al., 1976) and cold (Hardy & Oppel, 1938; Stevens & Marks, 1979) stimuli, which means that identifying where a specific thermal change occurs is difficult. The localization of a thermal change can be facilitated by the tactile input associated with contact and for warm stimuli improves with increasing intensity of stimulation (Simmel & Shapiro, 1969). However, the interaction of thermal and tactile inputs can lead to mislocalization of thermal sensations when adjacent parts of the skin are differentially stimulated. These interactions between thermal and tactile inputs and spatial localization of thermal changes were the subject of the second

experiment. Of particular, interest was whether subjects could localize a thermal event based on relatively small changes in the skin temperature of the fingers as they made contact with different materials, and if this depended on which finger was stimulated.

In the present experiment, a range of materials with different thermal properties was used to induce thermal responses and subjects were required to indicate which of the three materials felt different from the other two. The materials were presented to the index, middle and ring fingers of the right hand and the position of the target material varied from trial to trial. It was predicted that subjects would have more difficulty in discriminating the target material in the presence of the other two stimuli (i.e., distractor material) as compared to the first experiment in which only two stimuli were presented on each trial, and that the differences in the thermal properties of the materials would need to be significantly larger for accurate localization.

3.3.1 Method

Subjects. Ten normal healthy adults (five women and five men), aged between 20 and 29 years, participated in this experiment. Two of them participated in the first experiment. The time between the two experiments was over 6 months. The subjects had no known abnormalities of the tactile or thermal sensory systems and no history of peripheral vascular disease. They all reported that they were right-handed. This research was approved by the local ethics committee.

Apparatus. Five materials were selected for this experiment. They were copper, stainless steel, granite, plastic (ABS), and foam. In order to have a set of materials that spanned the full range of thermal properties (see Figure 3-2 (A)), G10 was replaced by granite and bronze was no longer used. The thermal properties are listed in Table 3-4. The material samples were stored at room temperature, which was maintained at 24 °C. Each sample was 19.05 mm wide, 145 mm long and 38 mm thick. These sample dimensions were chosen to make the Fourier numbers of all the materials smaller than 0.05 in order to meet the assumption of the semi-infinite body model. The surfaces of the samples were

milled and then sanded to provide a flat, smooth contact surface. The surface roughness of each material was measured to ensure that differences in surface texture among the material samples were minimized; these data are listed in Table 3-2.

Table 3-4. Thermal Properties of the Materials

Material	Copper	Stainless Steel	Granite	ABS	Foam
Conductivity k (W/mK)	398	13.5	2.79	0.18	0.029
Density ρ (kg/m^3)	8954	8000	2630	1010	24
Specific heat c (J/kgK)	384	460	775	1386	1210
Contact coefficient $(k\rho c)^{1/2}$ ($J/m^2s^{1/2}K$)	36992	7048	2384	501	29
Skin temperature upon contact T_s (°C)[1]	24.3	25.3	27.0	30.3	32.8
Fourier number Fo[2]	0.05	0.0016	<0.001	<0.001	<0.001

[1] Based on semi-infinite body model with initial skin temperature at 33 °C and initial material temperature at 24 °C
[2] Based on 10 s contact time and the sample dimension

Two pieces of delrin were used to make a material localization fixture as shown in Figure 3-6. The combined size of these pieces when screwed together was 100 x 100 x 90 mm^3. One 84 mm x 45 mm rectangular pocket was machined into the upper piece to allow insertion of the index, middle and ring fingers. Three 19.8 x 95 x 34 mm^3 rectangular slots were machined into the lower piece. The material samples slid into these slots and their surfaces were 4 mm above the surrounding surface. When inserting their fingers into the fixture, the subjects' three fingers were able to make contact with the three samples. An extended roof and an acrylic housing were added around the fixture to prevent subjects from seeing the material samples. To ensure that the skin temperature of the hand remained constant, the fixture with the recirculating chiller described in the previous experiment was also used in this experiment.

(A) (B)

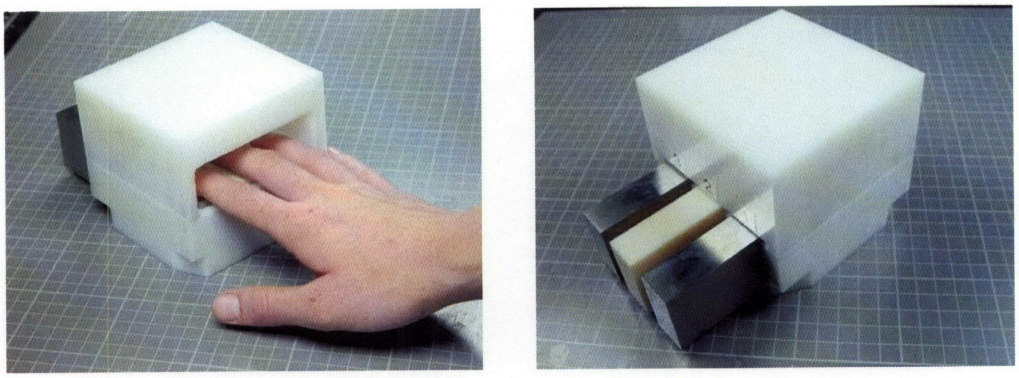

Figure 3-6. Front view (A) and rear view (B) of the material presentation fixture used in material localization experiment.

Procedure. Subjects washed their hands with soap prior to participating in the experiment. Subjects' initial skin temperatures ranged from 27 °C to 36 °C and the average value was 33.4 °C. The ambient temperature in the room was maintained at 24 °C, as measured with a k-type thermocouple (Omega) in free air.

Each of the five materials was paired with all other materials to give a total of 20 target-distractor combinations. There were three target positions, index, middle and ring finger, which gives 60 different combinations. These 60 combinations were then repeated three times for a total of 180 trials. Within each block of 60 trials, the order of presentation of the materials was randomized. There was at least one 60-s break between each block of trials, during which subjects placed their hands on the recirculating chiller. The experiment lasted about 90 minutes.

Prior to each trial, subjects were instructed to place their right hands on the recirculating chiller to maintain their skin temperature at 33 °C. Three material samples were inserted into the three rectangular slots as shown in Figure 3-6. Subjects inserted their index, middle and ring fingers into the fixture after hearing a sound cue. A three-alternative forced-choice (3AFC) method was used in which subjects were instructed to choose which finger felt different from the other two in terms of thermal changes on the fingerpad. They were asked to report the number of the corresponding finger: 1 for index

finger, 2 for middle finger and 3 for ring finger. Subjects were not told which materials were used and no feedback was given regarding the correctness of their judgments. They were encouraged to lift and replace their fingers on the material samples, but were discouraged from lateral scanning of the sample surface. The maximum time for each trial was 10 s. After 10 s, the experimenter asked the subjects to remove their hands from the fixture and place them back on the recirculating chiller.

3.3.2 Results

In this experiment the responses for the trials were analyzed in terms of the number of correct responses, that is, correctly identifying the location of the target in the presence of two identical distractors. The chance level in this experiment was 33%. A test of proportion indicated that at a 54% level of correct performance, subjects can discriminate the target from the distractors reliably ($p<0.0001$). The percentages of correct responses were converted into the corresponding d'values for a three-alternative forced-choice method (Gescheider, 1997). The percentage of trials in which the target location was correctly identified and the corresponding sensitivity, d', are shown in Table 3-5. A comparison of the results shown in Tables 3-3 and 3-5 indicates that the second experiment was considerably harder for subjects than the first, with the overall correct response rate averaging 57%, as compared to 90% in the first experiment. Performance was much poorer even for materials that were perfectly discriminated in the first experiment (e.g., copper and foam, and stainless steel and ABS).

In this experiment the material presentation mode was divided into high/low and low/high, where high/low describes those trials in which the contact coefficient of the target material was higher than that of the distractor, and low/high mode refers to those trials in which the contact coefficient of the target material was lower than that of the distractor. In the first condition, the target would feel colder than the two distractors, whereas in the latter condition, the distractors would feel colder than the target.

Table 3-5. Percentage of correct responses, p(c), and the corresponding average sensitivity, d', for the various combinations of materials regardless of target position.

Material combination	Contact coefficient ratio	High / Low[1]		Low / High[2]		Total[3]	
		p(c)	d'	p(c)	d'	p(c)	d'
Stainless steel / Granite	2.96	30	-0.12	43	0.33	37	0.13
Granite / ABS	4.76	53	0.65	44	0.36	49	0.52
Copper / Stainless steel	5.25	38	0.16	39	0.20	38	0.16
Stainless steel / ABS	14.07	72	1.31	59	0.85	66	1.09
Copper / Granite	15.52	56	0.75	44	0.36	50	0.56
ABS / Foam	17.28	68	1.16	46	0.43	57	0.78
Copper / ABS	73.83	69	1.20	51	0.59	60	0.89
Granite / Foam	82.21	68	1.16	61	0.92	64	1.02
Stainless steel / Foam	243.03	79	1.61	62	0.95	71	1.28
Copper / Foam	1275.59	82	1.75	66	1.09	74	1.39

[1.] High/low refers to those trials in which the first material listed in column one was the target and the other material was the distractor.
[2.] Low/high refers to those trials in which the first item listed was the distractor and the second material was the target.
[3.] Total refers to the percentage of correct responses for the combinations listed in the first column.

The results in Table 3-5 indicate that when the target had a higher contact coefficient than the distractor, subjects were able to identify the target's location reliably when the ratio of the contact coefficients of the target and distractor was higher than 14. For the low/high mode, three out of the four combinations that were reliably discriminated included foam as the target material, and the contact coefficient ratios for these combinations were all higher than 82. These results indicate that it is considerably easier to identify which finger is cooling the most, than to select the finger that has the smallest change in skin temperature.

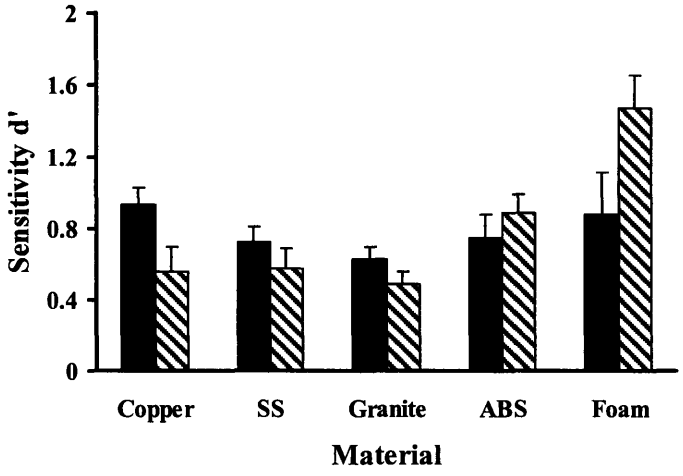

Figure 3-7. Group mean sensitivity (d') in identifying the location of the target as a function of whether a material was a target or distractor. Trials in which the material was a target are shown in black and those in which the material was the distractor are striped. The error bars show the standard error of the mean (SEM).

The group mean sensitivity, d', in identifying the location of the target as a function of whether the material was a target or distractor is shown in Figure 3-7. As can be seen in the figure, subjects performed better when presented with targets with extreme thermal properties (high or low contact coefficients) than those with median thermal properties. A repeated measures analysis of variance (ANOVA) of these values with materials and presentation mode (target or distractor) as factors indicated that there was a significant difference among the materials ($F(4,9)=11.92$; $p<0.001$) but no significant effect of presentation mode ($F(1,9)=1.90$; $p=0.20$). There was a significant interaction between materials and presentation mode ($F(4,36)=4.04$; $p = 0.008$). The latter reflects the finding that distractors with low contact coefficients, such as foam and ABS, interfered less with identifying the target location than distractors with high contact coefficients, such as copper and stainless steel.

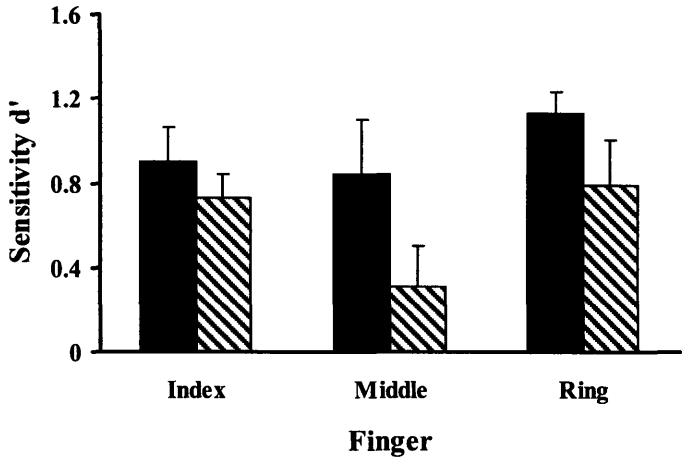

Figure 3-8. Group mean sensitivity (d') in identifying the location of the target material for each finger. The means are calculated across the five materials presented and are shown as a function of whether the target presented to the finger was in high/low (black) or low/high (striped) combination. The error bars represent the SEM.

It was of interest to determine whether performance was affected by the location of the target material, that is whether it was presented to the index, middle or ring finger. The group mean sensitivity, d', for each finger as a function of whether the target had a higher (high/low) or lower (low/high) contact coefficient than the distractor is shown in Figure 3-8. As can be seen in the figure, d' was lowest when the target was presented to the middle finger, especially when the target had a lower contact coefficient than the distractor. A repeated measures analysis of variance (ANOVA) of these values with presentation mode (high/low and low/high) and fingers as factors indicated that there was no significant effect of presentation mode ($F(1,9)=3.90$; $p=0.08$) and no significant difference among the three fingers ($F(2,9)=2.141$; $p=0.15$). There was also no significant interaction between fingers and presentation mode ($p=0.50$). These findings presumably reflect the high inter-individual variability in this task.

3.3.3 Discussion

In this experiment, subjects were required to identify which of three fingers was in contact with a material that was different from that in contact with the other two fingers.

As in the first experiment, textural cues from the surface of the various materials were minimized so that subjects would focus on the thermal responses on the fingertips when determining which material was the target. A comparison of the performance of subjects in the two experiments indicates that the second task was considerably more difficult than the first. For the same materials (i.e., copper, SS, ABS and foam), the decline in performance when three, rather than two, fingers were involved is 26%. This is not surprising as in the second experiment subjects had to compare the thermal responses of three fingers rather than two, and the stimuli were presented to the fingers of one hand, rather than to each hand separately. This result indicates that the effects of spatial summation across fingers within the hand have significantly reduced the ability of subjects to discriminate between the thermal responses and hence localize a target material.

The thermal properties of the materials were characterized by their contact coefficients and performance was then evaluated in terms of the ratio of the contact coefficients of the target and distractor materials. The ratio of the contact coefficients that is required to localize reliably a target in the high/low presentation mode is 14, whereas it is 82 for the low/high mode. These findings show that it is easier to identify which finger is in contact with a target material when that finger is cooled more than the other fingers, than when the two fingers are cooling more than the finger in contact with the target material. Although the change in skin temperature was not measured in this experiment, the results from the first experiment (see Figure 3-5) give some indication of the thermal responses of the fingers to contact with the various materials presented.

It is known that the perceived magnitude of cold sensation depends on the degree of cooling of the skin and on the areal extent of stimulation (Stevens & Marks, 1979). Studies on the hand, forearm, back and cheek have shown that there is pervasive spatial summation for cold, with the perceived magnitude of cold sensation depending almost as much on the size of the area of skin cooled as on the degree of skin cooling (Greenspan & Kenshalo, 1985; Stevens & Marks, 1979). In the Stevens and Marks (1979) experiment, the area of stimulation on the forearm was varied from 200 to 1900 mm^2, and the

decrease in skin temperature ranged from 2 to 12 °C, whereas Greenspan and Kenshalo (1985) applied thermal stimuli ranging from 0.1 to 1 °C to the thenar eminence of the hand and the area of stimulation varied from 50 to 700 mm^2. In the present experiment, the decreases in skin temperature were similar to the latter study, probably between 0.1 and 2 °C, and the total area of contact on the finger pads was around 400 mm^2. It is likely that spatial summation, and hence poor localization of thermal changes on the fingers, contributed to the inferior performance in this experiment as compared to the material discrimination experiment.

The position of the target material was varied across trials in the present experiment and it was predicted that target location would influence performance. This hypothesis was based on the findings of Green (1977) described earlier, in which temperature changes occurring at two adjacent fingers influenced the perceived magnitude of thermal sensation at the middle finger. In a further study of this phenomenon of "thermal referral," Green (1978) found that referral of cold sensation was greatest between the middle and ring finger, as compared to the index and middle and ring and little fingers, and for the latter fingers it was generally quite small (Green, 1978). In the context of the present experiment, the middle finger did perform more poorly than the other two fingers, although the differences between the fingers were not significant, due to the considerable variability between subjects.

3.4 CONCLUSION

In summary, the results from these two experiments indicate that subjects can discriminate between materials using thermal cues when the differences in the thermal properties of the materials are large. The ratio of the contact coefficients of the materials required for subjects to discriminate reliably between materials is substantially lower than the ratio necessary for subjects to identify a target material in the presence of two identical distractor materials. On the latter task, subjects found it easier to identify which finger was in contact with the target material when that finger was cooled more than the

other two fingers, than when the distractors resulted in a greater thermal change on the fingertips. These findings suggest, consistent with earlier results (e.g., Green, 1977, 1978), that spatial summation across the fingers impairs the localization of cooling responses.

The decrease in skin temperature when making contact with the materials was much smaller than the predictions calculated from the semi-infinite body model. This presumably reflects both the thermal properties of the skin, namely that it is a good insulator, and the vascular system in the finger that is a source of heat. The changes in skin temperature appeared to be localized to the area of contact and a more accurate measurement of the temperature changes in the finger would require a thermal imaging system.

CHAPTER 4

THERMAL DISPLAY DEVELOPMENT AND EVALUATION

In the process of developing a thermal model, it is important to evaluate an established thermal model in order to make sure that this model is able to provide reasonable predictions of the changes in temperature during hand-object interactions. Two approaches are commonly used to evaluate the validity of a thermal model. First, the thermal interaction between the skin and an object elicits a change in skin temperature and the ability of the model to provide reasonable predictions of this change in skin temperature is evaluated physiologically. This approach typically compares the theoretical predictions to the measured thermal responses of the skin during contact (Benali-Khoudja et al., 2003; Citerin et al., 2006; Ho & Jones, 2006a). A second aspect of the contact process is the responses of thermoreceptors in the dermis that sense the change in skin temperature and transmit this information to the central nervous system, which results in the perception of temperature. The accuracy of the model in generating appropriate perceptual responses is evaluated psychophysically. In this approach, a subject's performance in material identification and discrimination with real materials and simulated materials generated based on the thermal model are compared (Kron & Schmidt, 2003; Deml et al., 2006; Ho & Jones, 2004, in press; Ino et al., 1993).

In this study, a thermal display was constructed to generate various simulated materials based on the semi-infinite body model described in Section 3.1. Two psychophysical and one physiological experiments were conducted to evaluate the performance of the model. The first experiment compared the ability of subjects' to identify various materials which were presented physically or simulated with the thermal display. The second experiment examined the capacity of subjects to discriminate between a real and simulated material based on thermal cues. In the third experiment the changes in skin temperature that occurred when making contact with real and simulated materials were measured to evaluate how these compared to theoretical predictions.

4.1 THERMAL DISPLAY DESIGN

A thermal display based on the semi-infinite body model described in Section 3.1 was designed and built for simulating the thermal cues associated with making contact with different materials. A Peltier device was selected for use in the display as it was able to apply localized heating or cooling stimuli to the skin. Peltier devices are the most widely used thermal simulator for thermal displays, and pump heat based on the Peltier effect. The Peltier effect refers to the creation of a temperature difference at the junctions of two dissimilar conductors in contact when a DC current passes through the circuit. Depending on the direction of the current, unidirectional heat flows between the substrates and generates temperature differences between the substrates. This temperature difference and the rate of temperature change are controlled by varying the amplitude of the current passing through the device.

The major elements of the thermal display were the Peltier device, thermistors, and a digital PI temperature controller, which was integrated into the system to control the surface temperature of the Peltier device. The temperature control flow chart is shown in Figure 4-1. This thermal display simulated materials by maintaining the surface temperature of the Peltier device at the interface temperature, T_s, and presenting it to the fingerpad during contact. The interface temperature can be calculated based on Equation

3-1 with the initial skin and material temperatures set at 34 °C and 23.5 °C respectively. The interface temperature, T_s, is then a function of only the simulated material's contact coefficient.

As shown in Figure 3-1, the heat transfer process within the fingerpad when making contact with a material depends on the interface temperature, T_s, only. Therefore, by replacing the material with a thermal display that is able to maintain the same interface temperature, the heat flux conducted out of the skin will be the same as that which occurs when the fingerpad makes contact with the real material. The heat flux will cause a change in skin temperature that is encoded by thermoreceptors in the dermis. In this simulation method, the Peltier device only serves as a constant temperature source which maintains the interface temperature at T_s during contact. Its own thermal properties do not influence the heat transfer within the skin.

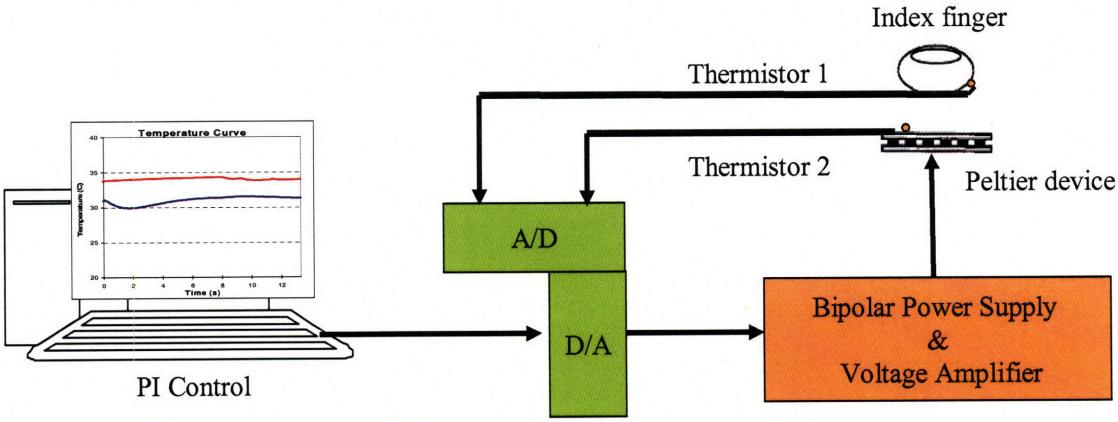

Figure 4-1. Schematic representation of the thermal display.

4.2. REAL AND SIMULATED MATERIAL IDENTIFICATION

In this experiment, the accuracy of the model in generating appropriate perceptual responses is evaluated by comparing subject's performance in material identification with real materials and simulated thermal cues based on the model.

4.2.1 Method

Subjects. Ten normal healthy adults (five women and five men) aged between 22 and 35 years participated in this experiment. They had no known abnormalities of the tactile or thermal sensory systems and no history of peripheral vascular disease. They all reported that they were right-handed. This research was approved by the local ethics committee.

Apparatus. Five materials that covered a broad range of thermal properties were selected. They were: copper, stainless steel, granite, acrylonitrile butadiene styrene (ABS, thermoplastic), and foam. Their properties are listed in Table 4-1. The surface roughness and asperity slopes of the materials were measured using a Mitutoyo Surface Roughness Tester (Model SV-3000S4). The material samples were stored at room temperature, 24 ^{o}C. Each sample was 12.4 mm in diameter and 100 mm long, and had a flat upper surface which was 12 mm x 60 mm.

Two pieces of delrin were used to make the material presentation fixture. A 20 x 20 mm rectangular hole was machined into the upper piece to allow for insertion of the right index finger. In the lower piece, a slot with a diameter of 12.5 mm was machined directly under the hole. The material samples slid into the slot and were flush with the surrounding surface as shown in Figure 4-2 (A).

The upper part of the simulated material presentation fixture was the same as that in the real material presentation fixture as illustrated in Figure 4-2(B). In the lower part of the fixture, a Peltier device (DT 6-6, Marlow) was placed in a rectangular slot, which was made of acrylic plastic. A thin acrylic sheet (0.8 mm) with a 12 mm x 20 mm rectangular

hole was placed on the Peltier device in order to control the contact area. Acrylic has similar thermal properties to delrin. This simulated material presentation fixture was placed on top of the copper plate of a recirculating chiller to maintain the hot side temperature of the Peltier device.

Table 4-1. Properties of the materials.

Material	Copper	Stainless Steel	Granite	ABS	Foam
Density ρ (kg/m^3)	398	13.5	2.79	0.18	0.029
Specific heat c (J/kgK)	8954	8000	2630	1010	24
Contact coefficient $(k\rho c)^{1/2}$ ($J/m^2s^{1/2}K$)	384	460	775	1386	1210
Skin temperature upon contact T_s (°C)[1]	36992	7048	2384	501	29
Surface roughness Rq[1] (μm)	0.31	0.19	0.46	0.45	8.03
Asperity slope (Radian)	0.045	0.031	0.048	0.046	0.157
Young's Modulus (GPa)	110.0	193.0	53	2.3	1.50E-03

[1] Rq: Root-mean-square surface roughness.

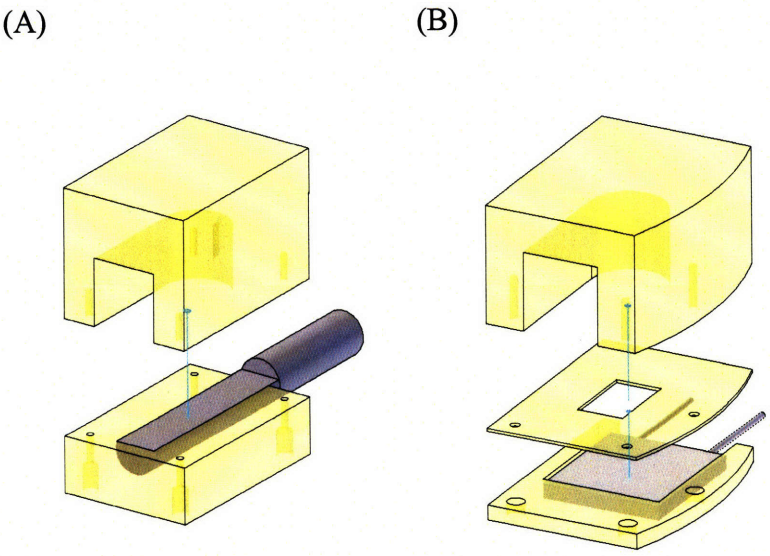

Figure 4-2. Real (A) and simulated (B) material presentation fixtures.

Thermistors (457 μm in diameter and 3.18 mm in length; 56A1002-C8, Alpha Technics) were used to measure the skin temperature of the subjects and the temperature of the thermal display. The thermistors were connected to a Data Acquisition Unit (34970A, Agilent Technologies), which was controlled using a Visual Basic program. The skin temperature and temperature control data were sampled at 20 Hz and 10 Hz respectively. To ensure that the skin temperature of the hand remained constant, the fixture with the recirculating chiller described in the previous experiments was also used in this experiment.

Procedure. Subjects washed their hands with soap prior to participating in the experiment. A thin layer of baking soda was spread on the ABS material sample that had been inserted in the real material presentation fixture. Subjects were instructed to insert the index finger into the fixture to make contact with the material sample after they wet the right index finger with water. Subjects retracted the finger after contact and the contact area was now demarcated by the baking soda. A thermistor was glued along the perimeter of the area covered with the baking soda using a biocompatible cyanoacrylate (Liquid Bandage, Johnson & Johnson). The baking soda was removed from the subject's finger after the thermistor was attached. Subjects' initial skin temperatures ranged from 30 °C to 35.5 °C and the average value was 33 °C. The ambient temperature was 24 °C, as measured with a k-type thermocouple (Omega) in free air.

At the beginning of the experiment, the five material samples described in the apparatus section were shown to subjects. These samples were placed on the table and subjects were instructed to make contact with the samples and attend to the thermal cues associated with each material. After subjects became familiar with the materials and their names, they were instructed to place their right hand on the recirculating chiller pad. The experiment began when the skin temperature was 34 °C.

In the material identification experiment, the real materials were presented to the subjects first, and then the simulated materials. The five real materials were presented to subjects in a random order with three repetitions of each material, giving a total of 15

trials. Subjects were blindfolded to eliminate any visual cues. At the beginning of each trial, a material sample was inserted into the presentation fixture. Subjects were instructed to place the right hand on the recirculating chiller pad to maintain their skin temperature at 34 °C. After hearing a sound cue, subjects inserted the right index finger into the fixture by tracing a thin wire which lead from the recirculating chiller pad to the fixture. When making contact with a material, subjects were encouraged to lift and replace their fingers on the material sample during each trial, but were discouraged from lateral scanning of the surface. They were instructed to name the material that they thought the finger was in contact with. Their responses were then entered into a Visual Basic program. No feedback was given regarding the accuracy of their judgments. Subjects moved their hands back to the recirculating chiller pad after naming the material. The maximum contact time for each trial was 10 seconds.

After finishing the real material identification part of the experiment, subjects removed the blindfold. The five material samples were shown to subjects and they touched them again. After subjects became familiar with the thermal cues associated with each material, they were instructed to place their right hand on the recirculating chiller pad to maintain the skin temperature at 34 °C. The blindfold was not used in this part of the experiment, because the simulated materials did not provide any visual cues that could assist in identification. The simulated material identification experiment began when the subject's skin temperature was 34 °C. Subjects were informed that the materials were simulated with a thermal display and they were instructed to report which material they thought the thermal display was simulating after making contact with the display.

Five simulated materials were presented to subjects in a random order with 9 repetitions of each material, giving a total of 45 trials. There was a rest period of one minute between every 15 trials, and during this time subjects were allowed to touch the five material samples. Prior to each trial, the temperature of the thermal display was set to the corresponding interface temperature of a simulated material based on the semi-infinite body model. After hearing a sound cue, subjects inserted the right index finger into the fixture. They moved their hands back to the recirculating chiller pad after

reporting the name of the material they thought the thermal display was simulating. The maximum contact time for each trial was 10 seconds. Subjects' responses were entered into a Visual Basic program.

It was decided to present the real materials first and then the simulated materials so that subjects had experience with the task and were familiar with the materials. As indicated in Chapter 3, discriminating between real materials using only thermal cues is difficult and as we were interested in achieving "optimal" performance from the subjects with the thermal display additional experience with real materials should facilitate performance.

4.2.2 Results

Subjects' responses when identifying real and simulated materials are summarized in Figure 4-3. The results indicate that materials with low contact coefficients such as ABS and foam were identified most easily, whereas materials with high contact coefficients such as copper and stainless steel were more difficult to identify. In general, for both real and simulated materials the higher the contact coefficient of the material, the more difficult it was to identify. For materials with high contact coefficients, the material that subjects usually confused with the target material was the one with the most similar contact coefficient. This suggests that subjects tended to group materials with similar interface temperatures. Since the thermal cues provided by these materials during contact were similar, subjects were not able to distinguish among them.

(A)

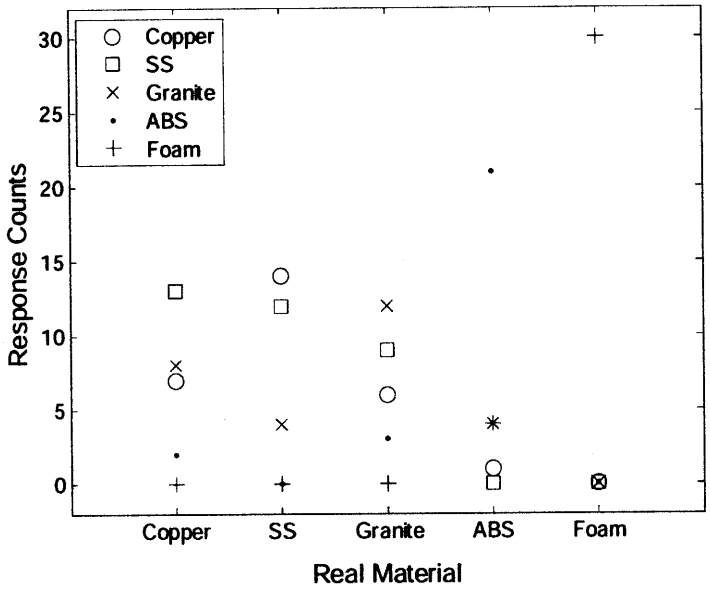

(B)

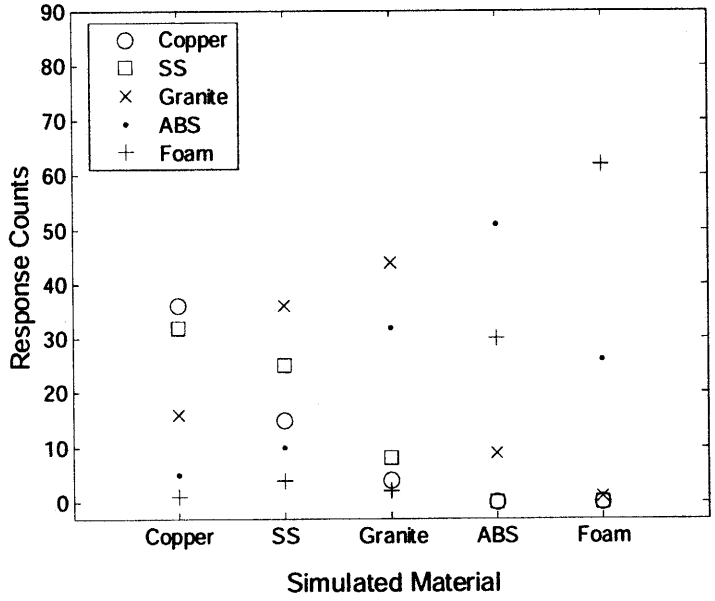

Figure 4-3. Subjects' responses in the real (A) and simulated (B) material identification experiment. The horizontal axis indicates the materials presented to the subjects and the marks represent subjects' responses in the identification task. The zero response count indicates that subjects never responded with that material when identifying a presented material. SS, stainless steel; ABS, a plastic.

In order to evaluate whether there was any response bias, the response counts for each material were calculated for each subject. A repeated measures ANOVA with the named material as the within factor and normalized response counts as the dependent variable indicated that there was no response bias for real materials ($F(4,36) = 1.24$, $p = 0.311$) but that there was for simulated materials ($F(4,36) = 7.54$, $p < 0.001$). A simple contrast test with copper as a reference indicated that subjects' response counts with simulated granite, ABS and foam were significantly different from those for simulated copper (granite: $F(1,9) = 56.49$, $p < 0.001$; ABS: $F(1,9) = 17.32$, $p < 0.01$; foam: $F(1,9) = 5.89$, $p = 0.038$). This indicates that subjects were more likely to name the simulated material granite, ABS or foam than copper.

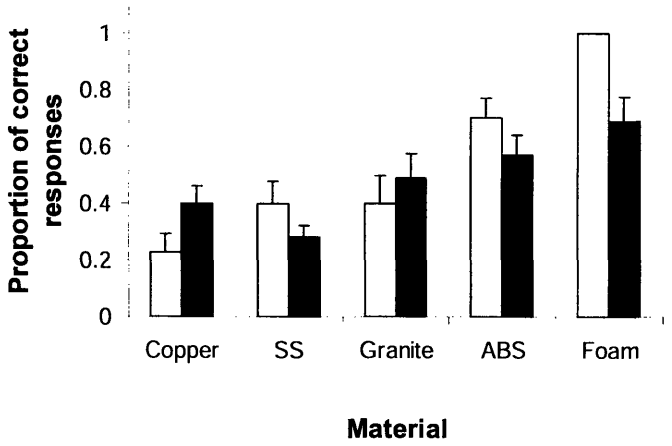

Figure 4-4. Group mean proportions of correct responses in material identification as a function of material and presentation mode. Trials in which the presented materials were real are shown in white and those in which the materials were simulated are black. The error bars show the standard error of the mean (SEM).

The proportions of correct responses were used to analyze the results from this experiment and are shown in Figure 4-4. The overall performance in this experiment was 55% correct for real materials (range: 23% - 100%) and 49% correct for simulated materials (range: 40% - 69%). The chance level in each trial was 0.2 because there were five alternative materials. A test of proportions indicated that at a 0.4 level of correct responses, subjects were able to identify the presented material reliably ($p < 0.01$). As

shown in Figure 4-4, there were two materials for which the proportion of correct responses was below the 0.4 level, real copper and simulated stainless steel. Copper and stainless steel have relatively high contact coefficients and were often confused. With a low contact coefficient, foam was the easiest material to identify both physically (100% correct) and when simulated with the display (69% correct).

The analysis of variance for a split-plot design with presentation mode (real and simulated) and material as factors and the proportion of correct responses as the dependent variable indicated that there was no significant difference between the two presentation modes ($F(1,9) = 0.87$, $p = 0.375$), whereas there was a significant difference among the five materials ($F(4,36) = 21.04$, $p < 0.001$). The test also indicated that the interaction between presentation mode and material was significant ($F(4,36) = 2.98$ $p = 0.032$). For each material presented in the experiment, a post hoc Tukey test for a split plot design indicated that the subjects' performance was not significantly different with real or simulated materials except for foam ($q(2,36) = 3.67$, $p < 0.05$). It would appear that simulated foam was harder to identify than real foam, which is not surprising given its physical properties particularly its surface roughness (see Table 4-1). The correlation (Pearson's R) between the proportions of responses subjects made when identifying real or simulated materials regardless of whether their responses were correct or incorrect was 0.78.

Analyses of covariance (ANCOVA) were conducted to determine whether the surface roughness and elasticity of the materials (the latter defined in terms of Young's modulus which is the ratio of the stress to strain) influenced subjects' performance with the real materials. The covariates were the surface roughness of the materials or the Young's moduli. The analyses indicated that there was no significant effect of the materials' surface roughness ($p = 0.08$) or Young's modulus ($p = 0.23$) on the proportion of correct responses.

The number of trials with simulated materials (45) was greater than that for real materials (15). It seemed likely therefore that subjects' ability to identify the simulated

materials may have improved over the course of the experiment. A repeated measures ANOVA with blocks of trials (3 levels) as the within-subject factor was conducted. The results indicated that subjects' performance with the simulated materials did not change significantly across the three blocks of 15 trials ($F(2,18) = 0.68$, $p = 0.520$).

4.2.3 Discussion

In this experiment, subjects perceived the thermal cues by lifting and replacing their fingers on the surfaces, and the local thermal transients associated with contact were presumably used to identify the materials. The results indicate that when textural cues are minimized, material identification is possible but difficult. For most of the materials presented, both physically and with the thermal display, subjects' performance was well above the chance level, but was not at 100% correct. This difficulty in identifying materials using only thermal cues is consistent with the research on material discrimination described in Chapter 3, which showed that the differences in the thermal properties of materials had to be large for materials to be discriminated reliably (Ho & Jones, 2006a).

The thermal properties of the material influenced the ability of subjects to identify it. As shown in Figure 4-3, materials with higher contact coefficients, such as copper and stainless steel, were often confused. However, subjects were able to identify reliably materials with lower contact coefficients. This indicates that the contact coefficient is an important characteristic of a material and determines how easily it can be identified. It appears that subjects tended to group materials based on their contact coefficients. The distribution of responses suggests that the five materials were divided into two groups: group 1, comprising copper, stainless steel, and granite, and group 2, with ABS and foam. Group 1 is the 'cold group' with high contact coefficients, and group 2 is the 'no thermal response or neutral group' with low contact coefficients. This grouping is consistent with the semi-infinite body model. With an initial skin temperature of 34 °C, the theoretical interface temperatures when making contact with materials in group 1 would range from 23.8 to 27 °C, whereas they would be 30.8 to 33.7 °C for materials in group 2. The ranges

of the interface temperatures for the two groups were both about 3 °C, and the two groups were separated by 4 °C. This suggests that subjects may have set the boundary between 'cold' and 'neutral' materials somewhere between 27 and 30.8 °C. When calculated from the semi-infinite body model, the boundary lay between contact coefficients of 513 and 2340 $J/m^2s^{1/2}K$. Therefore, materials whose contact coefficients are higher than 2340 $J/m^2s^{1/2}K$ are likely to be perceived as cold materials, whereas materials whose contact coefficients are lower than 513 $J/m^2s^{1/2}K$ tend to be perceived as neutral materials.

An analysis of the responses made by subjects indicated that there was no response bias with the real materials, that is, there was no tendency to name one material in preference to another. However, with the simulated materials there was a significant response bias, with subjects being biased toward naming materials with lower contact coefficients, such as granite, ABS and foam. This suggests that the simulated materials were not perceived to be as cold as expected during contact, and so subjects' responses were biased toward materials with lower contact coefficients.

In this study, the performance of subjects with the thermal display was compared to their performance in identifying real materials. The analyses indicated that subjects' responses when identifying real and simulated materials were moderately correlated and that with the exception of foam, there was no significant difference between the real and simulated materials in terms of the proportion of correct responses. This indicates that the thermal display was able to simulate the thermal sensations associated with making contact with real materials, and that the thermal sensations were presumably comparable to those provided by real materials during contact.

Previous studies of thermal displays (Caldwell & Gosney, 1993; Caldwell et al., 1996; Ino et al., 1993; Yamamoto et al., 2004) have usually evaluated the display's performance using material identification tasks. A comparison between the proportion of correct responses in this experiment and other studies indicates that subjects' performance depends on how the materials are simulated and the experimental procedure used in the material identification task. The overall material identification performance in

the present study of 55% and 49% correct for real and simulated materials, respectively, is comparable to the 61% and 56% correct for real and simulated material identification reported by Ino et al. (1993). These values are, however, considerably lower than the 92% and 74% correct reported by Caldwell and Gosney (1993) and Yamamoto et al. (2004) respectively, for materials simulated by the thermal displays that they developed. The excellent performance reported by Caldwell and Gosney (1993) presumably resulted from the large thermal transients they used to simulate materials, which were not maintained at the same initial temperature (e.g. a cube of ice and a soldering iron), unlike the materials used in the present study. Yamamoto et al. (2004) allowed their subjects to touch the real materials while they were identifying the simulated materials, which presumably facilitated performance.

Although the thermal cues associated with contact were presumably used to discriminate between the materials, differences in surface texture and elasticity could have influenced subjects' performance with the real materials. Analyses indicated that performance was not significantly affected by the surface roughness or the Young's moduli of the materials. The ease with which foam was identified is probably due to its distinctive thermal characteristics, and its surface roughness and elasticity. Based on the typical contact pressure for material identification, it would seem reasonable to assume that with the exception of foam, no deformation occurred during contact in this experiment. Although the surface roughness and compliance of foam may have provided additional cues to assist in material identification, the best performance in identifying a simulated material was for foam. This suggests that the thermal properties of foam alone are sufficient to identify it.

4.3 Real and Simulated Material Discrimination

The results from the real and simulated material identification experiment indicated that subjects could identify both real and simulated materials with a comparable level of performance. The objective of the second experiment was to examine the ability of

subjects to use thermal cues to discriminate between various materials when one was presented physically and the other was simulated with the display.

4.3.1 Method

Subjects. Ten normal healthy adults (five women and five men) aged between 22 and 30 years participated in this experiment. Three of the subjects participated in the first experiment. The time between the two experiments was over 18 months. They had no known abnormalities of the tactile or thermal sensory systems and no history of peripheral vascular disease. They all reported that they were right-handed. This research was approved by the local ethics committee.

Apparatus. In this experiment, copper, stainless steel, granite and ABS were selected as the test materials. Foam was eliminated because of its distinguishable surface texture. Each sample was 19.05 mm wide, 145 mm long and 38 mm thick and was stored at room temperature, 21.6 ^{o}C. These sample dimensions were chosen to meet the Fourier number requirement of the semi-infinite body model (Fo < 0.05). The thermal properties and surface roughness of the samples are reported in Table 4-1.

The real and simulated material presentation fixtures were three-piece fixtures as shown in Figure 4-5 and were made with a rapid prototyping system (Viper Laser Stereolithograpy Forming Center, 3D systems). A 23 mm x 20 mm x 46.5 mm rectangular pocket was machined into the upper piece to allow insertion of the index finger, and a 19.8 mm x 55 mm x 38 mm rectangular slot was machined into the lower piece. For the real material presentation fixture, the material sample slid into the slot and was flush with the surrounding surface. For the simulated material presentation fixture, a 30 mm x 34mm x 4 mm rectangular pocket was machined on the surface of the lower piece to fit the Peltier device (DT 6-6, Marlow). For both fixtures, a 20 mm wide channel was machined into the middle piece, which was sandwiched between the upper and lower pieces. At the end of the channel was an elliptically shaped opening with a primary axis of 7 mm and secondary axis of 10 mm, which gave a surface area of 220 mm^2. This

opening controlled the contact area between the fingerpad and real or simulated material. An extended roof and an acrylic housing were added around the fixture to prevent subjects from seeing the material samples.

Three thermistors (457 μm in diameter and 3.18 mm in length; 56A1002-C8, Alpha Technics) were used in this experiment. One measured the initial skin temperature of the index finger in each trial; another monitored the temperature of the thermal display, and the third recorded the room temperature during the experiment. These thermistors were connected to a Data Acquisition Unit (34970A, Agilent Technologies), which was controlled using a Visual Basic.NET program. Temperature data were sampled at 10 Hz. To ensure that the skin temperature of the hand was maintained constant prior to each trial, the recirculating chiller pad used in the previous experiments was also used in this experiment.

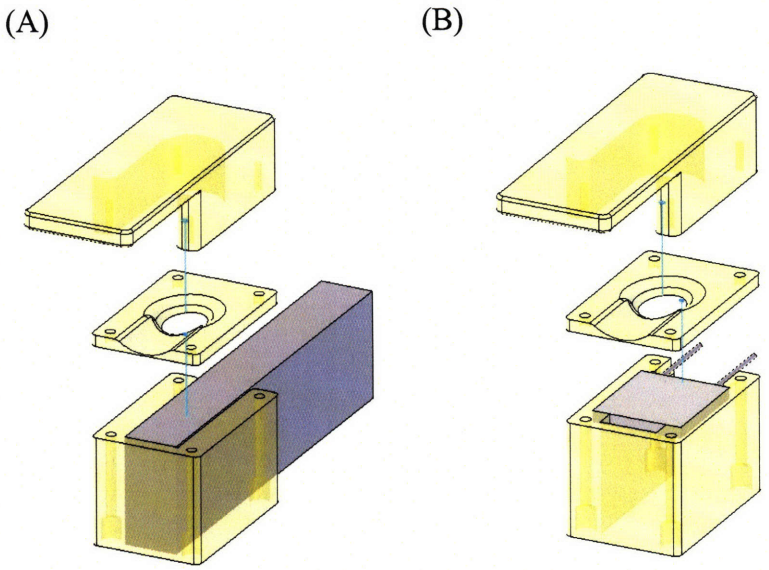

Figure 4-5. Real (A) and simulated (B) material presentation fixtures.

Procedure. Subjects washed their hands with soap prior to participating in the experiment. The width and length of each subject's index fingerpad were then measured with digital calipers (Absolute digimatic, Mitutoyo). The mean width and length were 16.83 mm and 26.15 mm, respectively. Subjects' initial skin temperatures ranged from

24.5 °C to 32 °C, with the average of 28.6 °C. The average ambient temperature was 21.16 °C, as measured with the thermistor in free air.

Each of the four real materials was paired with each of the four simulated materials, which gave a total of 16 different combinations. These 16 combinations were repeated four times for a total of 64 trials. The order of presentation of the material pairs and the position of the real and simulated materials was randomized across trials. There was at least a 1-minute break between each block of 16 trials, during which the subjects placed their hands on the recirculating chiller to maintain their skin temperature.

Prior to each trial, subjects were instructed to place both of their hands on the recirculating chiller pad. A material sample was inserted into the presentation fixture and the real and simulated material presentation fixtures were placed in the position indicated by the Visual Basic.NET program. The data acquisition system started to record the room and thermal display temperatures after the subject's skin temperature reached 34 °C. When hearing a sound cue, subjects moved their hands from the chiller pad and inserted their left and right index fingers into the fixtures. Subjects moved their index fingers vertically downward and made contact with the real and simulated materials when hearing the second sound cue. The set temperature of the thermal display was calculated in real-time using the semi-infinite body model and was based on the subject's initial skin temperature and the recorded room temperature.

A two-alternative forced choice (2AFC) method was used in which subjects were instructed to choose the colder of the two materials presented by reporting which hand made contact with the colder material. Subjects were not told which materials were used in this experiment and no feedback was given regarding the accuracy of their judgments. They were encouraged to lift and replace their fingers on the material samples during each trial, but were discouraged from lateral scanning of the sample surface. After subjects reported which hand felt colder, they withdrew their hands from the fixture and placed them back on the recirculating chiller pad. A maximum of 10 s was allowed for each trial.

4.3.2 Results

In this experiment, the responses for the trials involving different materials were analyzed in terms of the number of correct responses, that is, correctly identifying the "colder" of the two materials as defined in terms of the predicted thermal responses based on the semi-infinite body model. The chance level in this experiment was 50%, and a threshold level of 72% correct was chosen as indicating that subjects could reliably discriminate between a pair of materials. The proportion of correct responses for the various combinations of the materials is shown in Figure 4-6. In this figure, the material presentation mode was divided into $R/S > 1$ and $R/S < 1$, where $R/S > 1$ describes those trials in which the contact coefficient of the real material was higher than that of the simulated material, and $R/S < 1$ refers to those trials in which the contact coefficient of the real material was lower than that of the simulated material. In the first mode, the real material would feel colder than the simulated one, whereas in the second mode, the simulated material would feel colder than the real one. As shown in Figure 4-6, there were 4 material combinations of which the proportions were below threshold level, and they were copper - stainless steel (in both $R/S > 1$ and $R/S < 1$ modes), stainless steel - granite (in $R/S < 1$ mode), and granite - ABS (in $R/S < 1$ mode).

A repeated measures ANOVA with presentation mode and material combination as within-subject factors and the proportion of correct responses as the dependent variable indicated that there was no significant difference between the two presentation modes ($F(1,9) = 2.49$, $p = 0.149$), but there was a significant difference among the material combinations ($F(5,45) = 10.71$, $p < 0.001$). The analysis also indicated that the interaction between presentation mode and material combination was not significant ($F(5,45) = 1.02$, $p = 0.397$). A simple contrast test indicated that subjects' performance in discriminating copper and ABS ($F(1,9) = 6.13$, $p = 0.035$) and stainless steel and ABS ($F(1,9) = 34.61$, $p < 0.001$) was significantly above the mean, and that their performance with copper and stainless steel was significantly below the mean ($F(1,9) = 21.68$, $p= 0.001$).

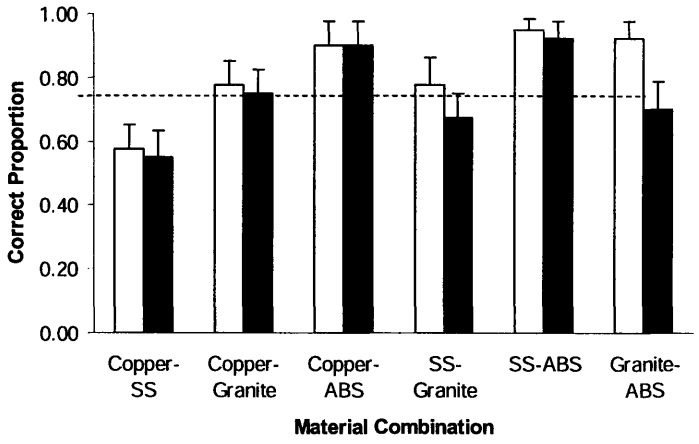

Figure 4-6. Group mean proportion of correct responses in discriminating which material felt colder as a function of presentation mode and material combination. Trials in which the contact coefficient of the real material was higher than that of the simulated material are shown in white and those in which the contact coefficient of the real material was lower than that of the simulated material are shown in black. The dashed line indicates the 0.72 threshold. The error bars show the standard error of the mean (SEM).

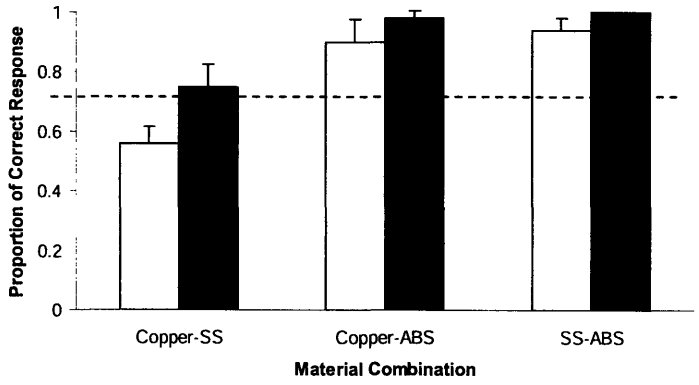

Figure 4-7. Group mean proportion of correct responses in discriminating which material felt colder as a function of presentation mode and material combination. Trials in which a real and simulated material were presented are shown in white and those in which both materials were real (from section 3.2; Ho & Jones, 2006a) are in black. The dashed line indicates the 0.72 threshold. The error bars show the standard error of the mean (SEM).

The results from this experiment were compared to those from an earlier study on material discrimination which used only real materials (Section 3.2; Ho & Jones 2006a) in order to see if discrimination was affected by the presentation mode (i.e., real or simulated). These data are shown in Figure 4-7. A Chi-square test was used to compare these two sets of data in preference to an ANOVA because of the near perfect performance of subjects when discriminating real copper and ABS, and real stainless steel and ABS. The test indicated that there was no significant difference between the two presentation modes ($\chi^2(2) = 0.51$, $p = 0.775$) in terms of discriminating between materials.

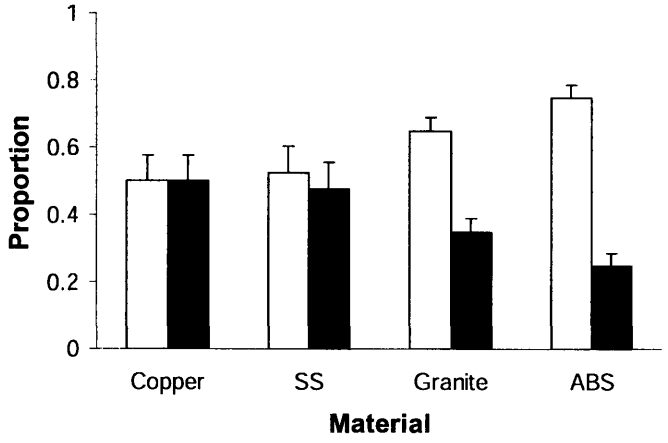

Figure 4-8. Group mean proportion of responses in discriminating which material felt colder when presented with identical materials as a function of presentation mode and material. Trials in which subjects thought the real material was colder are shown in white and those which subjects thought simulated material was colder are in black. The error bars show the standard error of the mean (SEM).

For trials involving identical material combinations (e.g., real and simulated copper), subjects reported the material on the right index finger felt colder on 49% of the trials, and on 51% of the trials they reported that the left index finger felt colder indicating that there was no bias toward the right or left index finger. Subjects' responses as to which material felt colder as a function of presentation mode (real or simulated) and material are shown in Figure 4-8. When real and simulated copper or real and simulated stainless steel were presented, subjects performed at chance in terms of indicating which

material felt colder. This indicates that subjects were unable to discriminate between real and simulated copper or real and simulated stainless steel when making contact with them simultaneously. However, it appears that real granite and ABS felt colder than simulated granite and ABS.

4.3.3 Discussion

The performance of the thermal display in simulating materials was evaluated in this experiment. For trials involving different materials, it was predicted that the change in skin temperature elicited by the thermal display which was based on the semi-infinite body model should be comparable to the change that occurs with contact with the real material. Trials were divided into two presentation modes based on the contact coefficients of the two materials, $R/S > 1$ and $R/S < 1$. There was no significant difference between the two presentation modes indicating that subjects' performance did not depend on whether the colder material was presented physically or simulated with the thermal display. A comparison between the present results and those obtained when subjects discriminated between real materials (Section 3.2; Ho & Jones, 2006a) further confirms that subjects' performance in the present experiment was comparable to that obtained with real materials. These results suggest that the thermal sensations provided by the thermal display were similar to those provided by the real materials.

The results also indicated that thermal cues can be used to discriminate between materials only when the differences in their contact coefficients are relatively large. Among all the material combinations, subjects performed best when discriminating between copper and ABS or stainless steel and ABS, and were at chance when trying to discriminate between copper and stainless steel. The thermal cues used to discriminate between materials are the heat fluxes conducted out of skin, which are determined by the interface temperatures during contact and therefore depend on the contact coefficients of the materials. The difficulty in discriminating between materials relates to the differences in their contact coefficients, regardless of whether the pair comprises real materials or a combination of a real and simulated material.

In this experiment, subjects were not able to discriminate reliably between real and simulated materials when the contact coefficient ratio was smaller than 5.25. This is slightly larger than the ratio of 3 reported in our previous study (Section 3.2; Ho & Jones, 2006a) that was required to discriminate between two real materials. Dyck et al. (1974) also found that normal healthy subjects were not able to reliably distinguish copper and stainless steel on the palm of the hand as "cold" and "warm" (Dyck et al., 1974). Using both real and simulated materials, Kron and Schmidt (2003) reported that subjects were not able to discriminate between PVC and wood reliably when they were presented in either real or simulated modes. Their results suggest that subjects cannot discriminate between materials when the ratio of the contact coefficients is smaller than 2.04. Based on these findings, it appears that the ratio required for subjects to discriminate between two materials thermally is between 2 and 5. The differences between the studies probably reflect variations in the surface finishes of the samples, the method of simulating materials, and experimental procedures.

For trials involving identical materials, the results indicated that the thermal display was able to simulate copper and stainless steel successfully in that subjects were not able to discriminate between the real and simulated material. However, subjects perceived that real granite and ABS were colder than the simulated versions. This suggests that the interface temperatures of the granite and ABS calculated by the semi-infinite body model were not low enough and so simulated granite and ABS were not able to conduct the same heat fluxes out of the skin as real materials did during contact. Several assumptions were made in the semi-infinite body model, and these findings suggest that the present model is not adequate for materials with lower contact coefficients.

In the present model, thermal contact resistance is omitted and this may be the source of inaccuracy in simulating materials with lower contact coefficients. With the addition of thermal contact resistance, there would be a temperature difference between the skin and material surface, instead of the zero temperature difference in the present model. This temperature difference will cause the material surface temperature to be

lower than the interface temperature predicted with the present model. Without thermal contact resistance, the simulated materials have higher surface temperatures than the real ones during contact, and so subjects feel that real materials are colder than simulated materials.

Although subjects were able to discriminate between real and simulated materials with lower contact coefficients in direct comparisons of the same material (see Figure 4-8), this did not affect their capacity to discriminate between two different materials. The ability to discriminate between two different materials based only on thermal cues was not affected by whether one of the materials was real or simulated. This indicates that the thermal sensations provided by the thermal display were adequate for the task.

4.4 CHANGES IN SKIN TEMPERATURE DURING CONTACT

The objective of this experiment was to measure the changes in skin temperature as the fingerpad made contact with the real and simulated materials. This provided a basis for evaluating the effectiveness of the thermal display in simulating the temperatures associated with making contact with different materials. A second goal was to determine how these changes compared to the theoretical predictions based on the semi-infinite body model. Further refinements to the model would be made based on these comparisons.

4.4.1 Procedure

Subjects. Ten normal healthy adults (five women and five men) aged between 21 and 29 years participated in this experiment. They had no known abnormalities of the tactile or thermal sensory systems and no history of peripheral vascular disease. They all reported that they were right-handed. This research was approved by the local ethics committee.

Apparatus. The five materials used in the material identification experiment were used in this experiment; they were copper, stainless steel, granite, ABS, and foam. Their

thermal and physical properties are listed in Table 4-1. The material samples were stored at room temperature, 24 °C. Each sample was 19.05 mm wide, 145 mm long and 38 mm thick.

The real and simulated material presentation fixtures were the same as those used in the material discrimination experiment shown in Figure 4-5 except that the lower part of the simulated material presentation fixture was made of acrylic plastic to fit in a Peltier device (DT 6-6, Marlow) as shown in Figure 4-9. This fixture was placed on top of the copper plate of a recirculating chiller to maintain the temperature of the hot side of the Peltier device. An extended roof and an acrylic housing were also added around the real material presentation fixture to prevent subjects from seeing the material samples.

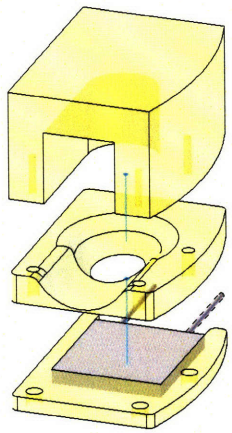

Figure 4-9. Simulated material presentation fixture

Two Thermistors (457 μm in diameter and 3.18 mm in length; Model 56A1002-C8, Alpha Technics) placed at each side of the contact area were used to measure the skin temperature of the right index finger. The thermistors were connected to a Data Acquisition Unit (Model 34970A, Agilent Technologies) which was controlled using a Visual Basic.NET program. The skin temperature and temperature control data were sampled at 20 Hz and 10 Hz respectively. To ensure that the skin temperature of the hand was maintained constant prior to each trial, the recirculating chiller pad used in the previous experiments was also used in this experiment.

Procedure. At the beginning of the experiment, the width and length of each subject's fingerpad were measured with calipers (CD-6" CS, Mitutoyo). The contact area on the fingerpad when making contact with a material was marked using the method described in the material identification experiment. Photographs of the right index finger were taken with a digital camera (DSC-F707, Sony), and Matlab was used to process these images in order to calculate the surface area of the fingerpad and the contact area.

After the fingerpad images were taken, two thermistors were glued, using a biocompatible cyanoacrylate (Liquid Bandage, Johnson & Johnson), on the right and left side of the fingerpad along the perimeter of the area covered with the baking soda. The baking soda was removed from the subject's finger after the thermistors were attached. The thermistors were positioned so that they did not interfere with the contact surface between the fingerpad and material and did not deform the fingerpad during contact. Subjects' initial skin temperatures ranged from 31.4 °C to 36.4 °C, with an average value of 34.96 °C. The ambient temperature was 23 °C, as measured with a k-type thermocouple (Omega) in free air.

In this experiment, the real materials were presented to the subjects first, and then the simulated materials. In the first part of the experiment, five real materials were presented to subjects in a random order with three repetitions of each material, giving a total of 15 trials for each subject. Prior to each trial, a material sample was inserted into the presentation fixture. Subjects were instructed to place their right hands on the recirculating chiller pad to maintain their skin temperature at 34 °C. After hearing a sound cue, subjects inserted their right index finger into the fixture. After making contact with a material, they were instructed to leave their index fingers on the material sample for 10 s. The data acquisition system recorded the temperature from the thermistors attached to the subjects' fingerpads during contact at 20 Hz. Subjects moved their hands back to the recirculating chiller pad after each trial was completed.

After the first part of the experiment, subjects were given a rest period of one minute. Five simulated materials were then presented to subjects in a random order with three repetitions of each material, giving a total of 15 trials for each subject. Prior to each trial, the temperature of the thermal display was set to the corresponding interface temperature of a simulated material. After hearing a sound cue, subjects inserted the right index finger into the fixture. Subjects moved their hands back to the recirculating chiller pad after 10 s of contact. The skin temperature responses were recorded at 20 Hz with the same data acquisition system.

4.4.2 Results

The mean fingerpad area of the subjects was 355.87 mm^2 (standard deviation: 51.26 mm^2) and the mean contact area was 134.84 mm^2 (standard deviation: 23.87 mm^2). The changes in skin temperature during 10 s of contact with the real and simulated materials were analyzed in terms of ΔT, that is the difference in the skin temperature prior to and at the end of the 10 s contact period. These data are summarized in Figure 4-10. As expected, the subjects' skin temperatures decreased when making contact with the real and simulated materials, and the changes in skin temperature were smaller for materials with lower contact coefficients. Prior to performing an analysis of variance of these changes in skin temperature, Levene's test of equal error variance was performed due to the considerable range of variances (Levene, 1960). The test indicated that there was a significant difference in the error variances among the ten groups ($F(9,90) = 3.94$, $p < 0.001$). The data were therefore transformed using a power (0.5) transformation. The Levene's test of equal error variance on the transformed data indicated that there was no significant difference among the error variances of the groups ($F(9,90) = 0.93$, $p = 0.505$).

An analysis of variance for a split-plot design, with presentation mode and material as factors and changes in skin temperature during contact as the dependent variable, indicated that there was a significant difference between the two presentation modes ($F(1, 9) = 16.48$, $p = 0.003$), and among the five materials ($F(4,36) = 236.11$, $p < 0.001$). The interaction between presentation mode and material was also significant ($F(4,36) =$

19.88, $p < 0.001$). For each material presented in the experiment, a post hoc Tukey test for split plot design indicated that the subjects' performance was significantly different for real and simulated stainless steel, ABS and Foam ($q(2,36) = 3.88$, $p < 0.05$; $q(2,36) = 9.45$, $p < 0.05$; $q(2,36) = 7.96$, $p < 0.05$). In general, the decreases in skin temperature elicited by real materials during contact (range: 0.46 - 2.80 °C; mean: 1.84 °C) were greater than those with the simulated materials (range: 0.15 - 2.57 °C, mean: 1.54 °C).

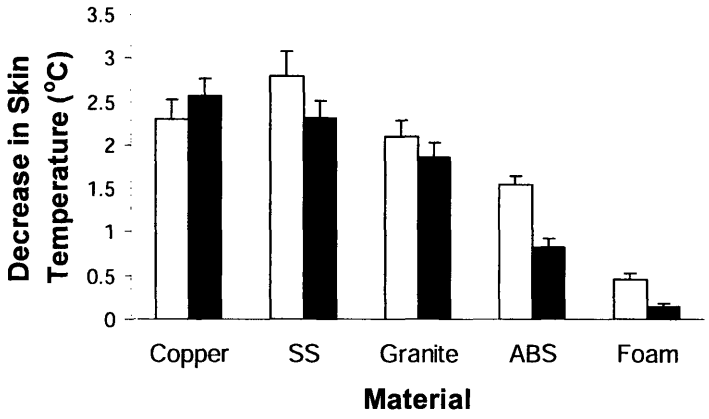

Figure 4-10. Mean changes in skin temperature during 10 s of contact with real (white) and simulated (black) materials. The error bars show the standard error of the mean (SEM).

In order to evaluate the effectiveness of the semi-infinite body model in describing the heat transfer process during contact, a comparison was made between the decreases in skin temperature during contact with the real and simulated materials and the theoretical values predicted from the model. These data are shown in Figure 4-11. The decreases in skin temperature during contact for the five real and simulated materials were all considerably smaller than the theoretical values, ΔT ($T_{skin,i} - T_s$), derived from the model. However, the mean decreases in skin temperature during contact with the real and simulated materials were highly correlated with the predicted values (Real materials: Pearson's $R = 0.93$, $p = 0.021$; simulated materials: Pearson's $R = 0.99$, $p < 0.001$). This suggests that for both the real and simulated materials, the decreases in skin temperature are consistent with the contact coefficient $(k\rho c)^{1/2}$ of the material, as predicted by the semi-infinite body model, but are considerably smaller than predicted.

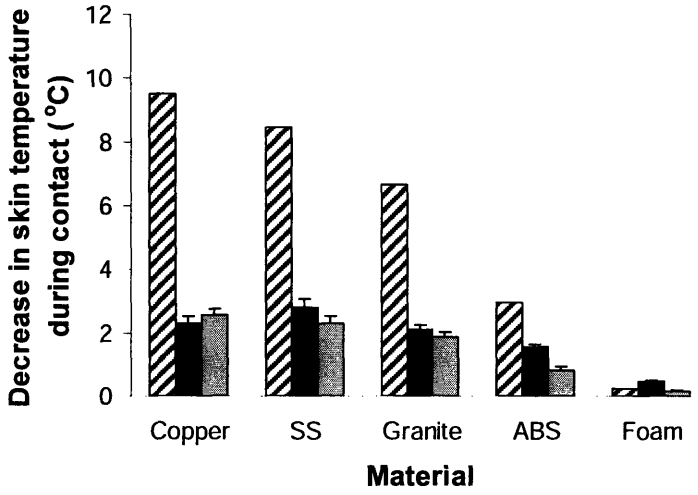

Figure 4-11. Decreases in skin temperature during contact predicted from the model (striped), with the real material (black), and with the simulated material (grey). The error bars show the standard error of the mean (SEM).

The changes in skin temperature during the 10 s of contact with the real and simulated materials are shown in Figure 4-12. The differences in the initial skin temperatures when making contact with the real and simulated materials was around 0.4 °C, which suggests that subjects' skin temperature increased slightly during the experiment. In contrast to the model, the skin temperature changed with time instead of changing instantaneously to the interface temperature at the moment of contact. Exponential functions were fitted to these skin temperature responses and with the exception of real and simulated foam, the functions fitted well. When the finger made contact with real or simulated foam, the skin temperature reached a steady state soon after contact with little change thereafter. The constants and the time constants for each real and simulated material indicated that the skin temperature responses elicited by the real and simulated materials were similar for copper, stainless steel, and granite, but not for ABS and foam. The simulated ABS and foam had larger time constants than real ABS and foam. This indicates that simulated ABS and foam elicited smaller changes in skin temperature than real ABS and foam.

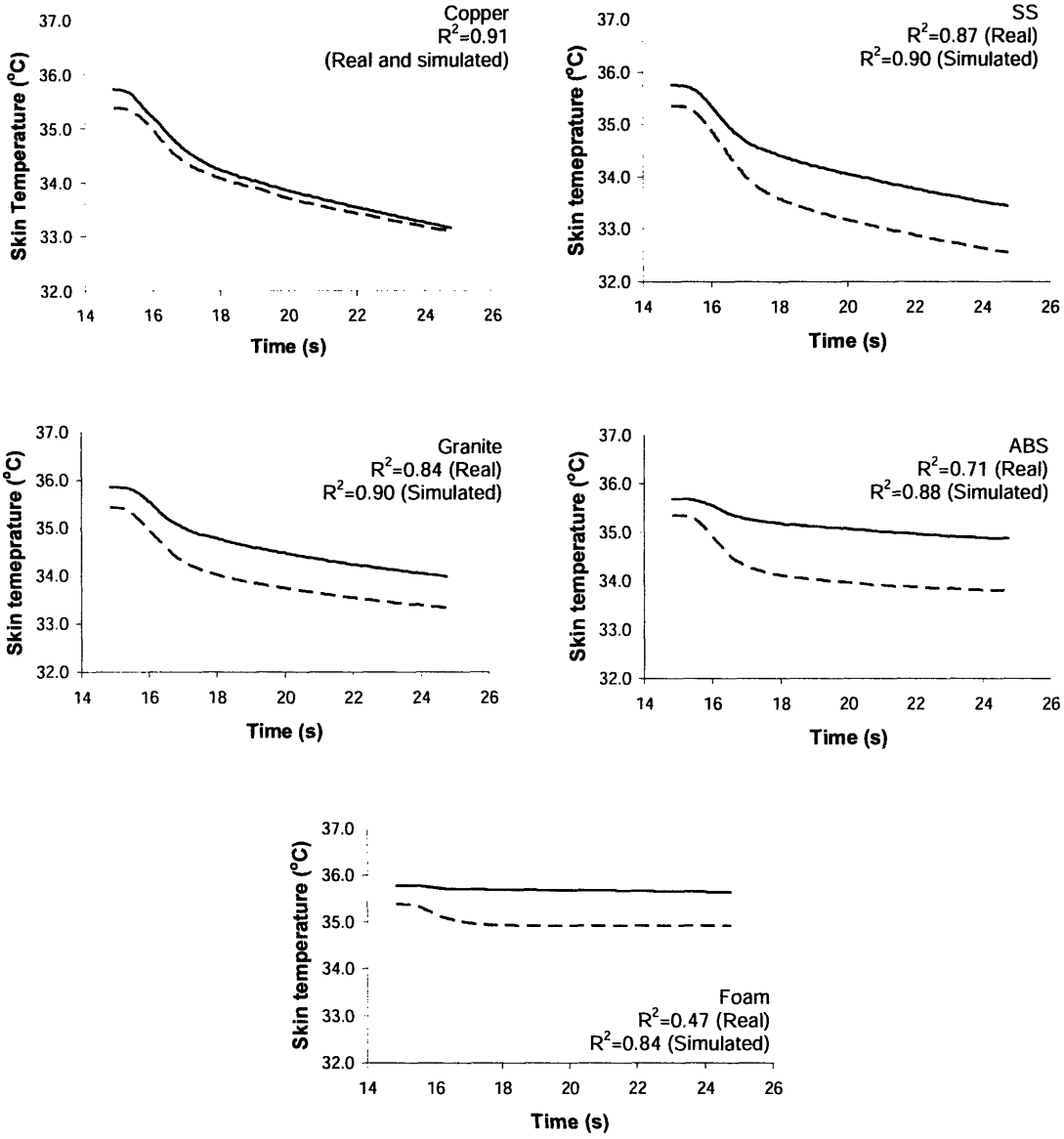

Figure 4-12. Mean changes in skin temperature during 10 s of contact with the real (dashed) and simulated (solid) materials. R^2 value indicates the goodness of fit of the exponential functions.

4.4.3 Discussion

In this experiment, the contact area was controlled and did not vary much across subjects despite variations in the size of the fingerpad. Therefore, it seems unlikely that the changes in skin temperature during contact were influenced by the fingerpads' dimensions. The magnitude of the changes in skin temperature during contact was a function of the material's contact coefficient, which is consistent with the semi-infinite body model. According to the model, the change in skin temperature from its initial value should occur instantaneously at the moment of contact. During the contact period, the temperatures of the skin and material surface should equal the interface temperature and should not change with time. However, the results indicate that during contact the measured skin temperature changed over time and that it was always higher than the predicted interface temperature. As a result, the changes in skin temperature during contact, $T_{skin,i}$-$T_{skin,10s}$, with either real or simulated materials were much smaller than the theoretical values predicted by the model, $T_{skin,i}$-T_s. This discrepancy may result from the skin's thermal properties. Skin is a good thermal insulator ($\alpha = 10^{-7}$ m^2/s), which means that changes in temperature can be localized to a small region (Eberhart, 1985). It is possible that with the localized nature of the change in skin temperature, the thermistors attached to the edge of the contact area may not have detected the full extent of the temperature change. However, if the thermistors were placed in the middle of the fingerpad, it would interfere with the contact between the fingerpad and material and would have deformed the fingerpad during contact. This would influence the heat transfer during contact and make it difficult to analyze the skin temperature changes.

The difference between the theoretical and measured temperature changes may also result from the thermal contact resistance between the finger and the material. In its present form, the semi-infinite body model does not account for thermal contact resistance and assumes that the skin temperature is the same as the interface temperature during contact. Thermal contact resistance can occur between the fingerpad and real materials or a thermal display during contact (Benali-Khoudja et al., 2003; Yamamoto et al., 2004), with the result that there would be a temperature difference between the skin and material surface, instead of the zero temperature difference assumed in the present

model. This temperature difference would cause the skin temperature to be higher and the material surface temperature to be lower than the interface temperature predicted with the present model. The skin temperature would therefore not decrease as much as predicted with both the real and simulated materials. In addition, the decreases in skin temperature when making contact with simulated materials would be smaller than those for real materials as the simulation did not account for thermal contact resistance. This is consistent with the results from the material discrimination experiment in which subjects felt that some real materials, such as granite and ABS, were colder than their simulated versions.

The significant interaction between the presentation mode and material in this experiment reflects the thermal responses elicited by real copper. The change in skin temperature when making contact with real copper was lower than that which occurred when the finger made contact with simulated copper. This differs from the general trend in which real materials elicited greater changes in skin temperature during contact than simulated materials. It is possible that real copper elicited smaller changes in skin temperature than anticipated because the copper oxidized during contact which would have increased the thermal contact resistance between the fingerpad and the material.

The slight increase in the subjects' skin temperature during the experiment may be due to the use of the recirculating chiller, which is set at 38 ^{o}C in order to achieve a surface temperature of 34 ^{o}C. Because the simulated material presentation fixture was placed on the top of the recirculating chiller fixture in order to maintain the hot side temperature of the Peltier device, the temperature of the delrin housing might have increased during the experiment. As a result, the subjects' skin temperatures increased slightly when their fingertip was in the fixture while waiting for the sound cue to make contact with the material. This problem can be solved by replacing the recirculating chiller with a heat sink to maintain the hot side temperature of the Peltier device.

In this study, the skin temperature decreased relatively rapidly during the first 3 to 4 seconds of contact and then changed much more slowly for the next 5 seconds. For most

of the materials except foam, the skin temperature did not stabilize during this 10 s period of contact (shown in Figure 4-12). These data are consistent with the long reaction and decision times reported for thermal stimuli (Lederman and Klatzky, 1997; Stevens, 1991). The time course of these thermal responses suggests that semi-infinite body model is not adequate for simulating different materials and that thermal contact resistance should be included in a future model.

4.5 CONCLUSION

The thermal display described in the present study is capable of simulating materials that cover a broad range of thermal properties. The performance of subjects in identifying and discriminating between materials is similar regardless of whether the materials are real or simulated. However, an analysis of the performance of the thermal display in terms of the changes in skin temperature during contact indicated that the display did not elicit the same thermal responses during contact as did contact with the real material. Despite these differences, there was no significant effect of presentation mode (real or simulated) on the ability of subjects to identify and discriminate between materials. This suggests that thermal perception is not precise, as has often been noted (e.g. Stevens, 1991), and that the thermal cues provided by the display are sufficient to simulate a range of materials.

At present, the thermal display is based on the semi-infinite body model. Although this model serves as a reasonable description of the skin temperature response, it overestimates the changes in skin temperature and the material surface temperature during contact. These overestimations presumably reflect the absence in the model of thermal contact resistance, which exists between the fingerpad and material. Therefore, it will be important to estimate and incorporate thermal contact resistance in the future development of the thermal model.

In this study, the skin temperature was measured with thermistors attached to the perimeter of the contact area. The locations of the thermistors were chosen to prevent the sensors from deforming the fingerpad and affecting the surface area between the fingerpad and material. However, the localized nature of the change in skin temperature during contact with an object may mean that the sensors were not able to detect the full extent of the temperature change in these studies. A non-contact measurement system based on an infrared camera was therefore developed to overcome the limitations of contact thermal sensors. This system is described in Chapter 5. Measurements obtained with this system will enable further evaluation and refinement of the thermal model.

CHAPTER 5

THERMAL MEASUREMENTS FOR HAND-OBJECT INTERACTIONS

5.1 LIMITATIONS OF CONTACT THERMAL SENSORS

When evaluating a thermal model from a physiological perspective, the temperature responses of the skin during contact are typically measured with small thermal sensors, such as thermistors or thermocouples, that are affixed to the skin. In some studies, the sensors have been placed directly on the contact area (Ino et al., 1993; Yamamoto et al., 2004) and in others (Ho & Jones, 2004, 2006a), the sensors were attached to the perimeter of the contact area.

As indicated in Figure 5-1, it is difficult to obtain consistent temperature measurements with sensors attached to the fingerpad. When the sensor is placed directly on the contact area, it affects the contact between the fingerpad and material, which may result in a smaller change in skin temperature during contact. When the sensor is attached to the perimeter of the contact area, the localized nature of the change in skin temperature means that the sensor is not able to detect the full extent of the temperature change during contact. As shown in Figure 5-2, the thermal sensors were not able to detect the instantaneous decreases in skin temperature at the moment of contact and the measured time courses and amplitudes of the skin temperature changes during contact were significantly different from the theoretical predictions.

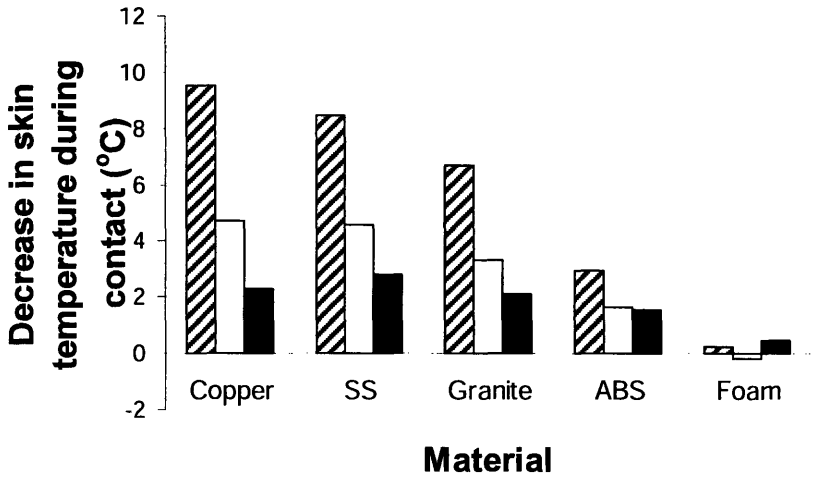

Figure 5-1. Decreases in skin temperature during 10 s of contact with real materials predicted by the model (striped), with the sensor attached on the center of the contact area (white), and with the sensor attached to the perimeter of the contact area (black).

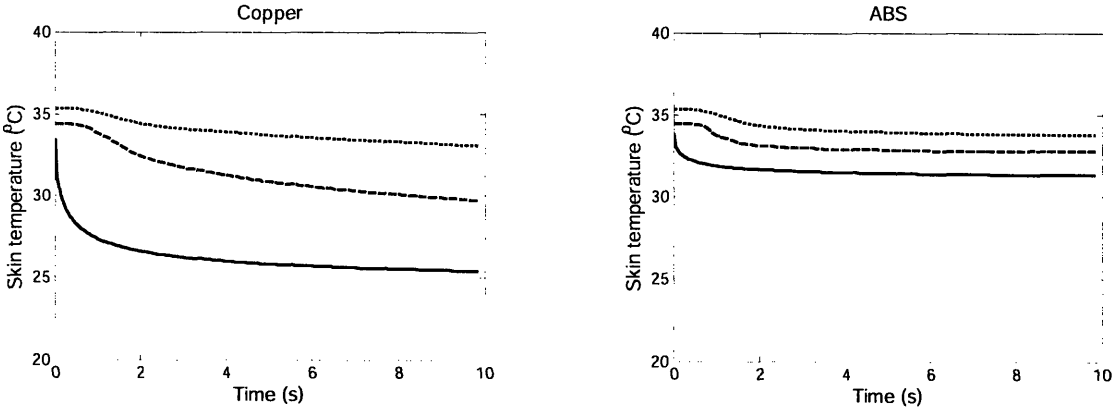

Figure 5-2. Changes in skin temperature during 10 s of contact with real materials from the predictions made by the revised model introduced in Chapter 6 (solid), with the sensor attached on the center of the contact area (dashed), and with the sensor attached to the perimeter of the contact area (dotted).

5.2 INFRARED THERMAL MEASUREMENT SYSTEM

In order to eliminate the limitations of contact thermal sensors and examine the influence of the contact pressure on skin thermal responses during contact, an infrared thermal measurement system has been developed. This measurement system is able to provide an image of the temperature distribution across the fingerpad during contact rather than a single point measurement from a thermal sensor. With special system layout, this system can measure contact area and contact force simultaneously during contact. With this system, detailed analyses of the skin temperature responses during contact can be conducted. These measurements permit the validation of different thermal models which can then be incorporated into haptic displays.

5.2.1 System layout

By utilizing an infrared camera to measure temperature, the optical components placed between the infrared camera and the fingerpad must be infrared transmissive to prevent obstruction of the thermal radiation emitted from the fingerpad. The layout of the system designed to fulfill these requirements is shown in Figure 5-3. An infrared camera (A40M, FLIR Systems) was used to measure the thermal radiation emitted from the fingerpad. It eliminates the measurement limitations of contact thermal sensors, which can only record localized changes in skin temperature and can deform the skin during contact.

In order to measure the contact area and temperature distribution on the fingerpad simultaneously two infrared windows that can transmit wavelengths in both the visible and infrared spectrum were selected as contact materials. They were barium fluoride (BaF_2) and zinc sulphide (ZnS) (Crystran LTD). They were stored at room temperature and were 43 mm in diameter and 10 mm thick. Their surface roughness was measured with a Mitutoyo Surface Roughness Tester (Model SV-3000S4). Their thermal and mechanical properties are listed in Table 5-1. A beamsplitter, made of germanium (Ge) with an anti-reflection coating, was used to separate the infrared radiation and visible

light from the contact area. It measured 32 mm in diameter and was 3 mm thick. The contact area was captured by a digital camera (EOS D60, Canon) with a 100 mm macro lens (EF 100 mm, Canon). A 6-axis force transducer (Nano 43, ATI Industrial Automation) with a 20-mm diameter hole in the center was attached to the contact material and measured the contact force without obscuring the infrared and visible radiation from the fingerpad.

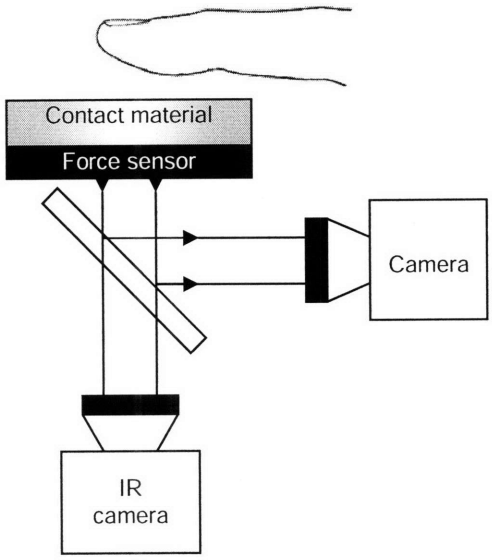

Figure 5-3. Layout of the infrared thermal measurement system

Table 5-1. Properties of the contact materials

Material	BaF_2	ZnS
Conductivity k (W/mK)	11.7	27.2
Density ρ (kg/m^3)	4890	4090
Specific heat c (J/kgK)	410	515
Contact coefficient $(k\rho c)^{1/2}$ ($J/m^2s^{1/2}k$)	4843	7569
Surface roughness R_q[1] (μm)	0.008	0.006
Asperity slope Δa (radian)	0.009	0.006
Young's Modulus E (GPa)	53.1	74.5

[1] R_q: Root-mean-square surface roughness.

The fixtures that held the contact material and force transducer, and the beamsplitter are shown in Figure 5-4 (A) and (B), respectively. They were made with a rapid prototyping system (Viper Laser Stereolithograpy Forming Center, 3D systems). The contact material and transducer holder is a three-piece fixture. A 20 mm wide channel was machined into the main piece. At the end of the channel was an elliptically shaped opening with a primary axis of 7.5 mm and secondary axis of 10 mm, which gave a surface area of 240 mm^2. The design of this opening and the other piece on the right helped subjects to position their fingerpad in a consistent location during skin temperature measurements. A circular pocket, which was 43 mm in diameter and 22 mm in depth, was machined into the other side of the middle piece to hold the contact material and transducer with the other piece on the left of Figure 5-4 (A). The beamsplitter holder held the beamsplitter at a 45^{o} inclination without obscuring the infrared radiation from the fingerpad.

(A) (B)

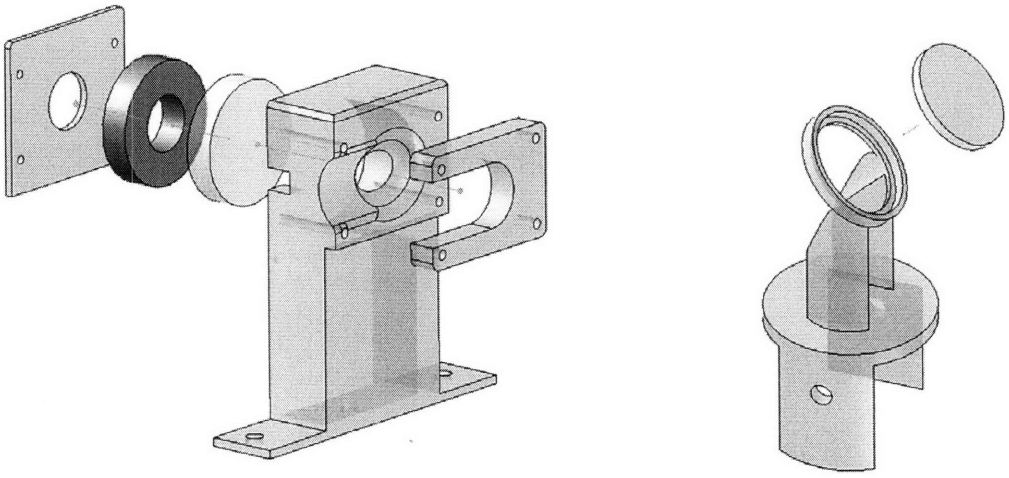

Figure 5-4. Fixtures for contact material and force transducer (A) and beamsplitter (B).

A lighting unit was also incorporated into the system to improve the luminance level while the contact area was being imaged with the digital camera. Two LEDs (Luxeon III Emitter, LumiLEDs) were attached to a thin clear acrylic structure, which was designed to guide the emitted light toward the fingerpad. This lighting unit was placed between the contact material and the transducer holder and beamsplitter holder. During measurement, the distance between the fingerpad and the infrared camera was 300 mm, which was the minimum distance required for focusing. The optical components and fixtures were arranged to prevent radiation loss. The overall setup of the infrared thermal measurement system is shown in Figure 5-5.

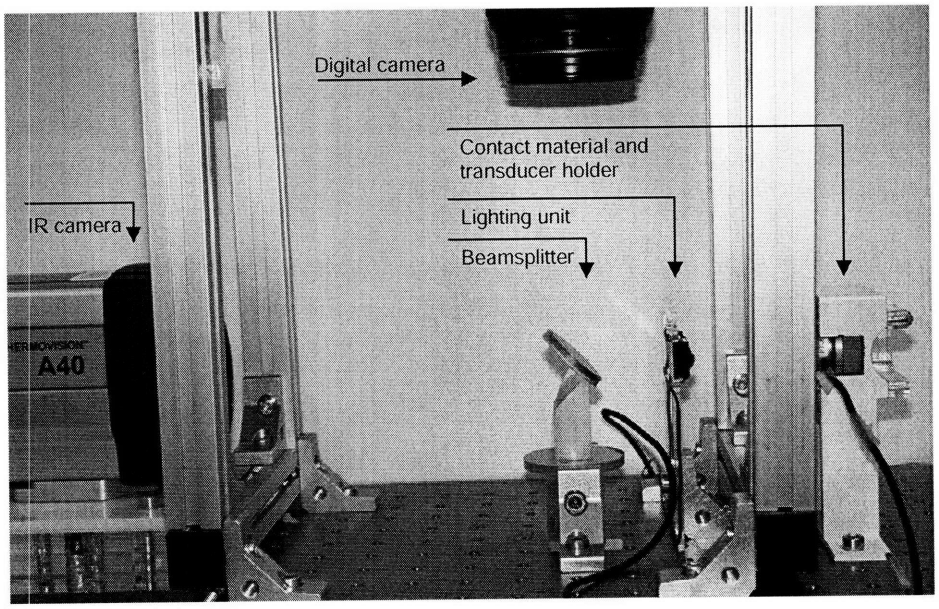

Figure 5-5. Infrared thermal measurement system.

5.2.2 Parameters in infrared measurement

In this thermal measurement system, the radiation measured by the infrared camera not only originates from the fingerpad, but also from the surroundings and the optics placed in between the camera and finger. In addition, the radiation from these sources can be influenced by the absorption of the atmosphere. To measure the fingerpad temperature accurately, it was necessary to establish an IR model to compensate for the effects of the

different radiation sources. In order to achieve this goal, the optical parameters listed in Table 5-2 needed to be considered.

Table 5-2. Parameters considered for IR model derivation

Target parameters
Target emissivity
Target distance
Ambient parameters
Relative humidity
Ambient temperature
External optics parameters
Optics temperatures
Optics transmissivity
Optics reflectivity
Optics emissivity

Target parameters

The fingerpad was the target of this thermal measurement system. In this study, the fingerpad was assumed to be a gray body with a constant emissivity of 0.95 (Incropera & DeWitt, 1996) within the spectral range of the infrared camera, that is 7.5-13 μm. A calibration test was conducted with the system to validate this assumption and will be discussed in Section 5.2.5. The target distance in this system was 300 mm, which was the minimal focal distance required for the infrared camera.

Ambient parameters

The target distance, relative humidity, and ambient temperature together determine the transmission of the air between the target and the infrared camera. The total transmissivity of the atmosphere over a distance is $D = T_m \times T_s$, where T_m is the molecular absorption by constituent gases and T_s is scattering by particles in the atmosphere. In the present configuration, the target distance was 300 mm and therefore the transmissivity of

the atmosphere equals to 1 (Gaussorgues, 1994). The ambient temperature determines the amount of thermal radiation from the surrounding sources.

External optics parameters

The infrared camera selected for this system measures over the waveband between 7.5 and 13 μm. In order to characterize the optical properties of the external optics, that is the contact materials and beamsplitter, in this spectral range, the spectral transmissivity and reflectivity of the optics were measured with a spectrometer (Nicolet Magna 860 Fourier Transform Infrared Spectrometer) and the angles of incidence of the measurement were chosen to be the same as the system configuration, that is normal and 45° for the two contact materials and beamsplitter, respectively.

The optics used in the system were real body radiators and exhibited a bandpass transmissivity that depended on the waveband response of the infrared camera, the spectral response of the optics, and the temperatures of the optics and the target. Based on the model proposed by Madding (2004, 2005) with the assumptions that the surfaces of the target and optics were diffuse and that the optics' temperature equaled the ambient temperature, the bandpass transmissivity, τ, can be estimated from (Madding, 2004; Madding, 2005):

$$\tau = \frac{\int_{7.5}^{13} \tau(\lambda) \cdot R_{\text{det}}(\lambda) \cdot [E(\lambda, T_{\text{tar}}) - E(\lambda, T_{\text{amb}})] d\lambda}{\int_{7.5}^{13} R_{\text{det}}(\lambda) \cdot [E(\lambda, T_{\text{tar}}) - E(\lambda, T_{\text{amb}})] d\lambda} \tag{5-1}$$

where τ is transmissivity, R_{det} is the detector response of the infrared camera, E is the spectral emissive power of a blackbody, λ is wavelength, and T is temperature in Kelvin. Subscripts tar and amb represent target and ambient, respectively.

The bandpass reflectivity ρ, is defined as the fraction of the spectral irradiation that is reflected by the surface (Incropera & DeWitt, 1996). With respect to the reflectivity of optics at the infrared camera side, the ambient radiation was assumed to be the only

source of irradiation. With the assumption that the surface of the optics is diffuse, the bandpass reflectivity can be calculated accordingly:

$$\rho = \frac{\int_{7.5}^{13} \rho(\lambda) E(\lambda, T_{amb}) d\lambda}{\int_{7.5}^{13} E(\lambda, T_{amb}) d\lambda} \tag{5-2}$$

By working with the bandpass properties of the optics, the optics can be treated as gray bodies within the infrared camera's spectral range. The bandpass emissivity, ε, can therefore be estimated from the relation $\varepsilon + \tau + \rho = 1$. For a typical hand-object interaction with the initial temperatures of the skin and object of 34 and 24 °C, respectively, the skin surface temperature for 10 s of contact should be around 27 °C based on the thermal model proposed by Ho & Jones (2006b). The bandpass optical properties of this system were therefore evaluated based on the ambient and target temperature of 24 and 27 °C, respectively and their values are listed in Table 5-3.

Table 5-3. Bandpass optical properties of this system

	Transmissivity τ	Reflectivity ρ	Emissivity ε
BaF_2	0.77	0.04	0.19
ZnS	0.65	0.22	0.13
Germanium	0.54	0.42	0.04

5.2.3 IR model for target temperature derivation

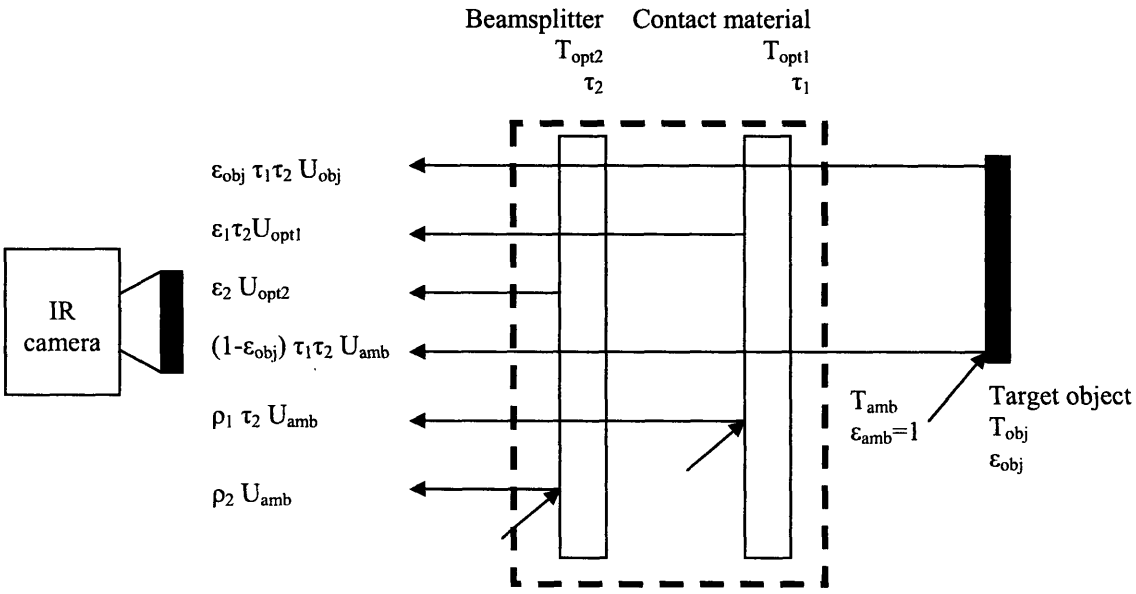

Figure 5-6. Schematic representation of the IR model.

In order to derive the temperature of the fingerpad during contact that is based on the thermal energy measured by the infrared camera, an IR model was developed to compensate for the effects of the contact material and beamsplitter that were placed between the fingerpad and IR camera. The schematic representation of the IR model is shown in Figure 5-6. This model takes into account various sources of thermal radiation that can be detected by the IR camera. They include the radiation emitted by the contact material, beamsplitter, and the target, and the ambient radiation reflected by the contact material, beamsplitter and the target. Based on this model, the radiation emitted by the target can be derived as:

$$U_{tot} = \varepsilon_{obj}\tau_1\tau_2 U_{obj} + (1-\varepsilon_{obj})\tau_1\tau_2 U_{amb} + \varepsilon_2 U_{opt2} + \varepsilon_1\tau_2 U_{opt1} + \rho_1\tau_2 U_{amb} + \rho_2 U_{amb}$$

$$\Rightarrow U_{obj} = \frac{U_{tot} - (1-\varepsilon_{obj})\tau_1\tau_2 U_{amb} - \varepsilon_2 U_{opt2} - \varepsilon_1\tau_2 U_{opt1} - \rho_1\tau_2 U_{amb} - \rho_2 U_{amb}}{\varepsilon_{obj}\tau_1\tau_2} \quad (5\text{-}3)$$

where U is the energy signal received by the infrared camera, ε is emissivity, τ is transmissivity, and ρ is reflectivity. Subscripts tot, obj, amb, and opt stand for total, object, ambient, and optics, respectively, and 1 and 2 represent the contact material and beamsplitter, respectively. The infrared camera measures the total energy signal U_{tot}. The infrared camera calibration curve provided by the camera manufacturer enables the conversion between temperature and energy signal. The energy signals of the ambient and optics, U_{amb} and U_{opt}, could therefore be estimated from their corresponding temperatures. Based on the model and the calibration curve, the temperature of the target was calculated from U_{obj}.

5.2.4 Spatial resolution of the thermal image

The spatial resolution of the thermal image recorded by the IR camera in the current setup was 400 μm. In order to ensure that this spatial resolution was able to capture the essential thermal information on the fingerpad during contact, a 2-D fast Fourier transform was performed on a thermal image of a fingerpad as it made contact with BaF_2. The lens had a spatial resolution of 50 μm. The frequency content of this image was analyzed and the power spectrum of the transform is shown in Figure 5-7. Most of the power in the thermal image lies in the low frequency range between 0 and 1.25 (1/mm). This suggests that the spatial frequency needed for capturing the essential thermal information from the fingerpad during contact should be at least 2.5 (1/mm), which equals a spatial resolution of 400 μm.

(A)

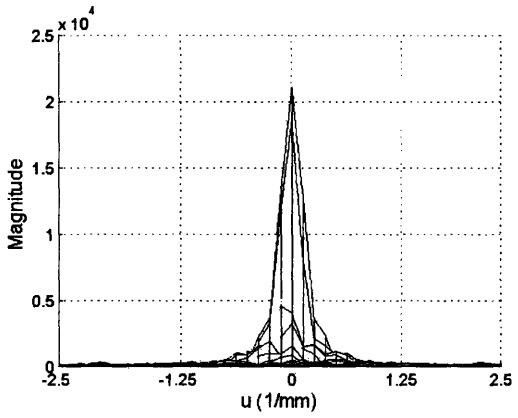

(B)

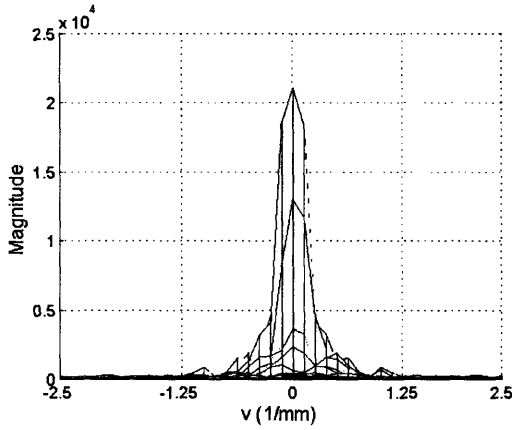

Figure 5-7. Power spectrum of the thermal image for horizontal (A) and vertical (B) frequency

5.2.5 Calibration test

The performance of this system was evaluated with two calibration tests by comparing the temperature readings from a thermal sensor attached to the fingerpad with those measured by the thermal measurement system.

Subject. Two normal healthy adults (1 woman and 1 man), aged 27 years, participated in this test. They had no known abnormalities of the tactile sensory system and no history of

peripheral vascular disease. This research was approved by the MIT Committee on the Use of Humans as Experimental Subjects.

Apparatus. Although the overall average emissivity of the skin is a generally accepted value, it could vary among different subjects. Using only a subject's fingerpad as the target in the calibration test might therefore introduce variability into the system and make it difficult to evaluate its performance. In order to have a better control of the target emissivity, standard black insulation tape (Scotch Super 33+, 3M) with emissivity similar to the skin (0.95) was used to simulate the fingerpad surface in the first set of calibration tests. The tape was attached to a Peltier device (DT6-6, Marlow) and its surface temperature was controlled using a digital PI control system. In the second part of the test, the subject's fingerpad was used as the target.

Three thermistors (457 μm in diameter and 3.18 mm in length; Model 56A1002-C8, Alpha Technics) were used to monitor the temperatures that are necessary to derive the target temperature. These were the ambient temperature and the temperatures of the contact material and beamsplitter. In the first part of the test, the temperature of the target (black insulation tape) was monitored with a thermistor. In the second part, skin temperature was monitored with a thermistor that was attached to the center of the fingerpad. These thermistors were connected to a Data Acquisition Unit (Model 34970A, Agilent Technologies) which was controlled using a Visual Basic.NET program.

Procedure. An emissivity check was conducted to verify that the overall average emissivity of the target was adequate in characterizing its spectral emissivity within the system's range (7.5 – 13 μm) and to make sure that the system setup did not obscure any thermal radiation that passed through it. This check was done by measuring the target temperature with no contact material and beamsplitter in place. Five target temperatures were selected for this emissivity check: 28, 30, 32, 34 and 36 °C. Each target temperature was repeated three times for a total of 15 trials. The target was placed 10 mm in front of the contact material. For each trial, the temperature of the target was measured with a thermistor and the thermal measurement system simultaneously. The ambient temperature

was measured with a thermistor in free air and U_{amb} can therefore be calculated based on the calibration curve.

After the emissivity check was done, the contact material and beamspliter were placed in their corresponding fixtures for the evaluation of the system's performance. Two different contact materials and beamsplitter combinations were available in this system: BaF_2+beamsplitter and ZnS+beamsplitter. Six target temperatures were chosen: 27, 28, 29, 30, 31, 32 °C. There were 5 repetitions for each condition, which gave a total of 30 trials. The sequence of the trials was randomized. For each trial, the temperature of the target was measured with a thermistor and the thermal measurement system simultaneously. The ambient temperature and temperatures of the optics were measured with three thermistors. U_{amb}, U_{opt1} and U_{opt2} can therefore be calculated based on those temperatures and the calibration curves.

In the second part of the experiment, the subject's fingerpad was the target. Subjects washed their hands with soap prior to participating in the test. A thermistor was glued to the center of the right index fingerpad using biocompatible cyanoacrylate (Liquid Bandage™, Johnson & Johnson). The emissivity check was done with a procedure similar to that described above except that the fingerpad temperature was not controlled. There were 15 trials for each subject. For each trial, subjects placed their right index fingerpad in front of the contact material and transducer holder. The temperature of the fingerpad was measured with a thermistor and the thermal measurement system simultaneously. The ambient temperature was measured with a thermistor in free air to estimate U_{amb}.

After the emissivity check was done, the system's performance in measuring temperature was evaluated using the fingerpad as a target. The procedure was similar to the evaluation with the insulation tape except the fingerpad temperature was not controlled. There were 90 trials for each contact material+beamsplitter combination and they were divided into 6 blocks of 15 trials. These 6 blocks of trials were conducted on 3 successive days with 2 blocks of trials in each day. For each trial, the subject's fingerpad

was placed in front of the contact material without touching it. The temperature of the fingerpad was measured with a thermistor and the thermal measurement system simultaneously. The ambient temperature and temperatures of the optics were measured with three other thermistors to estimate U_{amb}, U_{opt1} and U_{opt2}.

Results. The result of the emissivity check for the standard black insulation tape is shown in Figure 5-8. The target temperature was the temperature controlled by the Peltier device. The calculated temperature was established from the tape emissivity and the following formula, which is based on the thermal radiation measured by the infrared camera:

$$\begin{aligned} U_{tot} &= \varepsilon_{obj} U_{obj} + (1 - \varepsilon_{obj}) U_{amb} \\ \Rightarrow U_{obj} &= \frac{U_{tot} - (1 - \varepsilon_{obj}) U_{amb}}{\varepsilon_{obj}} \end{aligned} \tag{5-4}$$

This formula assumes that the thermal radiation received by the infrared camera consisted of the energy emitted by the target and the ambient thermal energy reflected by the target. Based on the calibration curve, the target temperature can be calculated from U_{tot}. As shown in Figure 5-8, the intercept of the regression line was set to zero and the slope of the regression line was very close to 1 with a high r value. This indicated that the system was able to measure the target temperature accurately given the emissivity of the tape and the formula described in Eq. 5-4. This result further confirmed that the fixtures placed between the target and the infrared camera did not block or affect the thermal energy from the target and surroundings.

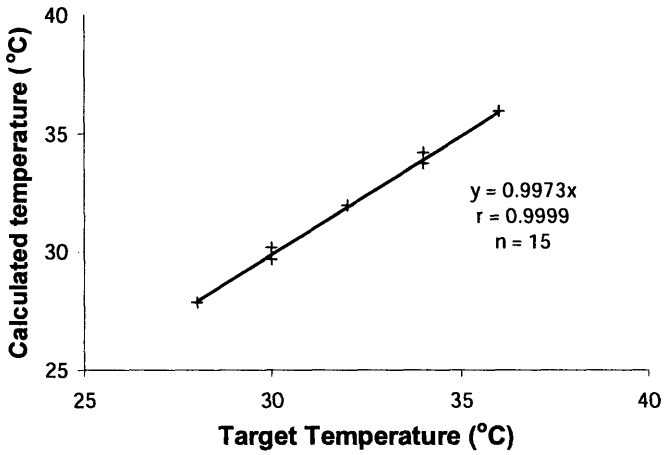

Figure 5-8. Result of emissivity check for black insulation tape.

Although the temperature and the emissivity of the fingerpad was not as uniform as the insulation tape, the result of the emissivity check of the fingerpad shown in Figure 5-9 indicated that the overall average emissivity of the skin was able to provide accurate temperature readings.

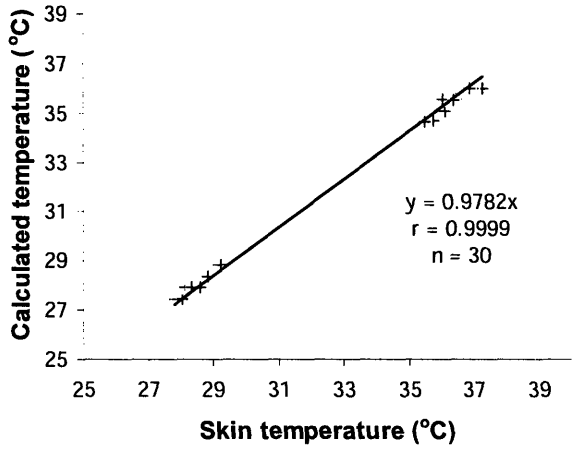

Figure 5-9. Result of emissivity check for fingerpad.

After verifying that the overall average emissivity of the insulation tape and skin was adequate for characterizing their spectral emissivity within the system's range (7.5 – 13 μm), the performance of the system was then evaluated with these targets. The result

of the evaluation with the insulation tape is shown in Figure 5-10. The calculated temperature was derived based on the measured thermal energy and the IR model proposed in this study. The intercept of the regression line was set to zero. The slope of the regression line was very close to 1 with high r values for both the BaF_2+beamsplitter and ZnS+beamsplitter combinations. The coefficients of the two regression lines indicated that the system tended to slightly underestimate the target temperature with the BaF_2+beamsplitter combination and overestimate it with ZnS+Beamsplitter combination.

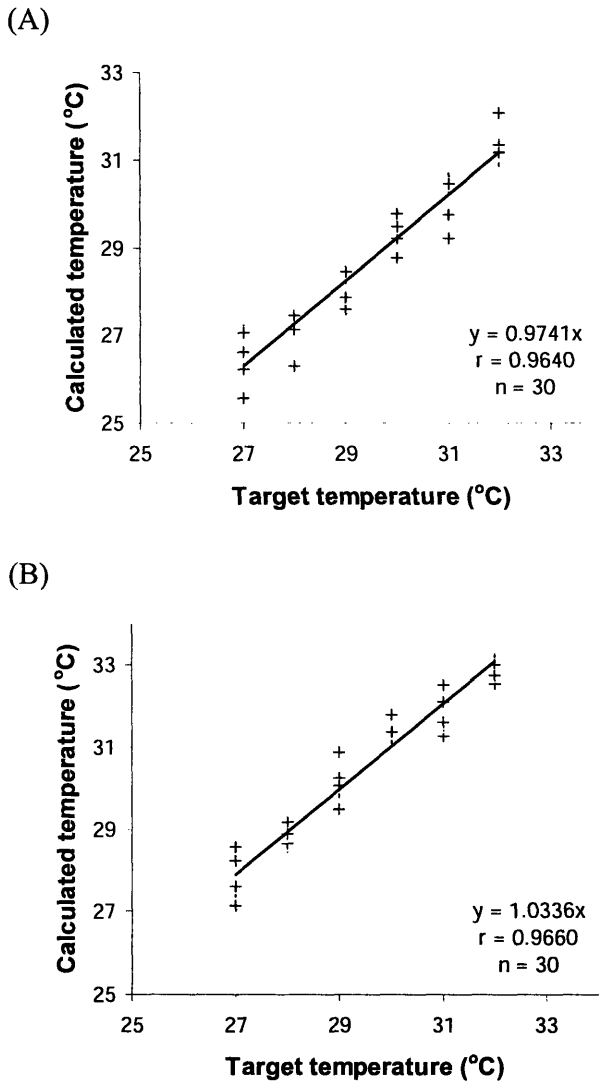

Figure 5-10. System performance evaluation with the insulation tape as the target with BaF_2+beamsplitter (A) and ZnS+beamsplitter (B). The solid line is the regression line.

The system's performance with the fingerpad as target is shown in Figure 5-11. The results were similar to those with the insulation tape and indicated that the system was able to provide accurate temperature readings. The lower r value reflected that the greater scatter among data points and was probably due to the fact that the fingerpad is not as uniform a surface as the insulation tape.

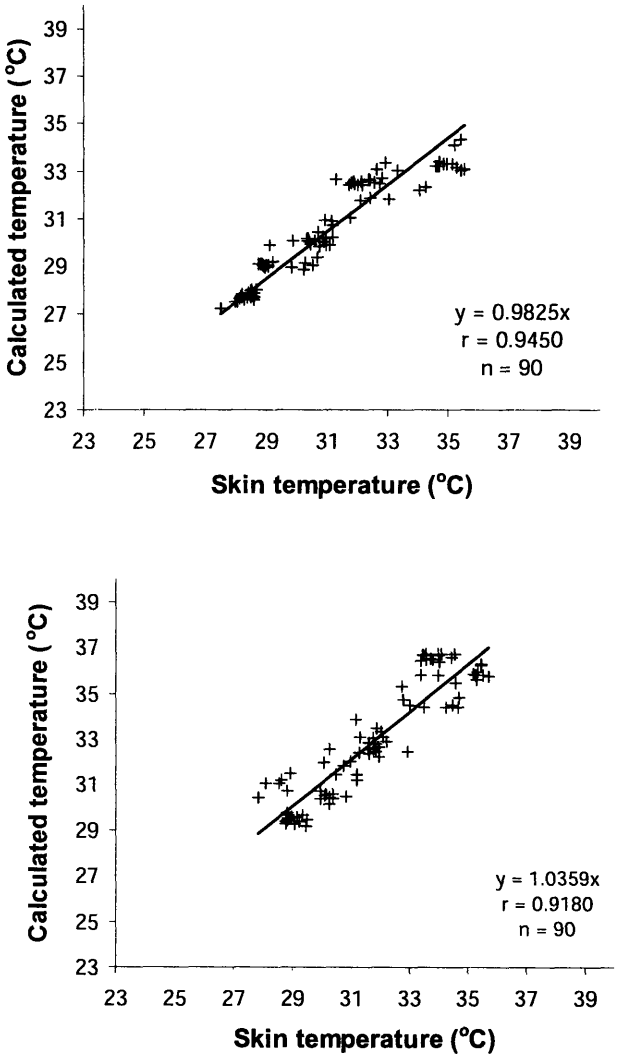

Figure 5-11. System performance evaluation with fingerpad as target with BaF_2+beamsplitter (a) and ZnS+beamsplitter (b). The solid line is the regression line.

After validating that this thermal measurement system was able to provide accurate temperature measurements, the temperature response of the fingerpad during contact with a thermistor attached to the center of the contact area was measured. The thermal image is shown in Figure 5-12. The outer grey section of the image is the background, and the white elliptical area is the fingerpad. The inner grey section inside the elliptical area indicates the region in which the skin temperature decreased during contact. The white region indicated by the arrow shows how a small thermistor (457 μm in diameter and 3.18 mm in length) can deform the fingerpad and influence the change in skin temperature during contact. The slight temperature gradient at the boundary of the inner grey section indicates that the decrease in skin temperature was localized within the contact area. This thermal image confirms the limitations of the thermal sensors in skin temperature measurement that were shown in Figures 5-1 and 5-2.

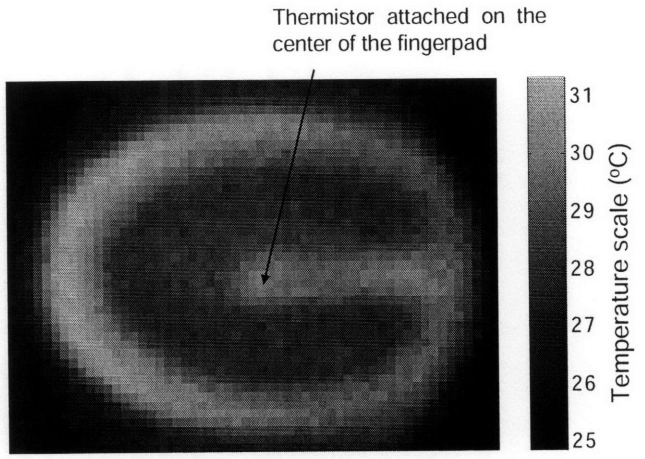

Figure 5-12. Thermal image of a fingerpad making contact with BaF_2 with a thermistor attached at the center of the contact area.

Discussion. In order to measure the contact force and area together with the skin temperature change during contact simultaneously, the contact materials selected for the system were required to be transparent in both infrared and visible spectrum. This requirement limited the selection of contact materials. In addition, the thermal measurement system needed several fixtures between the infrared camera and the target (see Figure 5-5). These fixtures were therefore carefully designed and positioned to prevent them from obscuring the thermal energy emitted from the target. This design goal

was validated by the consistency of the target and calculated temperatures in the emissivity calculation.

The two targets, insulation tape and the fingerpad, used in the present study were both non-transparent and had emissivity values close to 1. Based on the relation $\varepsilon + \tau + \rho = 1$, the effect of the reflection of ambient radiation through the target surface was not significant which greatly reduced the influence of the ambient condition on the measurement of the target temperature. The results of the emissivity check also indicated that using the overall average emissivity was adequate for measuring the target temperature in the present thermal measurement system.

When the contact materials and beamsplitter were added to the system, the sources of radiation that could be detected by the infrared camera increased because those optics were able to transmit, reflect and emit thermal radiation. In order to simplify the problem, it was necessary to assume that the optics were gray bodies and to use their bandpass optical properties to derive the target temperature based on the IR model proposed in this study. Since the beamsplitter was inclined at an angle of 45^{o}, the effect of radiation bouncing back and forth between the contact material and beamsplitter was not significant and therefore was not considered in the IR model.

In order to validate the IR model and evaluate the thermal measurement system, calibration tests were conducted with insulation tape and the fingerpad. During the test, the targets were placed as close to the contact material as possible without touching it in order to precisely monitor the temperature of the targets under conditions similar to the intended application, that is measuring the skin temperature when making contact with the contact material.

With two different contact materials, BaF_2 and ZnS, the results of the calibration tests indicated that the system tended to underestimate the target temperature with the BaF_2+beamsplitter and overestimate it with the ZnS+beamsplitter. This discrepancy may result from one major difference between BaF_2 and ZnS, that is the reflectivity of the two materials. When working with ZnS in the system, the infrared camera was able to 'see'

itself through the reflection from the ZnS surface. With the elevated working temperature of the infrared camera (approximately 30 °C), this extra thermal radiation, which was not considered in the model, caused a slight overestimation of the target temperature. This slight discrepancy in skin temperature measurement can be corrected by dividing the temperature readings with BaF_2 and ZnS by the corresponding slopes of the regression lines in Figure 5-11 (A) and (B).

As shown in Figure 5-12, the thermal sensors were not able to detect the full extent of the temperature change during contact even when they were attached to the center or to the perimeter of the contact area. It is presumably this limitation that caused the measured change in skin temperature to be much lower than the model predictions (See Figure 5-1). In addition, the thermal sensor's own thermal mass may result in its insensitivity to the instantaneous change in skin temperature upon contact so it was not able to capture the time course and amplitude of the change in skin temperature during contact as shown in Figure 5-2.

5.3 CONCLUSION

In this study, an infrared thermal measurement system was designed, fabricated and calibrated so that it could be used to assist in the development of a thermal display. The infrared thermal measurement system is able to provide a more accurate measurement of temperature without the limitations imposed by contact thermal sensors. The layout and optical arrangement of the system enables the measurement of the skin temperature distribution on the fingerpad together with contact force and contact area.

An IR model was proposed to account for the various sources of thermal radiation in order to derive the skin temperature based on the thermal energy detected by the infrared camera. Calibration tests with both insulation tape and the fingerpad as targets validated this IR model and confirmed that the thermal measurement system is able to provide accurate temperature measurements.

The infrared thermal measurement system required that the contact material be transparent in both the infrared and visible spectrum. It was therefore designed to assist in the development of the thermal model by providing a means for recording skin temperature more accurately during contact, and not as a system that would be integrated into a haptic interface. The thermal measurements recorded with the infrared thermal measurement system can then be compared directly to the model predictions of the changes in skin temperature during contact.

CHAPTER 6

THERMAL MODEL REVISION AND VALIDATION

6.1 Thermal Model with Consideration of Thermal Contact Resistance

6.2 Skin Surface Roughness Measurement

6.3 Model Simulation

6.4 Model Validation

6.5 Conclusion

Several thermal models have been proposed to describe the heat transfer process between the skin and an object during contact (Benali-Khoudja et al., 2003; Bergamasco et al., 1997; Citerin et al., 2006; Deml et al., 2006; Ho & Jones, 2004, Ho & Jones, 2006b; Kron & Schmidt, 2003; Shitzer et al., 1996; Yamamoto et al., 2004; Yang et al., 2006aa). With the exception of the model proposed by Benali-Khoudja et al. (2003), which was developed using an electrical analogy, all the other analytical models are based on the bio-heat equation formulated by Pennes (1948), each with different assumptions and boundary conditions. In these analytical models, the initial temperatures and thermal properties of the skin and materials, and the effects of blood perfusion have generally been considered. However, other factors such as the contact pressure and thermal contact resistance, which can affect the thermal responses of the skin, have rarely been evaluated.

The contact pressure imposed by a finger on an object can affect the temperature of the skin in two ways. First, compression of the cutaneous tissue may enhance thermal sensing by increasing the area of contact with the object (Westling & Johansson, 1987). Second, compression can change the finger's temperature by collapsing the blood vessels in the region of compression. This prevents continuous tissue-heat exchange and drives

the blood away from the contact area so that it now accumulates in the capillaries under the nail bed (Mascaro & Asada, 2001).

The presence of thermal contact resistance in the interface between the skin and an object results in a difference in temperature between the skin and object surfaces. As a consequence, the heat flux exchanged during contact will depend on this temperature difference and hence the thermal contact resistance. Analyses of the changes in skin temperature during contact (Chapter 4; Ho & Jones, in press; Yamamoto et al., 2004) have suggested that thermal contact resistance changes with contact force and has a significant effect on the temperature of the skin over the typical contact force range of 1 to 2 N (Ino et al., 1993; Jones & Berris, 2003). In the present study, a thermal model based on the semi-infinite body model (section 3.1; Ho & Jones, 2006a) was further developed to take into consideration the influence of thermal contact resistance on the thermal responses of the skin and object during contact. Since the semi-infinite body model had been validated psychophysically, the new model was evaluated physiologically by comparing the theoretical predictions of temperature changes to those measured experimentally using the infrared thermal measurement system described in Chapter 5.

6.1 Thermal Model with Consideration of Thermal Contact Resistance

The resting temperature of the skin is typically higher than the temperature of objects encountered in the environment. The thermal cues used to identify an object by touch are influenced by the skin surface temperature and the heat flux conducted out of the skin during contact. During this transient process, the heat flux is transferred across the interface by conduction and flows though a thermal contact resistance as shown in Figure 6-1. As long as the contact time is short enough (Ho & Jones, 2006a; Mills, 1999), both the skin and object can be modeled as semi-infinite bodies and the governing equations of the skin and object are:

$$\frac{\partial^2 T_{skin}}{\partial x_1^{\,2}} = \frac{1}{\alpha_{skin}} \frac{\partial T_{skin}}{\partial t} \quad , \quad \left\{ \begin{matrix} t = 0, \ \mathrm{T_{skin}} = \mathrm{T_{skin,i}} \\ \mathrm{x_1} = \infty, \mathrm{T_{skin}} = \mathrm{T_{skin,i}} \end{matrix} \right\} \tag{6-1}$$

$$\frac{\partial^2 T_{object}}{\partial x_2^{\,2}} = \frac{1}{\alpha_{object}} \frac{\partial T_{object}}{\partial t} \quad , \quad \left\{ \begin{matrix} t = 0, \ \mathrm{T_{object}} = \mathrm{T_{object,i}} \\ \mathrm{x_2} = \infty, \mathrm{T_{object}} = \mathrm{T_{object,i}} \end{matrix} \right\} \tag{6-2}$$

The boundary conditions at the interface are given by:

$$q''_{skin,s} = q''_{object,s} = q'' \tag{6-3}$$

$$q'' = \frac{T_{skin,s} - T_{object,s}}{R} \tag{6-4}$$

where T is temperature, α is thermal diffusivity, t is time, q" is heat flux, and R is thermal contact resistance. Subscripts i and s represent the initial and surface conditions, respectively.

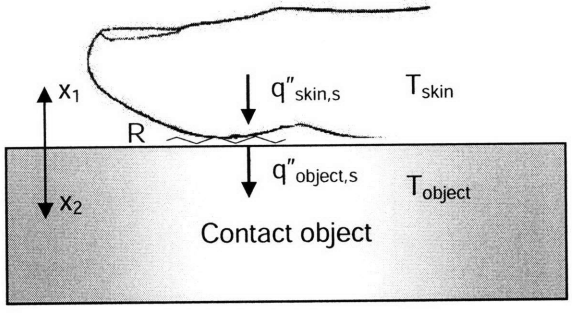

Figure 6-1. Schematic representation of the heat transfer process during hand-object interactions.

By determining the thermal contact resistance, R, and the initial temperatures of the skin, $T_{skin,i}$, and object, $T_{object,i}$, the skin surface temperature, $T_{skin,s}$, the object surface temperature, $T_{object,s}$, and heat flux exchanged during contact, q", can be solved as a function of t:

$$T_{skin,s}(t) = \frac{A}{B}\left\{1 - e^{\alpha_{skin}B^2 t}\,erfc\left[B\sqrt{\alpha_{skin}t}\right]\right\} + T_{skin,i}$$
$$A = \frac{-(T_{skin,i} - T_{object,i})}{k_{skin}R} \quad , \quad B = \frac{1}{k_{skin}R}\left[1 + \frac{(k\rho c)_{skin}^{1/2}}{(k\rho c)_{object}^{1/2}}\right] \tag{6-5}$$

$$T_{object,s}(t) = \frac{C}{D}\left\{1 - e^{\alpha_{object}D^2 t}\,erfc\left[D\sqrt{\alpha_{object}t}\right]\right\} + T_{object,i}$$
$$C = \frac{T_{skin,i} - T_{object,i}}{k_{object}R} \quad , \quad D = \frac{1}{k_{object}R}\left[1 + \frac{(k\rho c)_{object}^{1/2}}{(k\rho c)_{skin}^{1/2}}\right] \tag{6-6}$$

$$q''(t) = k_{skin}A\left\{-e^{\alpha_{skin}B^2 t}\,erfc(B\sqrt{\alpha_{skin}t})\right\} \tag{6-7}$$

where k is thermal conductivity, ρ is density and c is specific heat. The surface temperatures of the skin and object, $T_{skin,s}$ and $T_{object,s}$, and the heat flux exchanged during contact, q", are a function of time, thermal contact resistance, and the thermal properties and initial temperatures of the skin and object.

In order to calculate the thermal responses of the skin and object during contact, the thermal contact resistance must be estimated. The thermal contact resistance model that has been used by Benali-Khoudja et al. (2003) in developing their thermal display is based on the model proposed by Yovanovich (1981). In this model the thermal contact resistance is a function of mechanical, thermophysical and surface properties. With no fluid in the interfacial gap, the thermal contact resistance is given by:

$$R = \left\{ 1.25 k_s \frac{\Delta a}{R_q} \left(\frac{P}{H} \right)^{0.95} \right\}^{-1} \quad (\mathrm{m^2K/W}), \tag{6-8}$$

where k_s is the harmonic mean thermal conductivity of the interface:

$$k_s = \frac{2 k_{skin} k_{object}}{k_{skin} + k_{object}} \quad (\mathrm{W/mK}), \tag{6-9}$$

R_q is the effective root mean square surface roughness:

$$R_q = \left[R_{q\,skin}^2 + R_{q\,object}^2 \right]^{\frac{1}{2}} \quad (\mathrm{m}), \tag{6-10}$$

Δa is the effective absolute average surface asperity slope:

$$\Delta a = \left[\Delta a_{skin}^2 + \Delta a_{object}^2 \right]^{\frac{1}{2}} \tag{6-11}$$

H is the microhardness of the softer material, which is the skin in this situation, and is reported as 12.5 $\mathrm{gm/mm^2}$ (0.1225 MPa) by Dellon et al. (1995). P is the contact pressure and can be determined from the contact force and contact area for a specific contact condition. Refer to Appendix A for detailed definitions of R_q and Δa.

Given that the thermal cues used to identify an object by touch are the skin surface temperature and the heat flux conducted out of the skin during contact, the thermal display must be able to elicit the same responses when simulating a material. Based on equation 6-4, the set temperature of the thermal display, $T_{display}$, that is used to simulate a material can be determined from the following equations:

$$q'' = \frac{T_{skin,s}(t) - T_{object,s}(t)}{R_{skin-object}} = \frac{T_{skin,s}(t) - T_{display}(t)}{R_{skin-display}}$$
$$\Rightarrow T_{display}(t) = T_{skin,s}(t) \cdot \left[1 - \frac{R_{skin-display}}{R_{skin-object}}\right] + \frac{R_{skin-display}}{R_{skin-object}} \cdot T_{object,s}(t) \quad (6\text{-}12)$$

As indicated by Equation 6-12, the thermal display temperature depends on the ratio of the thermal contact resistance at the skin and display interface and skin and material interface, and the skin and object surface temperatures during contact that are predicted from Equations 6-5 and 6-6, respectively. By controlling the surface temperature of the thermal display at $T_{display}$, the display should be able to reproduce the same skin temperature response and heat flux conducted out of the skin as if the user were making contact with the corresponding real material.

6.2 Skin Surface Roughness Measurement

The surface properties of the skin did not appear to be available in the literature and so these had to be measured in order to estimate the thermal contact resistance. For this purpose, an experimental system was constructed to measure the RMS surface roughness and asperity slope of the fingerpad.

6.2.1 Method

Subjects. Ten normal healthy adults (five women and five men) aged between 20 and 30 years participated in this experiment. They had no known abnormalities of the tactile or thermal sensory systems and no history of peripheral vascular disease. There were no calluses on their right index fingerpads. This research was approved by the local ethics committee.

Apparatus. A surface roughness tester (SurfTest SV-3000S4, Mitutoyo) was used for the measurement. The detector of the tester has a 60 degree conical tip and a tip radius of 2

μm. The measuring force of the detector is 0.75 mN and the measuring speed is 1 mm/s. The vertical measurement range of the tester is 800 μm with a resolution of 0.01 μm.

A fixture was constructed using splinting materials (Smith & Nephew Rolyan) as the fingertip and hand supports as shown in Figure 6-2. Elastic fabric strips and Velcro were also used to adjust and fix each subject's hand and fingerpad position during the measurement.

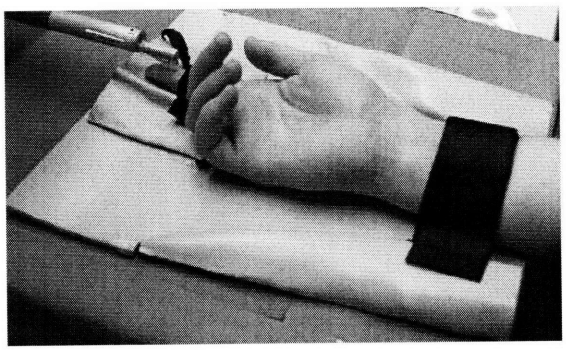

Figure 6-2. Fingertip and hand support.

Procedure. The procedure for selecting the cut-off wavelength, λc, for the surface roughness measurement followed the ISO standard 4288:1996 and was 2.5 mm. The short wavelength cut-off, λs, was 0.025 mm. The measurement was done in both the proximal-distal (PD) and medial-lateral (ML) directions on the right index fingerpad. The number of sampling intervals was three and two for the PD and ML directions, respectively.

Prior to the experiment, subjects washed their hands with soap. The width and length of each subject's right index fingerpad were measured with digital calipers (Absolute digimatic, Mitutoyo). The average width and length was 16.56 and 25.12 mm, respectively. Subjects were instructed to sit in a comfortable posture and place their right hand on the support with their palm facing up. Based on each subject's fingerpad size, the starting point of the measurement was decided and marked. The subject's right index fingerpad was then cleaned with alcohol. The position of the wrist and fingertip was adjusted in order to make the surface of the right index fingerpad level with respect to the

roughness detector and the midline of the fingerpad aligned with the detector. The elastic strips and Velcro were then used to fix the position of the hand. The measurement was repeated five times for the PD and ML directions with the order (PD or ML) randomized. There was a rest period of 5 minutes between the two directions and the total measurement time was approximately 30 minutes.

6.2.2 Results

Following the ISO standard 4287:1997, the roughness parameters that are available are RMS surface roughness, Rq, RMS surface asperity slope, RΔq, and the mean spacing of profile elements, RSm. The surface asperity slope parameter, Δa, used in the thermal contact resistance calculation is not defined in this ISO standard. However, it can be estimated based on the relationship between the average and RMS values of the asperity slope, as proposed by Mikic and Rohsenow (Mikic & Rohsenow, 1966):

$$\Delta a = \frac{R\Delta q}{1.25} \tag{6-13}$$

The results of the surface asperity slope were therefore analyzed in terms of the average asperity slope, Δa. Refer to Appendix A for the detailed definitions of these parameters.

The results for surface roughness, asperity slope and spacing of profile elements of the fingerpad skin are shown in Figures 6-3, 6-4, and 6-5, respectively. A repeated measures analysis of variance (ANOVA) of surface roughness with measurement direction and gender as within and between factors respectively, indicated that there was a significant difference between the two measurement directions ($F(1,8) = 7.409$; $p = 0.026$) but no significant effect of gender ($F(1,8) = 2.098$; $p = 0.186$). The analysis of the asperity slope indicated that there was no significant difference between the two measurement directions ($F(1,8) = 1.886$; $p = 0.207$) or gender ($F(1,8) = 4.280$; $p = 0.072$), although there was a trend for male subjects to have higher asperity slopes. A similar result was found for the spacing of profile elements with no significant difference

between measurement directions ($F(1,8) = 1.399$; $p = 0.271$) or gender ($F(1,8) = 0.001$; $p = 0.978$). The means and standard errors for surface roughness, asperity slope and spacing of profile elements of the fingerpad skin are listed in Table 6-1.

Table 6-1. Surface roughness, asperity slope and spacing of profile elements of the fingerpad skin

Parameter		Mean	Standard error
Rq_{skin} (μm)	ML	23.15	1.73
	PD	20.23	2.21
Δa_{skin} (radian)	ML	0.32	0.03
	PD	0.28	0.03
RSm_{skin} (mm)	ML	0.65	0.04
	PD	0.73	0.04

6.2.3 Discussion

In this experiment, the roughness detector exerted an extremely small force of 0.75 mN as it traveled across the fingerpad, and this caused a slight displacement of the skin. As a result, the surface roughness of the fingerpad measured here is assumed to be influenced by the ridges and furrows on the fingerpad skin and by the pulp tissue underneath, which is similar to the condition when making contact with an object.

The number of cut-offs used to evaluate the surface roughness in the ML and PD directions were two and three respectively which is less than the value of five recommended by the ISO standard. The vertical range of the detector is only 800 μm and the curvature and dimensions of the fingerpad are too small to provide a flat area for measurement with 5 cut-offs across the distance covered.

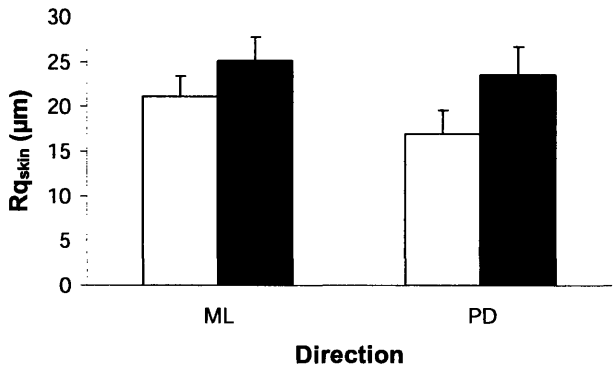

Figure 6-3. Mean and SEM of average root mean square roughness, Rq, as a function of direction and gender (women: white and men: black).

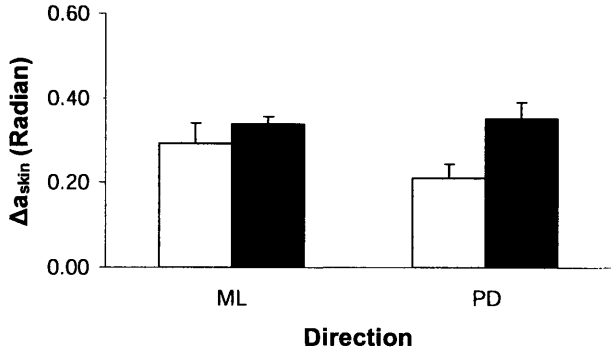

Figure 6-4. Mean and SEM of the asperity slope, Δa, as a function of direction and gender (women: white and men: black).

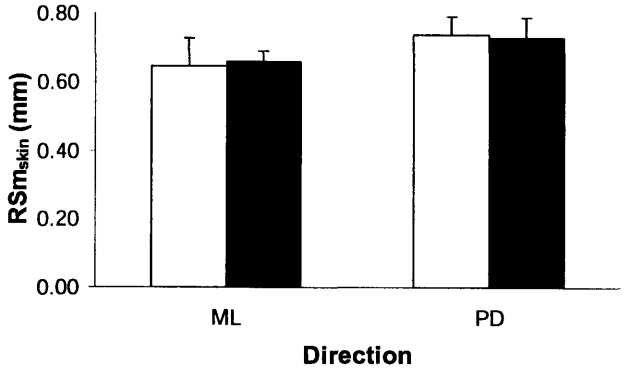

Figure 6-5. Mean spacing and SEM of profile elements, RSm, as a function of direction and gender (women: white and men: black).

Although the ridge lines on the fingerpad typically form a concentric pattern, they are not symmetric in the medial-lateral (ML) and proximal-distal (PD) directions. Therefore, the surface roughness of the fingerpad was measured in both directions. The results indicated that surface roughness is greater in the ML than the PD direction. Based on observations of the fingerprint, the surface roughness of the fingerpad would be expected to exhibit a periodic profile. Measurements of the spacing parameter, RSm_{skin}, indicated that the mean spacing of the ridges is consistent in both measurement directions and is similar for men and women.

The surface asperity slope parameter is not as commonly specified as the height parameter in the literature. Correlations between the surface asperity slope and surface roughness have been reported (Antonetti & Whittle, 1991). However, the surface texture data used to establish these correlations were from solid materials which have a lower surface roughness than the fingerpad ($0.216 < Rq < 9.6$ μm). The surface asperity slope was therefore measured directly in this study. The correlation between Rq_{skin} and Δa_{skin} was not significant for the fingerpad (Pearson's $R = 0.139$, $p = 0.167$), and Δa_{skin} was similar in both measurement directions.

In this small sample of subjects there was no significant difference between men and women with respect to any surface properties measured. This finding is consistent with other studies of the skin on the fingerpad and palm of the hand which have shown that there is no significant difference between men and women in skin thickness (Overgaard Olsen et al., 1995) or hardness (Dellon et al., 1995).

6.3 Model Simulation

Several parameters need to be calculated before performing the simulation using the thermal model. The thermal contact resistance used in this simulation was estimated using the mean RMS surface roughness, Rq_{skin}, and the mean surface asperity slope, Δa_{skin}, averaged across the two directions.

The simulation of the materials used in the experiments in Chapter 4 was performed in order to see if the present model is able to overcome some of the problems of the semi-infinite body model found in the psychophysical and physiological evaluations in Chapter 4. These include the overestimation of skin temperature during contact and the higher surface temperature of simulated materials than real materials during contact, especially for materials with lower contact coefficients. The contact pressure used in this simulation was calculated with a contact force of 2 N and a contact area of 135 mm^2 (measured in section 4.4). The initial temperatures of the fingerpad and materials were set at 34 and 24 ^oC respectively.

With these parameters determined, the skin surface temperature, material surface temperature, and heat flux exchanged were simulated for 10 s of contact. The results are shown in Figures 6-6, 6-7 and 6-8, respectively. As can be seen in Figures 6-6 and 6-7, the surface temperatures of the skin and material change with time and reach a steady state by the end of the contact period. The earlier semi-infinite body model (Section 3.1; Ho & Jones, 2006a; Ho & Jones, in press) predicted that the skin and material surface temperature changed to the interface temperature at the moment of contact and remained constant during the contact period. With the addition of thermal contact resistance to the model, the temperature responses of the skin and materials become more realistic (See Figure 4-12 for the skin temperature responses measured by the thermistor for these five materials).

The thermal responses of the skin and material during contact primarily depend on the material's contact coefficient, $(k\rho c)^{1/2}$, which is also the governing parameter in the semi-infinite body model. As shown in Figure 6-6, the decrease in skin temperature during contact, $T_{skin,i} - T_{skin,s}$ (10 s), increases with the material's contact coefficient. However, the increase in material surface temperature, $T_{material,s}(10\ s) - T_{material,i}$, is smaller for materials with higher contact coefficients. These results indicate that materials with high contact coefficients are able to maintain their own temperature while having a significant influence on the skin surface temperature during contact. As a result, the heat

flux exchanged during contact is also higher for materials with higher contact coefficients as shown in Figure 6-8.

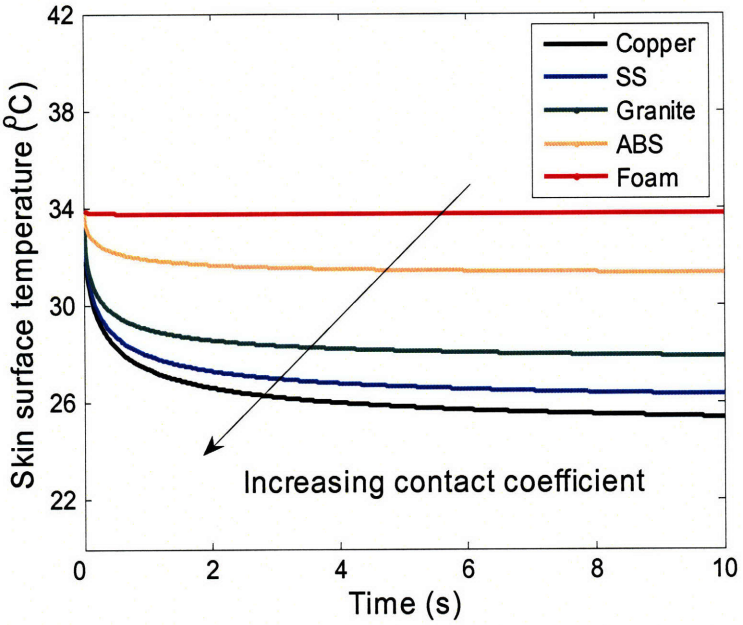

Figure 6-6. Skin surface temperature response when making contact with the materials.

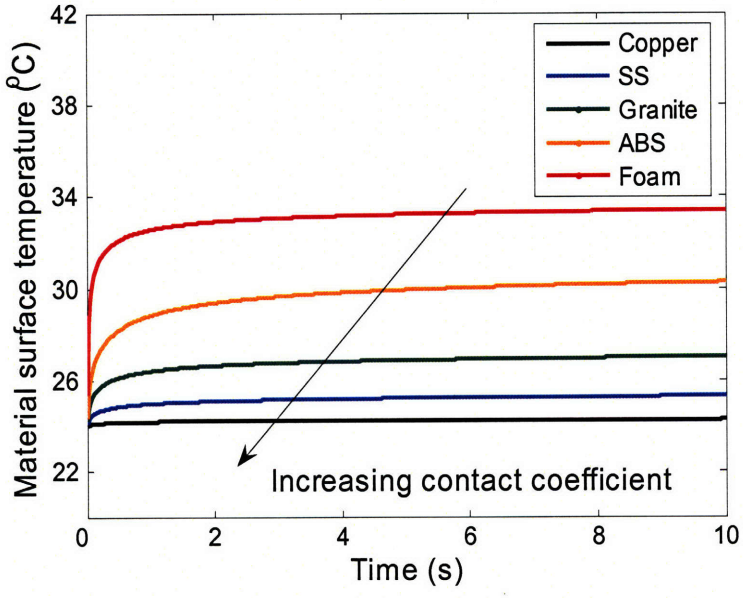

Figure 6-7. Material surface temperature response during contact.

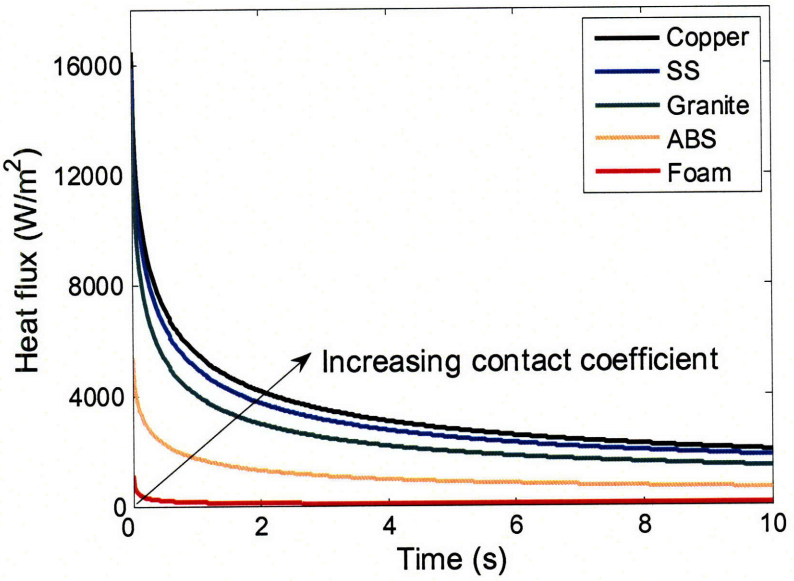

Figure 6-8. Heat flux exchanged during contact.

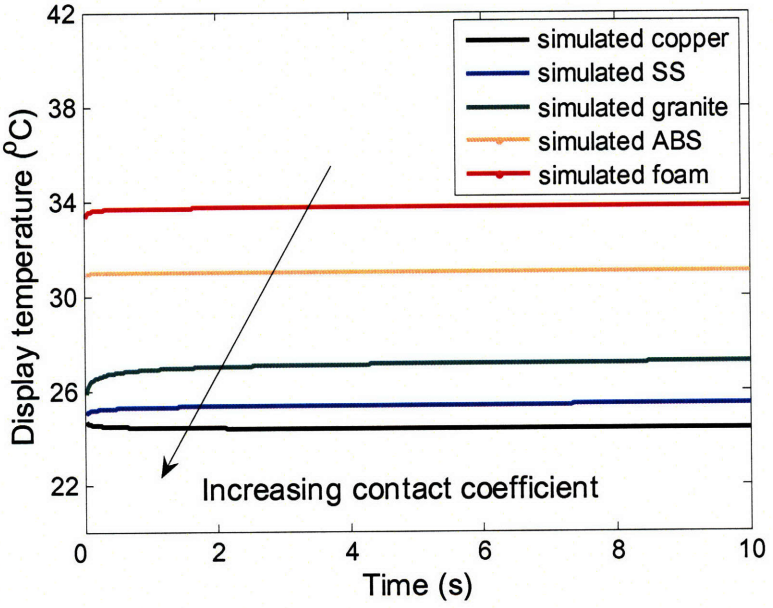

Figure 6-9. Surface temperatures of the thermal display for simulating various materials.

Based on Equation 6-12, the surface temperatures of the thermal display for simulating the five materials, $T_{display}$, are shown in Figure 6-9. These temperatures are a function of the thermal contact resistance between the skin and the real material and the skin and the thermal display, and the surface temperature responses of the skin and material surface during contact. These temperatures reached steady state quickly after contact and their steady state values are within the range of the skin and material surface temperatures. Whether they are closer to the skin or material surface temperature depended on the ratio of the thermal contact resistance between the skin and the real material and the skin and the thermal display. In the present simulation, the ratios of copper, SS and granite are 0.93, 0.90, 0.82, respectively which means that their display temperatures will be similar to their corresponding material surface temperatures during contact. However, the ratios for ABS and foam are 0.30 and 0.07 which indicates that the display temperatures will be closer to the corresponding skin temperature responses during contact.

A comparison between the results predicted by the present model and the semi-infinite body model for the materials used in the experiments is shown in Figure 6-10. It indicates that for all materials the predicted skin surface temperatures during contact are higher for the present model than for the semi-infinite body model. As a result, the present model predicts a smaller decrease in skin temperature than the semi-infinite body model, which means that the prediction is closer to the thermal data measured with the thermistors (see Figure 5-1). The difference between the two models in terms of the changes in skin surface temperature increases with the contact coefficient of the material. For materials with extremely low contact coefficients, such as foam, there is almost no difference between the two skin surface temperature responses, which is consistent with the data presented in Figure 5-1. As can be seen in Figure 5-1, the semi-infinite body model overestimates the change in skin temperature for materials with high contact coefficients, such as copper, but the difference decreases as the contact coefficient becomes smaller. The present model therefore provides a better prediction of the changes in skin temperature when the finger makes contact with materials that span a wide range of thermal properties.

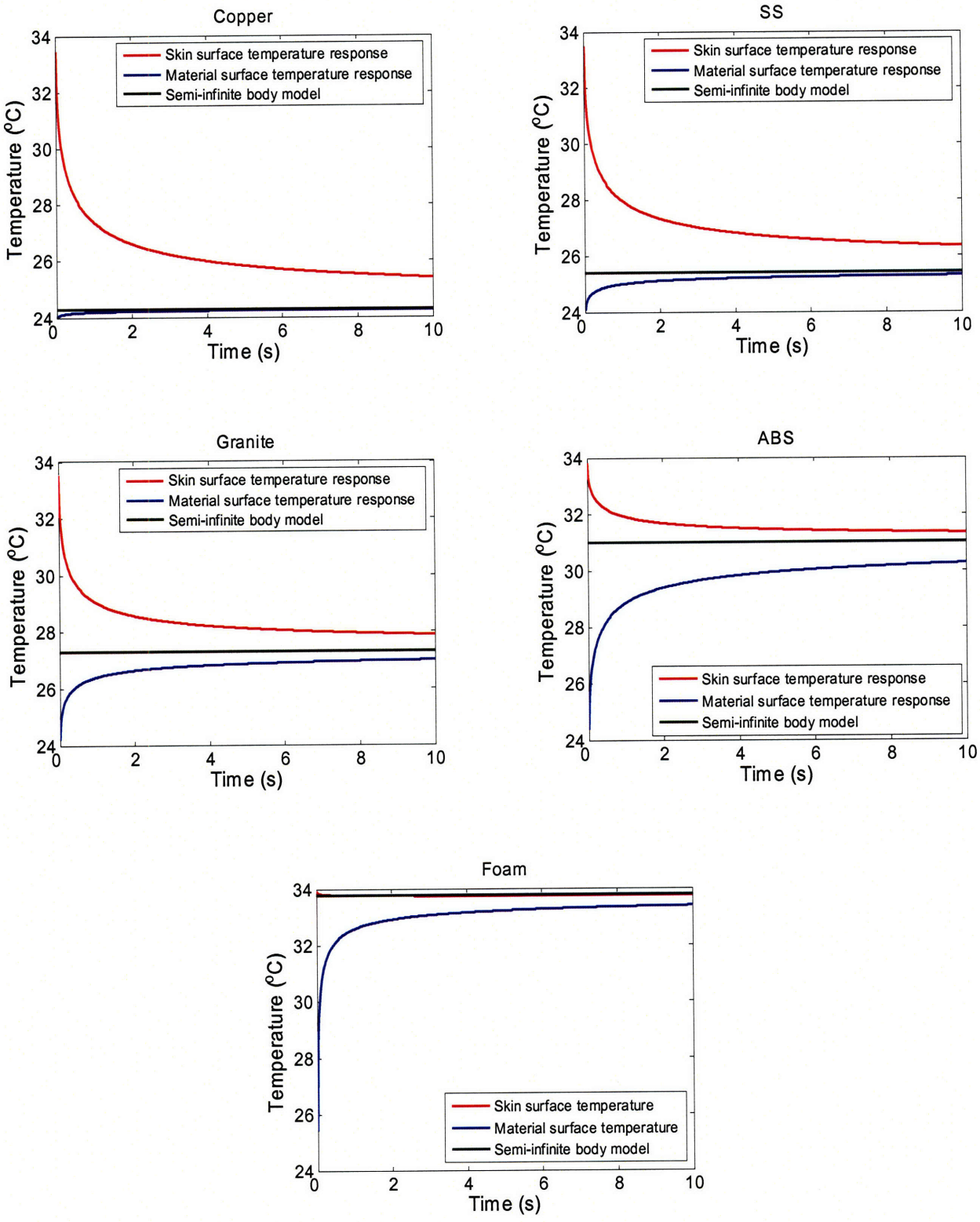

Figure 6-10. Temperature responses upon contact for the skin and material surface predicted by the semi-infinite body model and the revised model

The temperature changes predicted for the material surface during contact are smaller for the present model than for the semi-infinite body model. The difference between the models in their predictions of material surface temperatures becomes smaller for materials with higher contact coefficients. For materials with extremely high contact coefficients, such as copper, there is almost no difference between the two material surface temperature responses. This explains why subjects could not discriminate between real and simulated copper or stainless steel, but felt that the real granite and ABS were colder than the simulated versions based on the semi-infinite body model. For materials with low contact coefficients, the material surface temperature during contact should be lower, as the present model predicts, in order to conduct similar heat fluxes out of skin as real materials and induce similar thermal sensations.

In order to understand the influence of surface roughness and contact pressure on the perceived coldness of an object (which is related to the heat flux conducted out of the skin during contact), another set of simulations was conducted. Based on the present thermal model, these two factors influence the skin temperature response through thermal contact resistance. The material selected for this set of simulations was copper and its properties are listed in Table 4-1. The initial temperatures of the fingerpad and copper were set at 34 and 24 ^{o}C respectively.

In the surface roughness simulation, the typical RMS surface roughness obtained from milling and sawing processes was considered and they are about 8 and 30 μm, respectively (Kalpakjian, 1995). The contact pressure used is the same as that used in the previous simulation. As shown in Figure 6-11, the result of the simulation indicated that the surface roughness could influence the perceived coldness of an object with the major difference occurring within 1 s of contact. When making contact with a smooth surface, the perceived coldness, which depends on the heat flux conducted out of the skin, is greater than when making contact with a rough surface. This suggests that thermal sensations may be changed by altering an object's surface roughness.

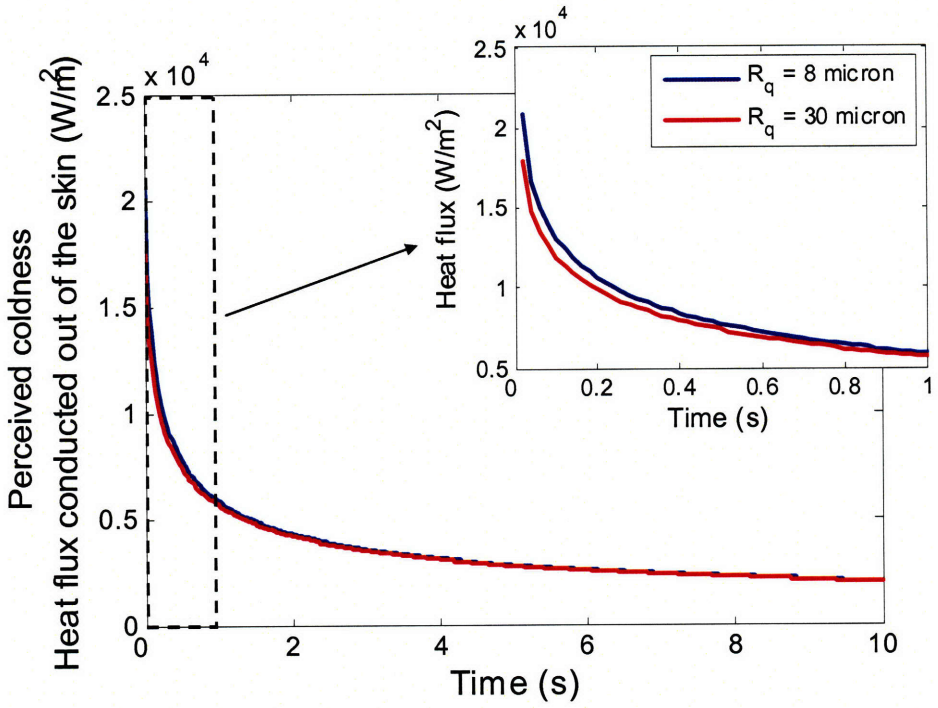

Figure 6-11. Perceived coldness as defined by the heat flux conducted out of the skin when making contact with surfaces with different surface roughnesses.

For the contact pressure simulation, the surface properties used are listed in Table 4-1. The selected contact pressures were 3.14, 5.90 and 10.98 kPa, which are within the typical range for object manipulation (Ino et al., 1993; Jones & Berris, 2003). As shown in Figure 6-12, the results of the simulation indicated that contact pressure could also influence the perceived coldness of an object and that contact pressure affects the heat flux conducted out of the skin throughout the period of contact. When pressing against the surface with a higher force, the perceived coldness, which depends on the heat flux conducted out of the skin, is higher than when making contact with a surface with a lower force. This suggests that the force used to make contact with an object may change the perceived coldness of the object. The simulation results also indicated that the contact pressure seems to have greater influence on the heat flux conducted out of the skin during contact than the surface roughness.

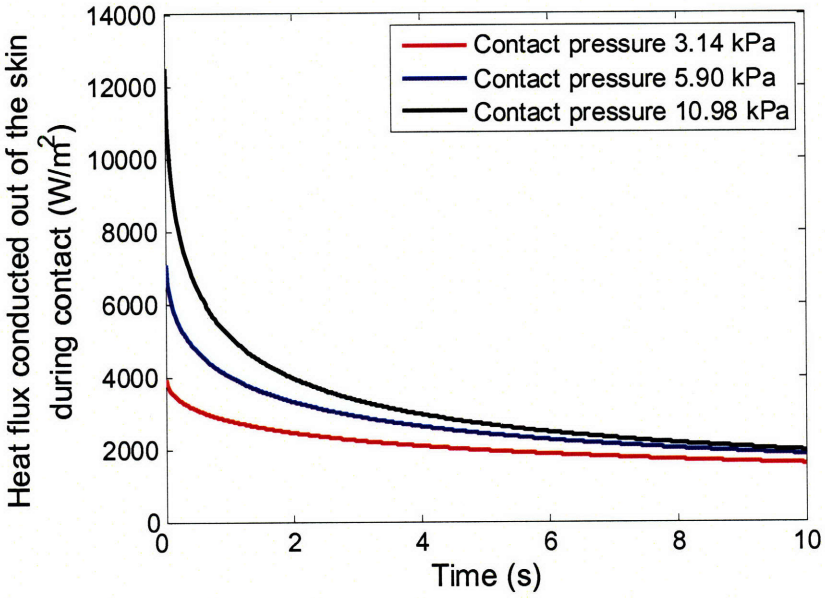

Figure 6-12. Perceived coldness as defined by the heat flux conducted out of the skin when making contact with different contact pressures.

In the present model the responses of the skin and material were determined by the thermophysical and surface properties of the skin and material and their initial temperatures. To simulate thermal contact in a virtual environment, the parameters in this model would need to be specified based on the contact condition. By simulating the temperature responses of the materials with this model, a haptic interface should be able to generate realistic thermal feedback for hand-object interactions.

6.4 MODEL VALIDATION

The simulations indicated that contact pressure could be an important factor in the skin's thermal responses during contact. An experiment was therefore conducted to investigate the influence of contact pressure on skin temperature responses and to determine whether skin temperature changes during contact are localized to the contact region. The thermal model was then evaluated by comparing the theoretical predictions of the changes in skin temperature to the experimental data measured with the infrared thermal measurement system.

6.4.1 Method

Subjects. Ten normal healthy adults (six women and four men), aged between 22 and 31 years, participated in this experiment. They included students and research staff at MIT and Harvard University. They had no known abnormalities of the tactile or thermal sensory systems and no history of peripheral vascular disease. They all reported that they were right-handed. This research was approved by the MIT Committee on the Use of Humans as Experimental Subjects.

Apparatus. The infrared thermal measurement system described in Chapter 5 was used in this experiment. In order to measure the contact area together with the skin temperature change during contact simultaneously, the contact materials used in this system need to be transparent in both the infrared and visible spectrum. In addition, these contact materials had to be safe to handle, and be able to withstand contact pressure and moisture from sweat during contact. With all these requirements, the selection of the contact materials was very limited. The two materials selected for this experiment, BaF_2 and ZnS, are actually very similar in their thermal properties as shown in Table 5-1. The predicted temperature responses based on the proposed model of the skin and material surfaces during contact with the initial skin and material surface temperatures of 34 °C and 26 °C, respectively (they are the average skin and contact material temperatures in this experiment), are shown in Figure 6-13 (A). The corresponding heat flux exchanged during contact is shown in Figure 6-13 (B). As indicated in Figure 6-13, the thermal responses elicited by the two contact materials during contact are very similar, as expected. However, we still chose to use both contact materials in the experiment in order to provide better validation of the model.

Four thermistors (457 μm in diameter and 3.18 mm in length; Model 56A1002-C8, Alpha Technics) were used in this experiment to monitor the ambient temperature and the temperatures of the fingerpad, contact material and beamsplitter. The thermistor, which monitored the skin temperature of the index finger, was attached on the side of the fingerpad so that it did not interfere with contact. These four thermistors and the force transducer were connected to two Data Acquisition Units (Model 34970A, Agilent

Technologies and NI DAQPad-6020E, National Instruments) which were controlled using a Visual Basic.NET program. The skin temperature and contact force were sampled at 20 Hz and 30 Hz, respectively, and the other temperature data were sampled at 1 Hz. To ensure that the skin temperature of the hand was maintained constant at 34 °C prior to each trial, the recirculating chiller pad used in the previous experiments was also used in this experiment.

(A)

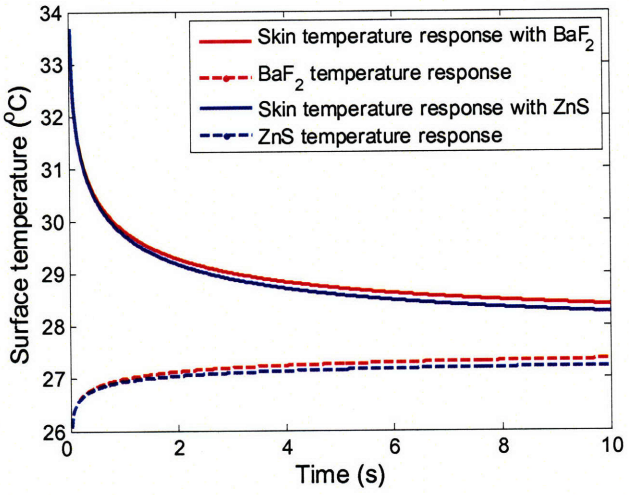

(B)

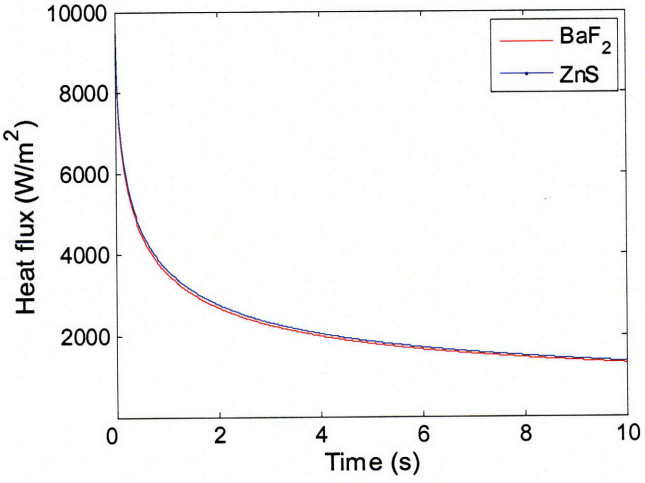

Figure 6-13. (A) Surface temperatures of the skin and material and (B) corresponding heat fluxes exchanged during contact based on the proposed thermal model.

Procedure. Subjects washed their hands with soap prior to participating in the experiment. The width and length of each subject's index fingerpad were then measured with digital calipers (Absolute digimatic, Mitutoyo). The mean width and length were 16.3 mm and 24.0 mm, respectively. Subjects' fingerpads were then cleaned with isopropyl rubbing alcohol. A thermistor was glued to the side of the index fingerpad using biocompatible cyanoacrylate (Liquid Bandage™, Johnson & Johnson). The thermistor was 457 μm in diameter and 3.18 mm in length, and was chosen on the basis of its small dimensions and thermal mass. Subjects' initial skin temperatures ranged from 31.2 °C to 35.6 °C, with the average of 34.6 °C. The average room temperature, contact material temperature and beamsplittter temperature during the experiment were 23.7 °C, 25.9 °C and 23.9 °C respectively, as measured with the thermistors.

Five target contact forces were chosen to investigate the influence of contact pressure on skin temperature. They were 0.1, 0.25, 0.5, 1 and 2 N. Each contact material (BaF_2 and ZnS) was paired with these five target contact forces, which gave a total of 10 combinations. These 10 combinations were repeated six times for a total of 60 trials. The contact materials were presented alternatively in each block of 15 trials, and the contact material that was presented in the first block was randomized across subjects. Within each block of 15 trials target contact forces were randomized. There was at least a 1-minute break between each block of trials, during which the subjects placed their hands on the recirculating chiller.

Prior to each trial, subjects were instructed to place their right hands on the recirculating chiller to maintain their skin temperature at 34 °C. After hearing a sound cue, subjects moved their hands toward the contact material and transducer holder. After 5 seconds a second sound cue was presented, and subjects were instructed to make contact with the contact material while trying to match the target contact force presented on a computer screen placed in front of them. The target force and real-time feedback of the actual contact force were presented on the screen as two lines and subjects were asked to overlap these two lines in order to match the force during contact. During 10 s of contact, the thermal and digital cameras captured images of the fingerpad, and the data

acquisition system recorded the data from the four thermistors and the force transducer. At the end of each trial, subjects withdrew their hand from the fixture. They were asked to wipe the contact material with a lens wipe and then placed their hands back on the recirculating chiller pad. A photograph of the hand in contact with the material is shown in Figure 6-14.

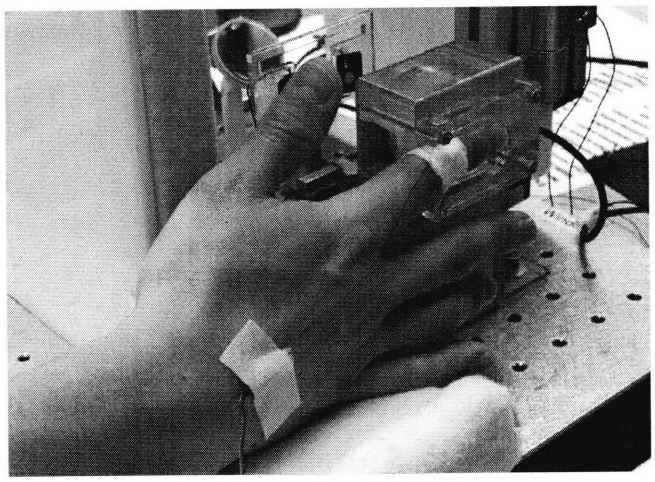

Figure 6-14. Hand position when subject made contact with the material.

6.4.2 Results

The finger forces measured in this experiment indicated that subjects were able to produce the target forces accurately. The time history of the measured contact force and the average contact force for the last 2 s of contact are shown in Figures 6-15 and 6-16, respectively. As can be seen in Figure 6-15, the time taken to reach the target force progressively increased as a function of force amplitude. However, by the end of the contact period, subjects were able to match all the target contact forces extremely well as judged by the very small standard deviations.

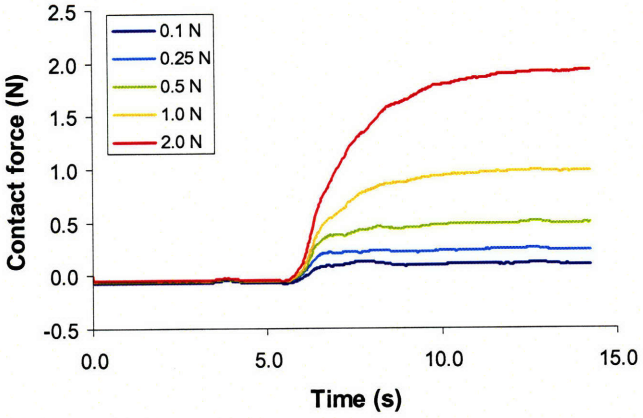

Figure 6-15. Time history of the measured contact force. Data averaged across 120 trials for each force level.

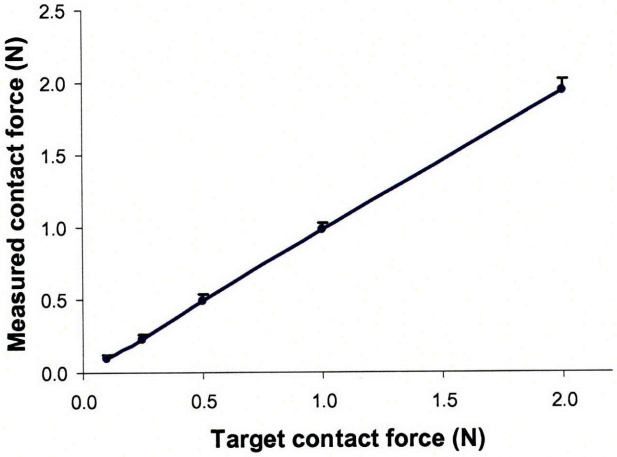

Figure 6-16. Average contact force for the last 2 s of contact. Data averaged across 120 trials for each force level. The data points are connected with a line and the standard deviations are shown.

Images of the change in contact area with contact force are shown in Figure 6-17. The contact area on the fingerpad was marked using image processing software (PhotoImpact, Ulead), and MATLAB (MathWorks, Inc) was used to process these images in order to calculate the contact area. The influence of contact pressure on blood flow is also shown in this figure. As contact pressure increased, the blood within the fingerpad was driven away from the contact area and the fingerpad started to whiten. The nonlinear relation between contact force and contact area is shown in Figure 6-18. The change in contact area between 0.1 and 2 N is about 50 mm^2, and 70% of this change

occurred at contact forces below 1 N. The contact pressures for the five contact forces were calculated from the corresponding contact areas and they were 0.73, 1.68, 3.14, 5.90 and 10.98 kPa, respectively.

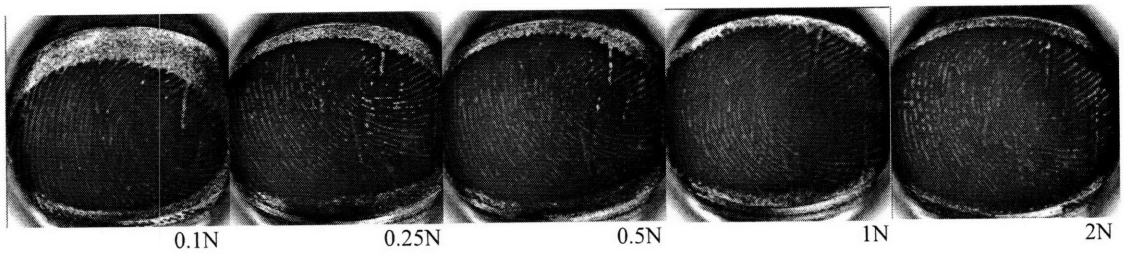

Figure 6-17. Typical images of the contact area at each target contact force.

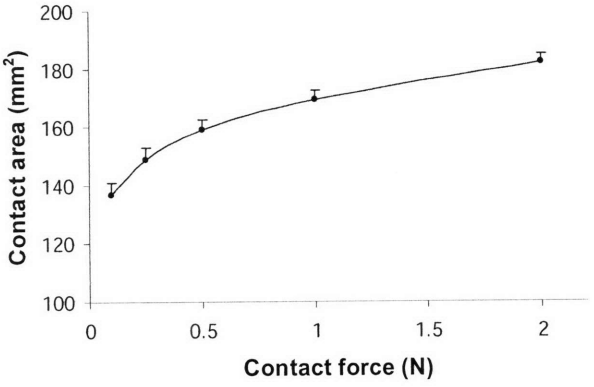

Figure 6-18. Relation between the contact force and contact area. Data averaged across two contact materials and 10 subjects. The data points are connected with a line and the standard errors of the mean are shown.

The decrease in skin temperature during 10 s of contact as measured by the IR camera was calculated as the difference between the initial skin temperature and the skin temperature that was averaged across the contact area at the end of the contact period. The model prediction and measured decrease in skin temperature when making contact with BaF_2 and ZnS are shown in Figures 6-19 (A) and (B), respectively. A repeated measures ANOVA with contact material and target contact pressure as within factors and the decrease in skin temperature as the dependent variable indicated that there was no significant difference between the two contact materials ($F(1,9)=2.726$, $p=0.133$), but a

significant difference among the five contact pressures ($F(4,36)=42.194$, $p < 0.001$). Tests of within subject contrasts indicated that the five contact pressures were all significantly different from one another except 1.68 and 5.90 kPa. There was no significant interaction ($F(4,36)=0.653$, $p=0.629$). These results indicated that there was no difference between the thermal responses induced by BaF_2 and ZnS, and that the contact pressure had an influence on the decrease in skin temperature during contact. The decrease in skin temperature generally increased with contact pressure but reached a maximum at a contact pressure of 3.14 kPa.

The thermal model predicted that skin temperature would decrease as a function of contact pressure. For contact pressures below 3.14 kPa, the model predicted that the decrease in skin temperature would increase rapidly with contact pressure, and that for contact pressures greater than 3.14 kPa, the decrease in skin temperature would change much more slowly with increases in contact pressure. A comparison between the measured data and the theoretical predictions indicates that the model tended to underestimate the decrease in skin temperature during contact for contact pressures below 3.14 kPa. For contact pressures larger than 5.90 kPa, the difference between the model predictions and the measured data was small and was generally within 1 ^{o}C.

The model predictions and the measured skin temperature response during contact are shown in Figure 6-20. The data indicate that the skin temperature approached a steady state value within 2 s of contact for both contact materials and all contact pressures. These skin temperature responses are consistent with the thermal model predictions, with a difference of about 1 ^{o}C at the end of the contact period.

(A)

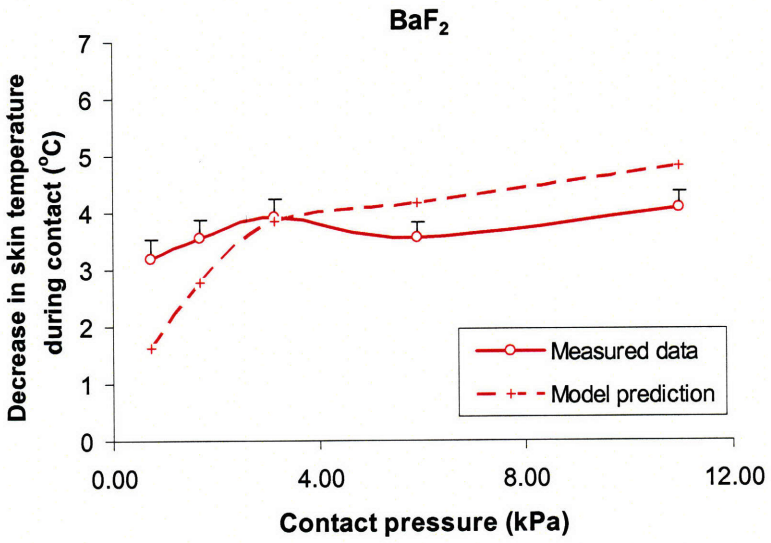

(B)

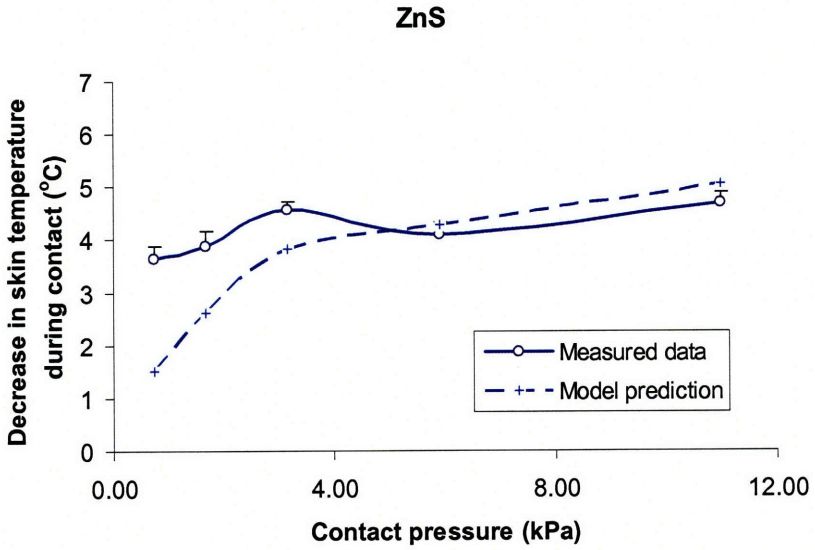

Figure 6-19. Model prediction (dashed line) and the mean of the measured decreases in skin temperature during 10 s of contact (solid line) with BaF_2 (A) and ZnS (B). The standard errors of the means are shown.

(A)

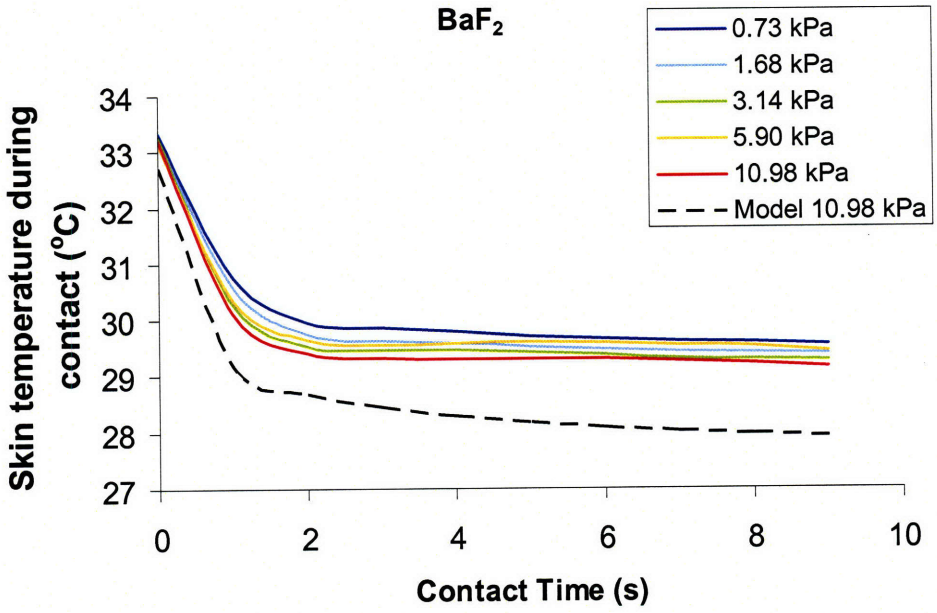

(B)

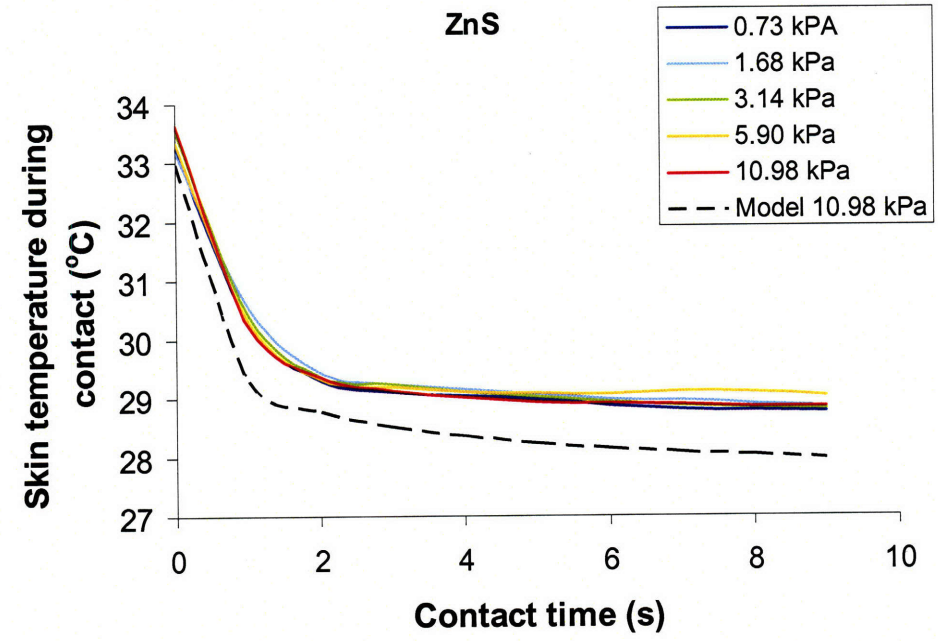

Figure 6-20. Model prediction (dashed line) and measured (solid line) time history of the change in skin temperature during 10 s of contact with BaF_2 (A) and ZnS (B).

The changes in skin temperature during 10 s of contact, $T_{skin,10s}$-$T_{skin,initial}$, as detected by the thermistor attached to the side of the fingerpad are very small as shown in Figure 6-21 and average 0.05 °C. This indicates that the thermistor was not able to detect the change in temperature even though it was only 2 or 3 mm away from the contact area. This result again confirmed the limitation of thermal sensors in skin temperature measurement during contact. A repeated measures ANOVA with contact material and target contact pressure as within factors and changes in skin temperature as the dependent variable indicated that there was no significant difference between contact materials ($F(1,9) = 0.860$, $p = 0.378$), but a significant difference among target contact pressures ($F(4, 36) = 11.191$, $p < 0.001$). There was no significant interaction ($F(4,36) = 2.111$, $p = 0.1$). These results indicate that contact pressure did influence the changes in skin temperature at the side of the fingerpad during contact and that the skin temperature tended to increase at low pressures and decrease at high pressures. This may be due to the effects of contact pressure on blood flow within the fingerpad during contact.

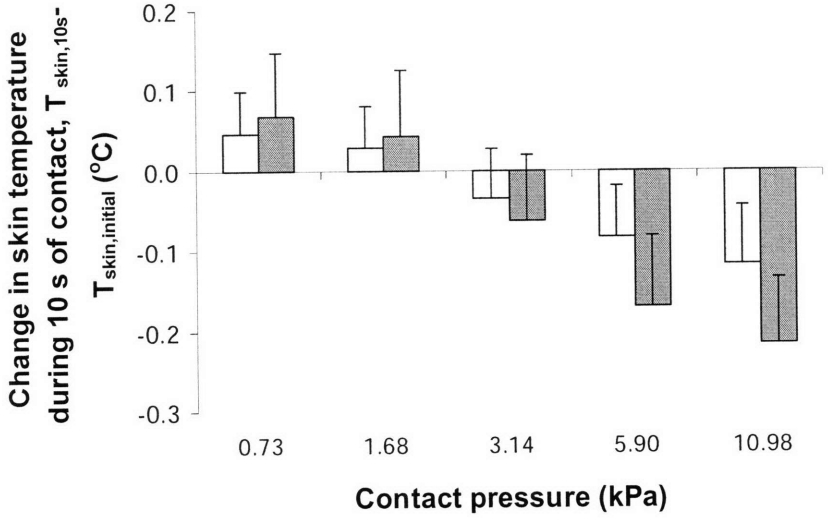

Figure 6-21. Group mean change in skin temperature during 10 s of contact as measured on the side of the fingerpad. Trials with BaF_2 are shown in white and those with ZnS are shown in grey. The error bars represent the standard errors of the mean.

6.4.3 Discussion

Previous studies have suggested that the change in skin temperature during contact is localized to the contact region because the change in skin temperature measured on the perimeter of this region is considerably lower than predicted (section 5.1; Ho & Jones, 2004; Ho & Jones, 2006a). One of the objectives of the present study was to determine how much skin temperature changed during contact and if this depended on the contact pressure. The changes in skin temperature captured by the infrared measurement system indicated that skin temperature decreased by about 3-5 °C during 10 s of contact. In comparison, the thermistor that was affixed 2 or 3 mm away from the contact area was only able to detect an average temperature change of 0.05 °C. The temperature changes detected by the thermistor attached on the perimeter of the contact area in the previous studies (section 5.1; Ho & Jones, 2004; Ho & Jones, 2006a) are consistent with these two sets of values. The image of the temperature distribution during contact (see Figure 5-12) shows that a small temperature gradient existed at the boundary of the contact area and hence a sensor placed on the perimeter would only be able to detect a small temperature change. These results demonstrate the localized nature of the change in skin temperature during contact and the limitations imposed by placing a thermal sensor on the margin of the contact area.

When the fingerpad makes contact with a surface, the contact area begins as a single point and grows rapidly in size at low contact forces (Pawluk & Howe, 1999). At forces of less than 1 N, the fingerpad is relatively compliant (Serina et al., 1997), but it stiffens at high contact forces and so the change in contact area with force becomes limited (Westling & Johansson, 1987). These viscoelastic properties determine the relation between contact force and contact area. In the present study, a nonlinear relation between contact force and contact area was determined with 70% of the overall change in contact area occurring at contact forces below 1 N. The contact forces used for tactile exploration with a single finger are typically less than 1.5 N and for some tasks such as determining surface friction (Smith & Scott, 1996) or locating a small feature in a smooth surface (Smith et al., 2002) are less than 0.5 N. The forces studied in this experiment are therefore comparable to those used for manual exploration (Jones & Lederman, 2006).

The thermal model proposed in this study is a function of the initial temperatures and thermal properties of the skin and object and the pressure during contact. Both the model predictions and the experimental data indicate that contact pressure is significant. As the fingerpad makes contact with a surface, the pressure imposed by the finger on the surface can affect thermal responses in two ways. First, the compression of the finger may enhance the heat flux conducted out of the skin by decreasing the thermal contact resistance at the interface. Both the model and experimental data indicated that the change in skin temperature generally increased with contact pressure. Secondly, compression can affect the finger's temperature by collapsing blood vessels and forcing the blood away from the contact region. Although the digital arteries, which are protected by the underlying bone, are unaffected by the pressure exerted by the fingerpad, the larger, more compliant digital veins which run lateral to the bone have a lower internal blood pressure and are more susceptible to collapse with pressure (Mascaro & Asada, 2001). The collapse of the blood vessels can easily be observed in the change in color of the fingerpad as shown in Figure 6-17.

For contact forces below some threshold, probably around 0.3 N, the blood vessels in the fingerpad are barely affected by compression (Mascaro & Asada, 2001) and a small amount of bloods tends to accumulate at the side of the fingerpad causing a slight increase in skin temperature during contact. This was apparent in the readings from the thermistor for the corresponding contact pressure range (See Figure 6-21). In the low pressure range, the major influence of contact pressure on skin temperature comes from thermal contact resistance. In the present study, the decrease in skin temperature increased with contact pressure for pressures smaller than 3.14 kPa, which was consistent with the model predictions. However, the model tended to underestimate the change in skin temperature at low contact pressures. Given the fact that the blood flow is barely affected in this pressure range, the effects of blood perfusion might have a significant influence on the skin temperature response. The results also suggests that the thermal contact resistance estimation model (Yovanovich, 1981) used in the present study is not adequate for predicting thermal contact resistance over this pressure range. A thermal

contact resistance model has not been developed specifically for skin-object interactions, and so the model proposed by Yovanovich (1981) is used in the present study and by Benali-Khoudja et al. (2003). However, this model is proposed for an interface formed by two conforming, rough surfaces with no fluid in the interface and with contact pressures ranging between 35 and 350 kPa. In the present study the contact pressures were considerably smaller than 35 kPa. As a result, the model is limited in its ability to predict the influence of thermal contact resistance on skin temperature.

When the contact force is between 0.5–1 N, the digital veins at the side of the finger and the capillaries in the pulp are collapsed with compression (Mascaro & Asada, 2001), and the fingerpad starts to whiten. Due to the collapse of the digital veins, blood flow is constrained and as a result, the skin temperature on the side of the fingerpad decreases during contact as indicated by the thermistor readings for the corresponding pressure range. In this pressure range, the contact pressure influences skin temperature through both thermal contact resistance and blood flow. Because the present thermal model only considered the effect of thermal contact resistance, it predicted that the change in skin temperature during contact would increase with contact pressure. However, the measured change in skin temperature during contact decreased with increasing contact pressure. This suggested that the collapse of the veins and capillaries resulted in an accumulation of blood in the capillaries under the nail bed (Mascaro & Asada, 2001) and an increase in skin temperature. This may contribute to the reduced decrease in temperature during contact in this pressure range.

For contact forces higher than 1 N, the veins and capillaries are almost blocked and the color of the fingerpad stops whitening with further increases in contact force (Mascaro & Asada, 2001). The continuous tissue-heat exchange provided by blood perfusion can no longer occur and thermal contact resistance again becomes the major influence on skin temperature during contact. This hypothesis is supported by the consistency between the model predictions and measured data over the corresponding pressure range. They both indicate that the decrease in skin temperature becomes greater with contact pressure and the difference between the model predictions and measured

data is less than 1 °C. One reason why the predicted decrease in skin temperature differed from the experimental data is that both the skin and object are not 'semi-infinite' objects as assumed in the model, and the skin has an internal source of heat generation. However, this slight difference suggests that the effects of blood perfusion and metabolic heat generation on skin temperature may not be significant for contact forces between 1 and 2 N.

In the present study the decrease in skin temperature stabilized within 2 s of contact with an amplitude range of between 3 and 5 °C for various contact pressures. The time course and amplitude of the thermal responses are comparable to those reported by Ino et al. (1993) and Yamamoto et al. (2004) who showed an immediate decline in skin temperature upon contact with materials which then stabilized within 2 s of contact. The reported decreases in skin temperature when the hand makes contact with glass, ceramic or aluminum, which have similar thermal properties to the contact materials used in the present study, are 3.1, 2.7 and 6.9 °C respectively. These values are comparable to the decrease in skin temperature measured in the present experiment.

6.5 CONCLUSION

The thermal model proposed in the present study is able to predict the temperature responses of the skin and material surface and the heat flux exchanged during contact. The simulation results obtained with this model account for the discrepancy between the previous semi-infinite body model and the results from the model evaluation in Chapter 4. The influences of surface roughness and contact pressure were also demonstrated in the simulation. Based on the present model, the predicted changes in skin temperature during contact for contact pressures larger than 3.14 kPa are within 1 °C of those measured using an infrared thermal measurement system. In addition, the model predictions of the time course and amplitude of the skin's temperature response during contact agree with the experimental data. This indicates that the present thermal model is

able to characterize the thermal responses of the skin during contact over the range of contact forces used in manual exploration.

The interaction between the fingerpad and an object during contact is dynamic, and the skin temperature responses are affected not only by thermal properties but also by the surface and mechanical properties of the skin and object. With the addition of thermal contact resistance to the model, the influence of surface and mechanical properties on skin temperature were characterized during contact and more realistic time constants for the thermal responses of the skin and material were obtained. The predicted decrease in skin surface temperature during contact was more similar to the empirical data than that predicted by the semi-infinite body model.

In addition to thermal contact resistance, contact pressure also influences the change in skin temperature by altering the blood flow in the fingerpad. However, this appears to be significant only for contact pressures between 3.14 and 5.90 kPa. For contact pressures lower than this range, the major influences on the change in skin temperature are thermal contact resistance and blood perfusion. For contact pressure higher than this range, thermal contact resistance is the major influence of the skin temperature response.

The thermal measurement system that has been developed in this study overcame the limitations of conventional contact thermal sensors and also provided an image of the temperature distribution across the fingerpad rather than a single point measurement from a thermal sensor. The measurements obtained with this system demonstrated that skin temperature changes during contact are localized to the contact area and that the proposed thermal model can predict the changes in skin temperature during contact.

CHAPTER 7
CONCLUSIONS

7.1 SUMMARY AND CONTRIBUTIONS

The goal of this thesis was to develop a thermal model that could be implemented in a thermal display as part of a haptic interface and provide realistic feedback about the thermal properties of objects during hand-object interactions. The thermal model was evaluated from both a psychophysical and physiological perspective by comparing the performance of the thermal display in which the model was implemented with the performance of subjects with real materials. The psychophysical studies evaluated whether the model was able to elicit realistic thermal sensations when simulating a material with the thermal display by comparing subjects' performance in material discrimination and identification with real and simulated materials. The physiological experiments examined if the model was able to provide reasonable predictions of the skin temperature responses during contact by comparing the measured changes in temperature to the model's predictions.

The first series of experiments was conducted to evaluate whether subjects could discriminate between real materials that spanned a wide range of thermal properties based only on thermal cues. The results confirmed that people are able to discriminate between materials using only thermal cues and further quantified the difference in thermal properties required for reliable discrimination. Of the various material combinations presented to the hands, subjects were able to discriminate reliably between two materials when the ratio of the contact coefficients of the materials exceeded three.

In a further study that examined the ability to localize thermal changes, subjects had to identify which of three fingers on the same hand was in contact with a target material that was different from the other two distractor materials using only thermal cues. The results indicated that subjects could reliably identify the location of the target material when the ratio of the contact coefficients of the materials exceeded 14 or 82, depending on whether the target or distractor material caused more cooling on the fingerpad. It is likely that spatial summation, and hence poor localization of thermal changes on the fingers, contributed to the inferior performance in this experiment as compared to the material discrimination experiment.

A semi-infinite body model was selected as the initial simple, but representative thermal model. The model was implemented in a thermal display comprising a Peltier device, thermistors and PI digital temperature control. This display simulated the thermal cues associated with making contact with materials that spanned a wide range of thermal properties. The performance of the model and display was evaluated in both psychophysical and physiological experiments by comparing subjects' performance in material discrimination and identification tasks with real and simulated materials and by comparing the measured skin temperature responses to those predicted by the model. Although performance with materials simulated by the display was not significantly different from that with real materials in material identification and discrimination tasks, subjects indicated that some real materials felt colder than their simulated counterparts (eg. real and simulated ABS) especially for materials with lower contact coefficients. In addition, the results of the physiological evaluation indicated that the measured changes in skin temperature when making contact with real or simulated materials were much smaller than the model predictions. These results showed that the semi-infinite body model was not able to provide a reasonable description of the change in skin temperature during contact.

It has been suggested that thermal contact resistance can influence the skin temperature response within the force range typically used for manual exploration. The thermal model was therefore further developed to account for the influence of thermal

contact resistance on skin thermal responses during contact. By incorporating the concept of thermal contact resistance, this model was able to capture the mechanical aspects of the process, such as contact pressure and surface roughness, on the thermal response of the skin. The model is therefore able to account for more contact conditions than the existing thermal models by changing input parameters, such as contact pressure, the initial temperatures of the skin and object, and the material properties and surface features of the object. The transient temperature responses of the skin and material, together with the heat flux conducted out of the skin during contact can also be simulated with this model.

In addition to the limitations of the semi-infinite body model, another source of error in measuring the skin temperature changes during contact may have resulted from the thermal sensors which were positioned on the margin of the contact area. An infrared thermal measurement system was therefore developed in this research to overcome the limitations of conventional contact thermal sensors and to assist in the physiological evaluation of the proposed thermal model. The infrared thermal measurement system was able to provide an image of the temperature distribution across the fingerpad rather than a single point measurement from a thermal sensor, and did not interfere with the contact between the skin and material. The system used a carefully devised layout and optical arrangement so that the skin temperature distribution on the fingerpad would be measured simultaneously with the contact force and contact area. Based on the data obtained with this system, the influence of contact pressure on the skin temperature response during contact was investigated.

The infrared thermal measurement system was used to conduct a physiological evaluation of the thermal model. A comparison between the thermal responses of the finger and the model predictions of the skin temperature responses during contact indicated that the difference between the measured and predicted changes in skin temperature was 1 ^{o}C for contact pressures higher than 3.14 kPa. In addition, the model's predictions of the time course and amplitude of the skin's temperature response during contact agreed with the experimental data. These results indicate that the thermal model

proposed in this research is able to characterize the thermal responses of the skin during contact over the range of contact forces used in manual exploration. A haptic display that incorporated thermal feedback based on this model should therefore be able to convey thermal cues that can be used to perceive and identify objects as effectively as those provided by real materials.

In summary, this thesis proposed and validated a thermal model that is able to characterize the thermal responses of the skin during contact over the range of contact forces used in manual exploration. Its implementation in a thermal display was able to elicit realistic thermal sensations when simulating materials with different thermal properties. The performance of the model was evaluated in both psychophysical and physiological experiments and an infrared thermal measurement system was developed to overcome the limitations of conventional contact thermal sensors in order to assist in the physiological evaluation of the thermal model.

7.2 FUTURE WORK

Pervasive spatial summation is a unique characteristic of the thermal perception system and influences the ability to identify materials using only thermal cues. It has been shown that presenting thermal cues to a larger area of skin improves subjects' ability in material identification (Yang et al., 2006b). However, presenting different thermal cues to different fingers in one hand can result in thermal illusions and degrade subjects' performance in material localization as described in Section 3.3. Further psychophysical experiments are needed to identify the extent to which spatial summation can assist in material identification and to clarify the conditions under which thermal illusions occur. The results from these studies should provide insight into determining the optimal presentation mode for a thermal display to achieve better performance in material identification.

The simulation results based on the revised thermal model indicated that surface roughness and contact pressure can influence the heat flux conduct out of the skin during contact, and hence presumably change the perceived coldness of an object. Further studies need to be conducted to examine the interaction between contact mechanics and temperature perception and investigate how these physical processes influence temperature perception. The influence of surface roughness and contact pressure on temperature perception may reflect the activity of cutaneous mechanoreceptors as some respond to thermal and mechanical stimuli. For example, it has been shown that warm and cold objects feel heavier than neutral objects (Stevens & Green, 1978). The interactions between thermal and tactile sensations can be addressed in future research.

The physiological evaluation of the revised model (Section 6.4) indicated that it tended to underestimate the change in skin temperature for contact pressures smaller than 3.14 kPa. This suggests that the thermal contact resistance estimation model (Yovanovich, 1981) used in the present study is not adequate for predicting thermal contact resistance over this pressure range. With the revised thermal model and the skin temperature responses measured using the infrared thermal measurement system, it is possible to derive the actual thermal contact resistance existing in the interface during contact. Based on the actual thermal contact resistance and the thermal and mechanical properties of the skin and contact material, a thermal contact resistance model could be developed specifically for hand-object interactions which should improve the performance of the model at low contact pressures. The influence of contact pressure on the skin temperature response during contact can also result from the collapse of blood vessels and blocking blood flow by compression (Section 6.4). Mascaro and Asada (2001) proposed several tentative values of contact forces that would induce different degrees of change in blood flow under normal force. Physiological experiments need to be conducted to determine those force or pressure thresholds.

Finally, the thermal model and experiments described in this thesis were all formulated within a normal temperature range for ambient and skin temperature. The modeling of thermal responses of the skin at extreme temperatures is very different from

the normal situations considered in the present studies, but may be relevant to some of the application domains of haptic displays (eg. underwater and space robotic systems). A thermal model could therefore be developed specifically for those extreme conditions to assist in predicting skin thermal responses.

APPENDIX A: DEFINITIONS OF SURFACE ROUGHNESS PARAMETERS*

1. Rq: Root mean square surface roughness

It is the square root of the arithmetical mean of the squares of profile deviations (Y_i) from the mean line (ISO standard 4287:1997).

$$R_q = \left[\frac{1}{n} \sum_{i=1}^{n} Y_i^2 \right]^{\frac{1}{2}} \tag{A-1}$$

2. Rdq: Root mean square asperity slope

The local slope dZ/dX is calculated with the data points which included three front points and three back points to all the measured data points in the profile. Let the square root of the arithmetical mean of the squares of the local slope be this parameter value (ISO standard 4287:1997).

$$R\Delta q = \left[\frac{1}{n} \sum_{i=1}^{n} \left(\frac{dZ_i}{dX} \right)^2 \right]^{\frac{1}{2}} \tag{A-2}$$

3. Δa: Arithmetical mean asperity slope

Divide the profile into sections at a predetermined interval Δx along the horizontal axis, and obtain the inclination of a line that connects the start point and the end point of the profile in each section. The arithmetical mean slope of the absolute values of the inclination is called the arithmetical mean asperity slope, Δa (ISO standard 4287:1984).

---

* These definitions are from "User's Manual: Surface Texture Parameter" of SURFPAK-TC, Mitutoyo Corporation.

$$\Delta a = \frac{1}{n-1}\left\{\sum_{i=1}^{n-1} \tan^{-1}\left|\frac{\Delta Y_i}{\Delta x}\right|\right\} \tag{A-3}$$

4. Rsm: Mean spacing of the profile elements

A peak projecting above the profile is called a "peak for profile element," and a valley dropping below the lower count level is called a "valley for profile element," and this peak and valley pair which appears continuously is called "profile element." Let the arithmetical mean of the width Xs of all profile elements be this parameter value (ISO standard 4287:1997).

$$Rsm = \frac{1}{n}\sum_{i=1}^{n} Xs_i \tag{A-4}$$

REFERENCES

Antonetti, V. W. & Whittle, T. D. (1991). "An approximate thermal contact conductance correlation," *ASME Experimental/Numerical Heat Transfer in Combustion and Phase Change*, 35-42.

Benali-Khoudja, M., Hafez, M., Alexandre, J. M., Benachour, J. & Kheddar, A. (2003). "Thermal feedback model for virtual reality," *Proceedings of the International Symposium on Micromechatronics and Human Science*, 153-158.

Benali-Khoudja, M. & Hafez, M. (2004). "VITAL: a vibrotactile interface with thermal feedback," *IRCICA International Scientific Workshop*, Lille, France.

Bergamasco, M., Alessi, A. A. & Calcara, M. (1997). "Thermal feedback in virtual environments," *Presence*, **6**: 617-629.

Brown, A. C. (1989). "Somatic sensation: peripheral aspects," *Textbook of Physiology*, Patton, H. D. (Ed.). Philadelphia: Saunders, 298-308.

Burdea, G. C. & Coiffet, P. (2003). *Virtual Reality Technology*, Second Edition. Hoboken, NJ: Wiley.

Cain, W. S. (1973). "Spatial discrimination of cutaneous warmth," *American Journal of Psychology*, **86**: 169-181.

Caldwell, D. G. & Gosney, C. (1993). "Enhanced tactile feedback (tele-taction) using a multi-functional sensory system," *Proceedings of the IEEE International Conference on Robotics and Automation*, **1**, 955-960.

Caldwell, D. G., Lawther, S. & Waedle, A. (1996). "Tactile perception and its application to the design of multi-modal cutaneous feedback systems," *Proceedings of the IEEE International Conference on Robotics and Automation*, **1**, 3215-3221.

Charny, C. K. (1992). "Mathematical models of bioheat transfer," *Advances in Heat Transfer*, Cho, Y. I. (Ed.). New York: Academic Press, 19-155.

Citerin, J., Pocheville, A. & Kheddar, A. (2006). "A touch rendering device in a virtual environment with kinesthetic and thermal feedback," *Proceedings of the IEEE International Conference on Robotics and Automation*, 3923-3928.

Darian-Smith, I. (1984). "Thermal sensibility," *Handbook of physiology: The nervous system* Darian-Smith, I. (Ed.). Bethesda, MD: American Physiological Society, 879-913.

Dellon, E. S., Keller, K., Moratz, V. & Dellon, A. L. (1995). "The relationships between skin hardness, pressure perception and two-point discrimination in the fingertip," *Journal of Hand Surgery*, **20**: 44-48.

Deml, B., Mihalyi, A. & Hanning, G. (2006). "Development and experimental evaluation of a thermal display," *Proceedings of 2006 EuroHaptics*, 257-262.

Dionisio, J., Henrich, V., Jakob, U., Rettig, A. & Ziegler, R. (1997). "The virtual touch: haptic interfaces in virtual environments," *Computer Graphics*, **21**: 459-468.

Dyck, P. J., Curtis, D. J., Bushek, W. & Offord, K. (1974). "Description of "Minnesota Thermal Disks" and normal values of cutaneous thermal discrimination in man," *Neurology*, **24**: 325-330.

Eberhart, R. C. (1985). "Thermal models of a single organ: skin," *Heat Transfer in Medicine and Biology, Vol. I*, Shitzer, A. and Eberhart, R. C. (Eds.). New York: Plenum Press, 269-271.

Gaussorgues, G. (1994). *Infrared Thermography*. New York: Chapman & Hall.

Gescheider, G. A. (1997). *Psychophysics: The Fundamentals*. Mahwah, NJ: Lawrence Erlbaum.

Green, B. G. (1977). "Localization of thermal sensation: An illusion and synthetic heat," *Perception & Psychophysics*, **22**: 331-337.

Green, B. G. (1978). "Referred thermal sensations: Warmth versus cold," *Sensory Processes*, **2**: 220-230.

Greenspan, J. D. & Kenshalo, D. R. (1985). "The primate as a model for the human temperature-sensing system: 2. area of skin receiving thermal stimulation," *Somatosensory Research*, **2**: 315-324.

Hardy, J. D. & Oppel, T. W. (1937). "Studies in temperature sensation. III. The sensitivity of the body to heat and the spatial summation of the end organ responses," *Journal of Clinical Investigation*, **16**: 533-540.

Hardy, J. D. & Oppel, T. W. (1938). "Studies in temperature sensation. IV. The stimulation of cold sensation by radiation," *Journal of Clinical Investigation*, **17**: 772-778.

Hensel, H. (1981). *Thermoreception and Temperature Regulation*. New York: Academic Press.

Ho, H.-N. & Jones, L. A. (2004). "Material identification using real and simulated thermal cues," *Proceedings of 26th Annual International Conference of the IEEE Engineering in Medicine and Biology Society*, 2462-2465.

Ho, H.-N. & Jones, L. A. (2006a). "Contribution of thermal cues to material discrimination and localization," *Perception & Psychophysics*, **68**: 118-128.

Ho, H.-N. & Jones, L. A. (2006b). "Thermal model for hand-object interactions," *Proceedings of the IEEE Symposium on Haptic Interfaces for Virtual Environment and Teleoperator Systems*, 461-467.

Ho, H.-N. & Jones, L. A. (in press). "Development and evaluation of a thermal display for material identification and discrimination," *ACM Transactions on Applied Perception.*

Incropera, F. P. & DeWitt, D. P. (1996). *Fundamentals of Heat and Mass Transfer.* New York: Wiley.

Ino, S., Shimizu, S., Odagawa, T., Sato, M., Takahashi, M., Izumi, T. & Ifukube, T. (1993). "A tactile display for presenting quality of materials by changing the temperature of skin surface," *IEEE International Workshop on Robot and Human Communication*, 220-224.

Johnson, K. O., Darian-Smith, I. & LaMotte, C. (1973). "Peripheral neural determinants of temperature discrimination in man: a correlative study of responses to cooling skin," *Journal of Neurophysiology*, **36**: 347-370.

Johnson, K. O., Darian-Smith, I., LaMotte, C., Johnson, B. & Oldfield, S. (1979). "Coding of incremental changes in skin temperature by a population of warm fibers in the monkey: correlation with intensity discrimination in man," *Journal of Neurophysiology*, **42**: 1332-1353.

Jones, L. A. & Berris, M. (2003). "Material discrimination and thermal perception," *Proceedings of the 11th International Symposium on Haptic Interfaces for Virtual Environment and Teleoperator Systems*, 171-178.

Jones, L. A. & Lederman, S. J. (2006). *Human Hand Function.* New York: Oxford University Press.

Kalpakjian, S. (1995). *Manufacturing Engineering and Technology.* Reading, MA: Addison-Wesley.

Kenshalo, D. R. (1976). "Correlations of temperature sensitivity in man and monkey, a first approximation," *Sensory functions of the skin with special reference to man* Zotterman, Y. (Ed.). Oxford: Pergamon Press, 305-330.

Kron, A. & Schmidt, G. (2003). "Multi-fingered tactile feedback from virtual and remote environments," *Proceedings of the IEEE Symposium on Haptic Interfaces for Virtual Environment and Teleoperator Systems*, 16-23.

LaMotte, R. H. & Srinivasan, M. A. (1991). "Surface microgeometry: Tactile perception and neural encoding," *Information processing in the somatosensory system*, Franzen, O. and Westman, J. (Eds.). London: Macmillan, 49-58.

Lecuyer, A., Mobuchon, P., Megard, C., Perret, J., Andriot, C. & Colinot, J. (2003). "HOMERE: a multimodel system for visually impaired people to explore virtual environments.," *Proceedings of IEEE Virtual Reality*, 251-258.

Lederman, S. J. & Klatzky, R. L. (1997). "Relative availability of surface and object properties during early haptic processing," *Journal of Experimental Psychology: Human Perception and Performance*, **23**: 1680-1707.

Levene, H. (1960). "Robust tests for the equality of variances," *In Contributions to Probability and Statistics: Essays in Honor of Harold Hotelling*, OLKIN, I. (Ed.). Palo Alto, CA: Stanford University Press, 278-292.

Lienhard, J. H. I. & Lienhard, J. H. V. (2003). *A Heat Transfer Textbook*. Cambridge, MA: Phlogiston Press.

MacLean, K. E. & Roderick, J. B. (1999). "Smart tangible displays in the everyday world: A hapic doorknob," *Proceedings of the IEEE/ASME International Conference on Advanced Intelligent Mechatronics*, 203-208.

Madding, R. P. (2004). "IR window transmittance temperature dependence," *Proceedings of InfraMation*, **5**, 161-169.

Madding, R. P. (2005). "Spectrally transmissive IR windows – how they affect your thermography results," *Proceedings of SPIE*, **5782**, 1-8.

Marks, L. E. & Stevens, J. C. (1973). "Spatial summation of warmth: Influence of duration and configuration of the stimulus," *American Journal of Psychology*, **86**: 251-267.

Marks, L. E., Stevens, J. C. & Tepper, S. J. (1976). "Interaction of spatial and temporal summation in the warmth sense," *Sensory Processes*, **1**: 87-98.

Mascaro, S. A. & Asada, H. H. (2001). "Photoplethysmograph fingernail sensors for measuring finger forces without haptic obstruction," *IEEE Transactions on Robotics and Automation* **17**: 698-708.

Mikic, B. B. & Rohsenow, W. M. (1966). "Thermal contact resistance," *Department of Mechanical Engineering Report No. 4542-41*, Massachusetts Institute of Technology.

Mills, A. F. (1999). *Heat Transfer.* Upper Saddle River, NJ: Prentice Hall.

Moore, K. L. & Agur, A. (1995). *Essential Clinical Anatomy.* Philadelphia: Lippincott Williams & Wilkins.

Ottensmeyer, M. & Salisbury, J. K. (1997). "Hot and cold running VR: Adding thermal stimuli to the haptic experience " *Proceedings of the Second PHANToM Users Group Meeting 34 Artificial Intelligence Laboratory Technology Report No. 1617.*

Overgaard Olsen, L., Takiwaki, H. & Serup, J. (1995). "High-frequency ultrasound characterization of normal skin. Skin thickness and echographic density of 22 anatomical sites," *Skin Research and Technology*, **1**: 74-80.

Pawluk, D. T. & Howe, R. D. (1999). "Dynamic contact of the human fingerpad against a flat surface," *Journal of Biomechanical Engineering*, **121**: 605-611.

Pennes, H. H. (1948). "Analysis of tissue and arterial blood temperatures in the resting forearm," *Journal of Applied Physiology*, **1**: 93-122.

Sarda, A., Deterre, R. & Vergneault, C. (2004). "Heat perception measurements of the different parts found in a car passenger compartment," *Measurement*, **35**: 65-75.

Serina, E. R., Mote Jr, C. D. & Rempel, D. (1997). "Force response of the fingertip pulp to repeated compression – effects of loading rate, loading angle and anthropometry," *Journal of Biomechanics*, **30**: 1035-1040.

Shitzer, A., Stoschein, L. A., Gonzalez, R. R. & Pandolf, K. B. (1996). "Lumped-parameter tissue temperature-blood perfusion model of a cold stressed finger tip," *Journal of Applied Physiology*, **80**: 1829-1834.

Simmel, M. L. & Shapiro, A. (1969). "The localization of non-tactile thermal sensations," *Psychophysiology*, **5**: 415-425.

Smith, A. M. & Scott, S. H. (1996). "Subjective scaling of smooth surface friction," *Journal of Neurophysiology*, **75**: 1957-1962.

Smith, A. M., Chapman, E., Deslandes, M., Langlais, J. S. & Thibodeau, M. P. (2002). "Role of friction and tangential force variation in the subjective scaling of tactile roughness," *Experimental Brain Research*, **144**: 211-223.

Spray, D. C. (1986). "Cutaneous temperature receptors," *Annual Review of Physiology*, **48**: 625-638.

Srinivasan, M. A. & LaMotte, R. H. (1995). "Tactile discrimination of softness," *Journal of Neurophysiology*, **73**: 88-101.

Stevens, J. C. & Green, B. G. (1978). "Temperature-touch interaction: Weber's phenomenon revisited," *Sensory Processes*, **2**: 206-219.

Stevens, J. C. & Marks, L. E. (1979). "Spatial summation of cold," *Physiology & Behavior*, **22**: 541-547.

Stevens, J. C. (1991). "Thermal sensibility," *The Psychology of Touch*, Heller, M. A. and Schiff, W. (Eds.). Hillsdale, NJ: Lawrence Erlbaum, 61-90.

Stevens, J. C. & Choo, K. C. (1998). "Temperature sensitivity of the body surface over the life span," *Somatosensory & Motor Research*, **15**: 13-28.

Taus, R. H., Stevens, J. C. & Marks, L. E. (1975). "Spatial localization of warmth," *Perception & Psychophysics*, **17**: 194-196.

Tortora, G. J. & Grabowski, S. R. (1993). *Principles of Anatomy and Physiology*. New York: Harper Collins.

Verrillo, R. T., Bolanowski, S. J., Checkosky, C. M. & McGlone, F. P. (1998). "Effects of hydration on tactile sensation," *Somatosensory and Motor Research*, **15**: 93-108.

Westling, G. & Johansson, R. S. (1987). "Responses in glabrous skin mechanoreceptors during precision grip in humans," *Experimental Brain Research*, **66**: 128-140.

Yamamoto, A., Cros, B., Hasgimoto, H. & Higuchi, T. (2004). "Control of thermal tactile display based on prediction of contact temperature," *Proceedings of the IEEE International Conference on Robotics and Automation*, 1536-1541.

Yang, G., Kyung, K., Srinivasan, M. A. & Kwon, D. (2006a). "Quantitative tactile display device with pin-array type tactile feedback and thermal feedback," *Proceedings of the IEEE International Conference on Robotics and Automation*, 3917-3922.

Yang, G., Jones, L. A. & Kwon, D. (2006b). "Use of simulated thermal cues for material discrimination and identification with a multi-fingered display," *submitted for publication.*

Yovanovich, M. M. (1981). "Thermal contact correlations," *AIAA 16th Thermophysics Conference.*